Order Number 9510648

Acetal copolymers: Synthesis, chemical modification and degradation study

Cho, Kumhee, Ph.D.

City University of New York, 1994

U·M·I
300 N. Zeeb Rd.
Ann Arbor, MI 48106

ACETAL COPOLYMERS: SYNTHESIS, CHEMICAL MODIFICATION AND DEGRADATION STUDY

by

Kumhee Cho

A dissertation submitted to the Graduate Faculty in Chemistry in partial fulfillment of the requirements for the degree of Philosophy, The City University of New York.

1994

This manuscript has been read and accepted for the Graduate Faculty in Chemistry in satisfaction of the dissertation requirement for the degree of Doctor of Philosophy.

July 26, 1994
Date

Prof. Nan-Loh Yang
Chair of Examining Committee

July 26, 1994

Executive Officer

Prof. Carol Steiner, City College

Prof. Micha Tomkiewicz, Brooklyn College

Supervisory Committee

The City University of New York

Abstract

Acetal Copolymers: Synthesis, Chemical Modification and Degradation Study

by

Kumhee Cho

Advisor: Professor Nan-Loh Yang

The degradation of trioxane-dioxolane copolymer in DMSO-d_6 solution at 120 °C caused by the addition of trifluoroacetic acid, AIBN, or Luperox was investigated by ^{1}H NMR spectroscopy. The degradation mechanisms in both acidic and radical processes were proposed based on the kinetic behaviors for triad sequences of the degraded copolymer and the small molecules formed during the processes. Formaldehyde was released through β-scisson reactions of both cationic and radical chain ends. The rate constants estimated based on available [H^+] and [$R^\bullet$] were 10^{-3} (sec^{-1}) and 10^{-2} (sec^{-1}) respectively. Cyclic acetals 1,3,5-trioxane, 1,3-dioxolane, 1,3,5,7-tetraoxane and 1,3,5-trioxepane were generated by backbiting of the cationic chain ends and intramolecular substitution of radical chain ends. The rate constant values for both reactions were about 10^{-3} (sec^{-1}).

The estimated free energy changes for the formation of

formaldehyde and cyclic acetals based on the enthalpy changes indicated that the formation of formaldehyde is more favored than cyclic acetals by 43 (kJ/mole). The difference of activation energies between formation of formaldehyde and cyclic acetals was calculated from the kinetic data. The difference in activation energy favoring the formation of formaldehyde over that of cyclic acetals was determined to be 4.5 (kJ/mole) and 9.8 (kJ/mole) in the acidic and radical degradation processes respectively. The smaller difference in the acidic process may be a consequence of lower activation energy for backbiting reaction involving stable tertiary oxonium ion and higher activation energy for the β-scisson involving heterolysis bond scission. The degradation rate of active chain end, evaluated in terms of the rate for elimination of monomer units per active chain, revealed that the radical chain end degrade at a rate more than eight times faster than the cationic one.

Trioxane copolymer carrying vicinal dibromo functional groups was synthesized and its chemical modifications were carried out for the introduction of amino and triple bond functional groups. The resulting copolymer with backbone -C≡C- group has been demonstrated to be not only more stable than the copolymer with backbone -C=C- against degrading agent, Br_2, but also in the oxidative thermal degradation. In the oxidative thermal degradation, the functionalized copolymer with pendant hindered phenol-amine group showed

better stability than the copolymers with comparable incorporation of octylamine pendant group or with higher incorporations of backbone -C=C- and -C≡C- groups.

Thanks To The Lord

Acknowledgements

I would like to express my sincere gratitude to Professor Nan-Loh Yang for his time, continuous support, guidance, encouragement through my graduate career.

I would like to thank Professors C. Steiner and M. Tomkiewicz, members of my thesis committee, for their interest in my project and advice as well as the generosity of their time. I would also like to thank the Chemistry Department of College for teaching support during my graduate study.

I am grateful to Tai Park for his expert advice on the IBM computers and NMR work stations. I would like to express my appreciation to the faculty, staff and graduate students in the Chemistry Department for their kindness.

I am indebted to every member of my family for their understanding, patience and continuous support. Specially, I am most grateful to my husband Jeong-Hwan and my son Seung-Wook, for their unending support and dedication throughout my studies.

Kumhee Cho

July, 1994.

Table of Contents

List of Tables

List of Figures

1. LITERATURE SURVEY

1.1. History of Polyacetals

Polyacetal may be considered as one of more recent polymers amongst traditional plastics. It rivals plastics such as ABS, some nylons, polycarbonate, and polysulfone resins in engineering applications (1). As a replacement for metal, polyacetal mainly competes with metals such as aluminum, brass and zinc.

Acetal homopolymers are completely characterized by $-(CH_2O)-$ repeat units and can be prepared either from formaldehyde or from its cyclic oligomers such as trioxane or tetraoxane. Whereas formaldehyde can be polymerized either anionically or cationically, only cationic polymerization take place in the case of trioxane or tetraoxane. High molecular weight acetal homopolymers with unique plastic properties were prepared first in 1892 by Kekule (2) from the cationic polymerization of trioxane. Extensive studies of the polymerization were published by Staudinger in 1932 (3). Acetal homopolymer includes unstable methylol end group, $-O-CH_2OH$ (hemiacetal), which normally results from polymerization in the presence of water. At elevated temperature, the unmodified homopolymer tends to split off formaldehyde at the chain ends through sequential elimination process, i.e. unzipping (4).

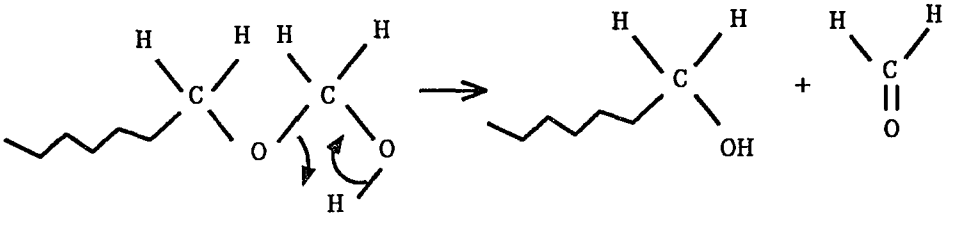

Unzipping process

The unzipping rate was reported to be proportional to the number of polymer chain ends and an exponential function of temperature.

Research efforts were made over twenty five years until, in 1959, Du pont produced chain end capped polyoxymethylene homopolymer (5), called Derlin, which possessed sufficient toughness and thermal stability. It has

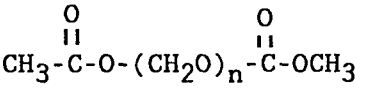

Derlin

stable acetate end groups, $-O-CH_2-OCOCH_3$, formed through esterification reaction of hemiacetal chain ends with acetic anhydride. Unzipping process is thus suppressed by the acetate chain end.

Trioxane can readily copolymerize with heterocyclic and some vinyl monomers. Commercial copolymer, Celcon, was prepared from copolymerization of trioxane with cyclic

acetal by Celanese in 1961 (6). Incorporated comonomer unit,

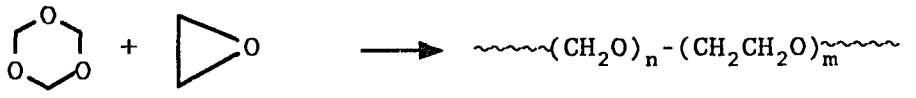

Trioxane *Ethylene oxide* *Celcon*

the ethylene oxide unit ($-CH_2CH_2O-$), acts as a stopper unit through interrupting $-CH_2O-CH_2-O-$ sequence linkages so that unzipping of the polymer chain can not proceed beyond this unit. The copolymer end groups, $-O-CH_2CH_2OH$, which resulted from base hydrolysis of the nascent copolymer either in solution (7) or heterogeneously (8), are not hemiacetal and also act as a stopper unit against unzipping process. Therefore the copolymer is more stable than the end capped homopolymer, Derlin.

1.2. Mechanism of Trioxane Copolymerization

Numerous works have been reported for the investigation of trioxane copolymerization mechanism in its copolymerization with ethylene oxide, or 1,3-dioxolane. Some unique features have been experimentally observed in these works, such as induction period and transacetalization.

Induction period is a result of consecutive reactions of intermediates which are formed during the early stage of the copolymerization and influenced by impurities such as

water (9). For example water appeared to prolong the induction period.

Weissermel et al. (10) reported much longer induction period for the initiation of trioxane copolymerization with ethylene oxide than that observed for the homopolymerization. During this period, cyclic oligomers such as 1,3-dioxolane, 1,3,5,7-tetraoxane, and 1,3,5-trioxepane and low molecular weight linear copolymer were observed.

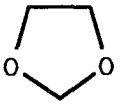

1,3-dioxolane

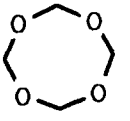

1,3,5,7-tetraoxane

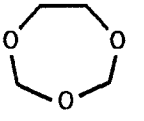

1,3,5-trioxepane

The formation of dioxolane was proposed as due to an insertion mechanism of formaldehyde to ethylene oxide by Weissermel et al. (11) and Collins et al. (12)

In an ^{1}H NMR study on the initial stage of trioxane homopolymerization, an insertion process involving the addition of formaldehyde to trioxane to form tetraoxane was proposed (13).

In the copolymerization of trioxane with dioxolane, the formation of trioxepane was considered from a insertion mechanism (14), or back-biting reaction. Insertion mechanism involves protonated dioxolane with formaldehyde was proposed

by Mengoli (14). Back-biting reaction was reported by Miki et al. (15) who described long growing polymer chain end reacting with oxygen of its own chain.

Other initiation mechanism, involving the existence of intermediates before the formation of trioxepane and dioxolane, was proposed for the copolymerization of trioxane and ethylene oxide by Asahi chemical researchers (9). They reported the isolation of nine and twelve membered rings of novel cyclic compounds during the copolymerization. They believe that nine membered ring, 1,3,5,7-tetraoxacyclononane (TOCN), was formed from the reaction of trioxane with ethylene oxide and act as intermediate to form trioxepane and dioxolane. A twelve-membered ring, 1,3,5,7,10-pentaoxacyclododecane (POCD), was considered as the product formed by 2:1 mole ratio reaction of trioxane and ethylene oxide.

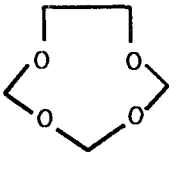

1,3,5,7,-Tetraoxa-cyclononane (TOCN)

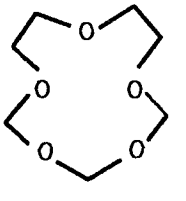

1,3,5,7,10-Pentaoxa-cyclododecane (POCD)

It was found that ethylene oxide, having higher basicity than trioxane, was nearly completely consumed very

early stage in the copolymerization of trioxane with ethylene oxide (16). Despite its consumption, ethylene oxide units were randomly distributed in the polymer with narrow molecular weight distribution of two (M_w / M_n= 2) (17). This was a good evidence of internal redistribution of comonomer units occurring frequently during the polymerization, which was termed transacetalization.

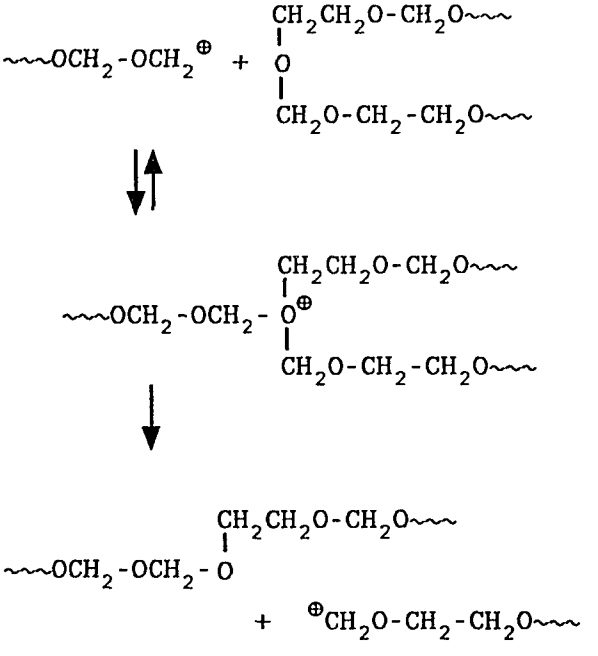

Transacetalization Scheme

For the copolymerization of trioxane with dioxolane, Jaacks proposed that in addition to transacetalization, depolymerization of the soluble polymer contributed to its random distribution of dioxolane units (18). He examined

viscometrically the polymer molecular weight changes with polymerization yield. The reduced viscosity was observed to be a maximum at close to a polymer conversion of 50 % and then decreased to a constant value with polymer conversion. He explained that in the later stage of copolymerization, the soluble copolymer was gradually degraded to give the dioxolane monomer which was incorporated into the crystalline copolymer almost randomly.

1.3. Polyoxymethylene Ionomers

Polyoxymethylene ionomers were prepared by Wissbrun et al. (19). They polymerized trioxane with epichlorohydrin and reacted the pendant chloromethyl groups with disodium thioglycolate to yield an ionomer with side group:

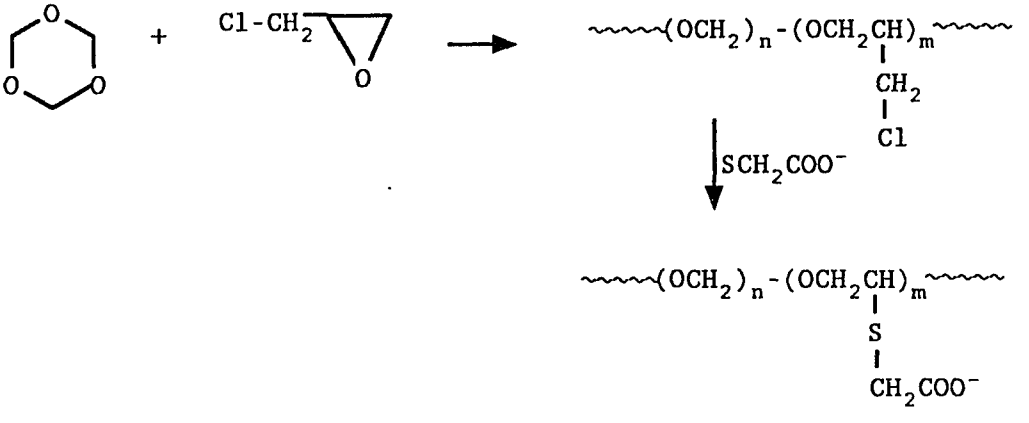

Some of ionomer polymers showed a substantial increase in their moduli over parent POM.

1.4. Trioxane Copolymer with Functional Groups

In addition to ethylene oxide and cyclic formals, usually used in commercial production of the trioxane copolymers, a great number of comonomers such as epoxy compounds (20, 21, 22), vinyl compounds (23 - 25), lactones and lactam (26) have been reported for the copolymerization of trioxane.

The copolymerization of trioxane with phenylglycidyl ether, derivative of epoxide, led to an increase in thermostability (27, 28).

Recently, acetal polymers with functional groups such as double bond (29, 30), hydroxy (31), epoxy and acrylate (31) have been prepared by copolymerization of trioxane with various functional comonomers. A copolymer with backbone double bond was obtained from the copolymerization of trioxane with unsaturated five membered ring, 1,3-dioxep-5-ene.

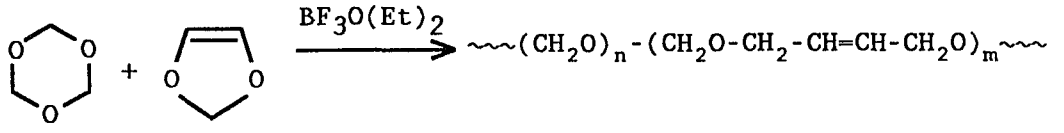

Shulz et al. (29) proposed further modifications of this copolymer through addition reaction of the double bond in the comonomer unit, oxy-2-butenylene, $-(CH_2O-CH_2-CH=CH-CH_2O)-$ as follows:

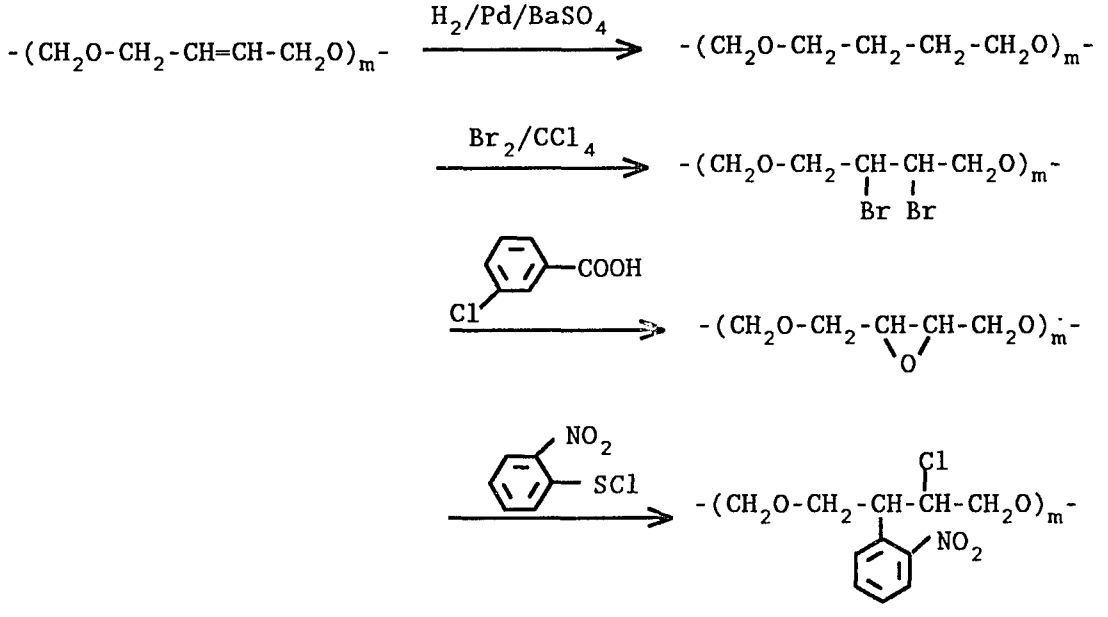

Oxy-2-butenylene have been shown to be an efficient stabilizer counit which improves thermostability of acetal copolymers by acting as a stopper unit against the unzipping process (30). Hydroxyl functional group of acetal copolymer was further reacted with acyl group as well as isocyanate group (31).

1.5. References

1. Stohler, F. R.; Berger, K., *Die Angew. Makromol. Chem.*, **1990**, 176/177, 323, 3074.
2. Kekule, A., *Ber.*, **1892**, 25, 2435.
3. Staudinger, H.; Johnen, H.; Signer, R.; Mie, G.; Henstenberg, J. Z., *Physik. Chem.*, **1927**, 126, p 257.
4. Morelli, F., *Ann. Chim.* (Rome), **1969**, 59, p 1.
5. U.S. Pat. 2,768,994 (Oct. 30, **1956**), Macdonald, R. N. (to E.I. Du pont de nemours & Co., Inc.)
6. U.S. Pat. 3,027,352 (Mar. 27, **1962**), Walling, C.; Brown, F.; Bartz, K. to Calanese Corp.
7. Wall, E., Smith, E.T.; Fisher, G. J. to Celanese Corp., U.S. Pat. 3,174,948, (Mar. 23, **1965**)
8. Clarke, C. M. to Celanese Corp., U.S. Pat. 3,318,848, (May 9, **1967**)
9. Masamoto, J.; Iwaisako, T.; Yoshida, K.; Matsuzaki,K; Kagawa, K.; Nagahara, H., *Makromolek. Chem., Macromolec. Sym.*, **1991**, 42/43, 409.
10. Weissermel, K.; Fisher, E.; Gutweiler, K., **1964**, 54, 410.
11. Weissermel, K.; Fisher, E.; Gutweiler, K.; Hermann, H. D.; Cherdron, H., *Angew. Chem. Int. ed.* **1967**, 6, 526.

12. Collins, G. L.; Greene, F. M.; Beradinelle, F. M.; Ray, W. H., *J. Polym., Sci. Polym. Chem. Ed.*, **1981**, 19, 1597.

13. Lu, N.; Collins, G. L.; Yang, N.-L., *Makromolek. Chem., Macromolec. Symp.*, **1991**, 42/43, 425.

14. Mengoli, G.; Furlanetto, F., *Makromolek. Chem.* **1975**, 176, 143.

15. Miki, T.; Higashimura, T.; Hayashi, K.; Okamura, S., *J. Polym. Sci., Polym. Lett.*, **1967**, **5**, 65.

16. Chen, C. S. H.; Diedwardo, A., *Advan. Chem. Series*, **1969**, 91, 359. & Chen, C. S. H.; Diedwardo, A., *J. Macromol. Sci.*, **1970**, A4, 349.

17. Dolce, T. J.; McAndrew, F. B., *ACS Poly. Prepr.*, **1986**, 27 (1), 476.

18. Jaacks, V., *Adv. Chem. Ser.*, **1969**, 91, 371.

19. Wissbrun, K.; Berardinell, F.; Price, M. B., U. S. pat. 3,488,322, **1970**, assigned to Hoechst Celanese; Wissbrun, K. F., *Makromolek. Chem.*, **1968**, 211, 1228.

20. Weissermel, K.; Fisher, E.; Gutweiler, H. D.; Cherdron, H., *Angew. Chem. Int. Ed.*, **1967**, 6, 526.

21. Jaacks, V., *Makromolek. Chem.*, **1967**, 101, 33.

22. Burg, K.; Fisher, E.; Weissermel, K., *Makromolek. Chem.*, **1967**, 103, 268.

23. Penczek, S.; Kubisa, P. ; Matjaszwski, K., Cationic Ring Opening Polymerization, part II, Synthetic Applications in *Adv. Polym. Sci.*, Springer-Verlag,

Berlin, **1985**, vol. 48, p 99.

24. Schulz, R. C.; Kubisa; P., Nienberg, J., Cyclic Compounds Containing Two or More Oxygen Atoms in "*Ring Opening Polymerization*" by Irvin, K. J. and Saegusa, T., Elsevier, New York, **1984**, p. 309.
25. Mateva, R.; Raschieva, E., PAN BAN TGP, **1982**
26. Mateva, R.; Pavlova, M.; Kabaivanov, V., *J. Polym. Sci., Polym. Chem. Ed.*, **1975**, 13, 825.
27. Mateva, R. Sirasiki, G., *J. Polym. Sci., Polym. Chem. Ed.*, **1988**, 26, 511.
28. Mateva, R.; Shirashiki, *Acta Polymerica*, **1989**, 40, 606.; Mateva, R.; Shirashiki, *Acta Polymerica*, **1989**, 40, 631.
29. Schulz, R. C. *Makromol. Chem. Suppl.*, **1985**, 12, 1.
30. Pesce-Rodriguez R.; Wang, S.; Yang, N.-L., *Makromol. Chem.*, **1990**, 191, 99.
31. Zheng, Y., *Acetal Copolymers: Synthesis and Modification* Doctoral Thesis, The City Univesity of New York, **1992**.

2. POLYACETAL DEGRADATION STUDY

2.1. Introduction

The main chain scission degradation of acetal polymers has been outlined as proceeding through two essential routes (Scheme 2-1) (1). Acetal polymers are susceptible to both radical and acidolytic degradation. Radical degradation may be initiated by radical abstraction of methylenic hydrogen. The unshared electron pairs of the oxygen atom of acetal unit may be attacked by acid. In both cases, β-scission will occur, resulting in the generation of formaldehyde. In the presence of heat and light, formaldehyde can produce radicals. Hydroperoxide produced during the degradation process can oxidized formaldehyde to formic acid (HCOOH), which can accelerate the degradation of the polyacetal.

The role of peroxides in oxidizing formaldehyde to formic acid has been reported in both thermal-oxidative and photo-oxidative degradation of TOX-DOL copolymer (1). As temperature increases the hydroperoxide decomposes readily and oxidizes formaldehyde efficiently.

In the presence of oxygen and at temperatures above 160 °C, auto-oxidative process (Scheme 2-2) of acetal polymer becomes effective. The auto-oxidative degradation was believed to be initiated by the formation of a polymer

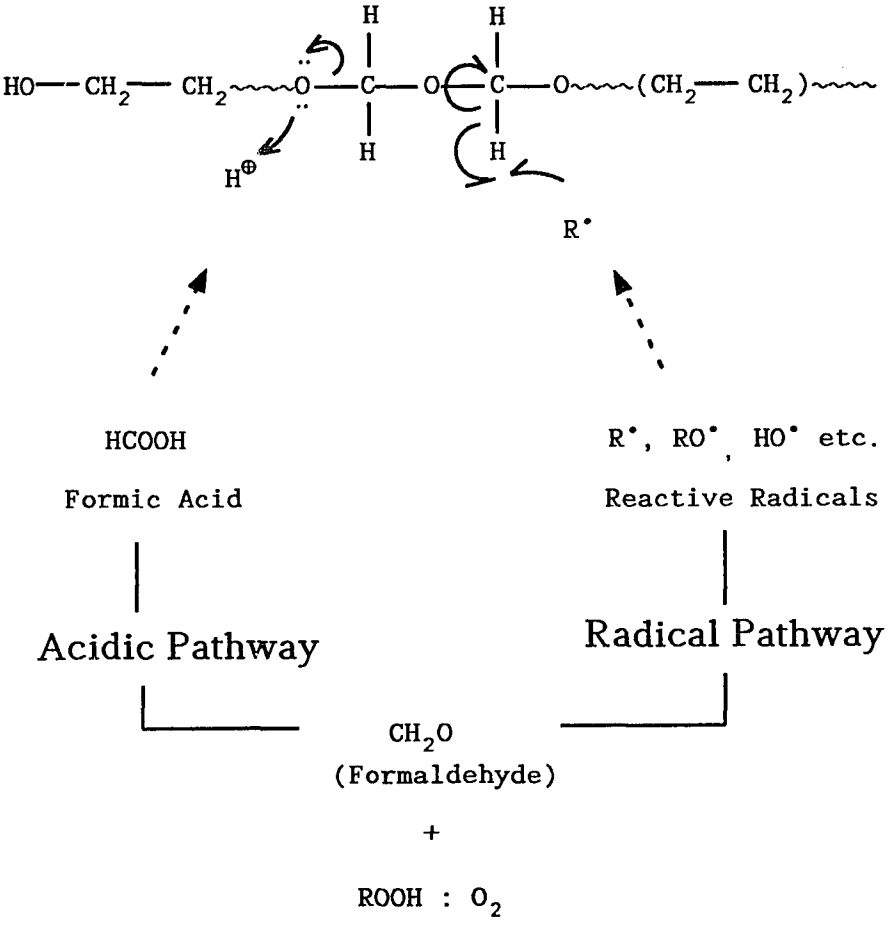

Scheme 2–1 Degradation Scheme

From reference (1)

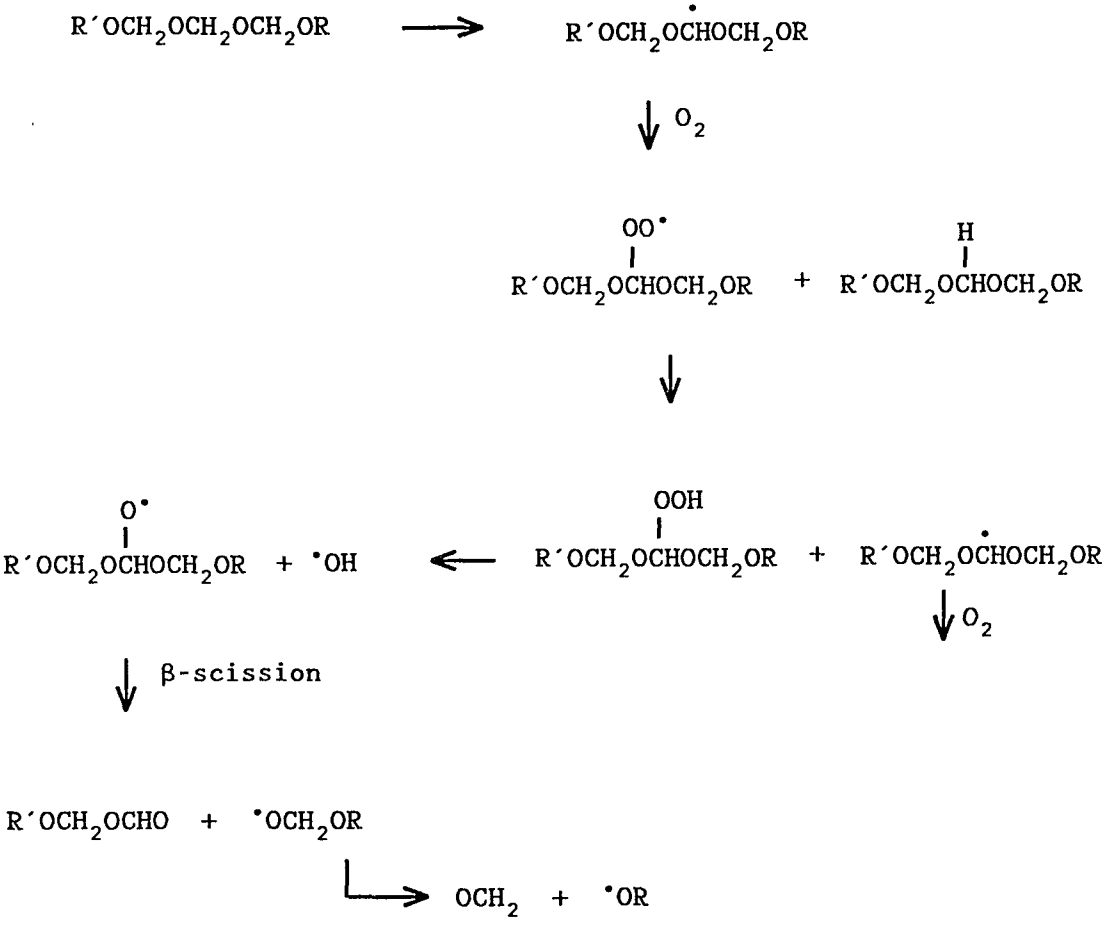

Scheme 2–2 Auto–Oxidative Degradation

From reference (2)

hydroperoxide in the amorphous region with subsequent cleavage of the chain by a β-scission mechanism followed by unzipping reaction of the active radical fragments (2).

Photochemical behavior of acetal copolymer under long wavelength excitation has been examined by Lemaire et al. (3). The final photo products were identified by chemical treatments and IR spectroscopy. The proposed mechanism involves the oxidation of the carbon atoms always in α-position of two oxygen atoms without participation of dimeric sequences and tertiary structures such as:

$$-CH_2-CH_2-O- \qquad \begin{matrix} -CH_2-O-CH_2-O-\underset{|}{CH}-O-CH_2-O- \\ -CH_2-O-CH_2-O-CH-O-CH_2-O- \end{matrix}$$

Previously, radical or acid initiated degradation of trioxane-dioxolane copolymer was followed in our laboratory using by ^{1}H and ^{13}C NMR spectroscopy (4). The degradation products of both processes have been identified to be formaldehyde and cyclic acetals 1,3,5-trioxane (TOX), 1,3-dioxolane (DOL), 1,3,5,7-tetraoxane (TEX), 1,3,5-trioxepane (TOP). The formation of cyclic acetals in the acidic degradation process has been considered in terms of chain end backbiting reaction on an oxygen of its own

chain. However, no extensive investigation of the degradation mechanisms of acidic or radical degradations has been carried out yet.

The main goal of the present study is to understand fundamental chemistry of the main routes of the polyacetal degradation in both of acidic and radical processes. There are several objectives: to confirm the degradation products in both of acidic and radical degradation processes; to investigate the kinetics of formation of these degradation products and degraded chain sequences during the entire course of the degradation processes; and to propose a kinetic mechanism consistent with experimental observation. The mechanisms are deduced from the experimental observations of the degradation process monitored by ^{1}H NMR spectroscopy. The rates of the two degradation processes, i.e. acidic versus radical, in terms of the degradation of the varied polymer chain sequences, the rate for elimination of monomer units, and the relative rate of formation of the products during the degradation processes were investigated.

2.2. Experimental

(a) Preparation of Model Acetal Copolymer

A model acetal copolymer for degradation study was prepared from bulk copolymerization of TOX and DOL using BF_3OEt_2 catalyst at 65 °C. In order to provide convenient concentrations for observation of the different comonomer sequences which are expected to vary during degradation processes, a high comonomer (DOL) incorporation (10 mol-% to formaldehyde) was employed as the model acetal copolymer, which has significantly higher concentration of ethylene oxide units than commercial materials. The molecular weight of the model copolymer was estimated from the inherent viscosity of the copolymer in hexafluoroisopropanol (HFIP) solution at 25 °C with a concentration of 0.200 g/dL. The viscosity average molecular weight (M_v) was found to be about 1.5×10^4 with degree of polymerization, DP = 600.

(b) Sample Preparations

To the solution of the model TOX-DOL copolymer, which was prepared in 5 mm NMR tube by dissolving 50 mg of the model copolymer in the 0.3 mL of DMSO-d_6, the required amount of trifluoroacetic acid was quickly introduced as an acidic initiator by a long needle syringe. Five to six μL of acid was used with quantitative uncertainty of ±20 %. As

radical initiator, either 12 mg of AIBN (2,2′-azobisisobutyronitrile) or 10 mg of Luperox (2,5-dihydroperoxy-2,5-dimethylhexane) was added. After addition of the initiator, the NMR tube was gently heated to dissolve the mixture at 120 °C and inserted into the spectrometer probe kept at 120 °C. The ^{1}H NMR spectra at desired time intervals were obtained during the entire degradation process.

(c) ^{1}H NMR Analysis of Degradation

The degradation progress of TOX-DOL copolymer was monitored from the initial stage to the final stage by carrying out sixteen scans for each of ^{1}H NMR spectra at desired time intervals in a 200 MHz ^{1}H NMR Bruker spectrometer. Integration of absorption peak area was carried out using "NMR 1" software. In the absence of acid or radical under the same condition, the degradation rate was found to be negligible.

2.3. Results and Discussion

2.3.1. Acidic Degradation

(a) Degradation Products

The ^1H NMR spectra covering processes taking place from the initial to the final stage of the acid catalyzed degradation are shown in Fig. 2-1. The degradation products have been identified to be formaldehyde, cyclic acetals including 1,3,5-trioxane (TOX), 1,3,5,7-tetraoxane (TEX), 1,3-dioxolane (DOL), 1,3,5-trioxepane (TOP), and formate end groups. The degradation products emerge with initial rates in the following order: formaldehyde > TOP > TEX > DOL > TOX > formate end groups. A broad peak at low field, corresponding to free acids and OH end groups, was also observed.

i. Formaldehyde and Cyclic Acetals

Identification of the degradation products, formaldehyde and cyclic acetals, were originally established by Pesce (4). The structure identification was carried out using ^1H NMR spectroscopy at 126 °C in DMSO-d_6 solution. The ^1H NMR chemical shifts values are presented in the Scheme 2-3.

Formaldehyde concentration increases rapidly within 10

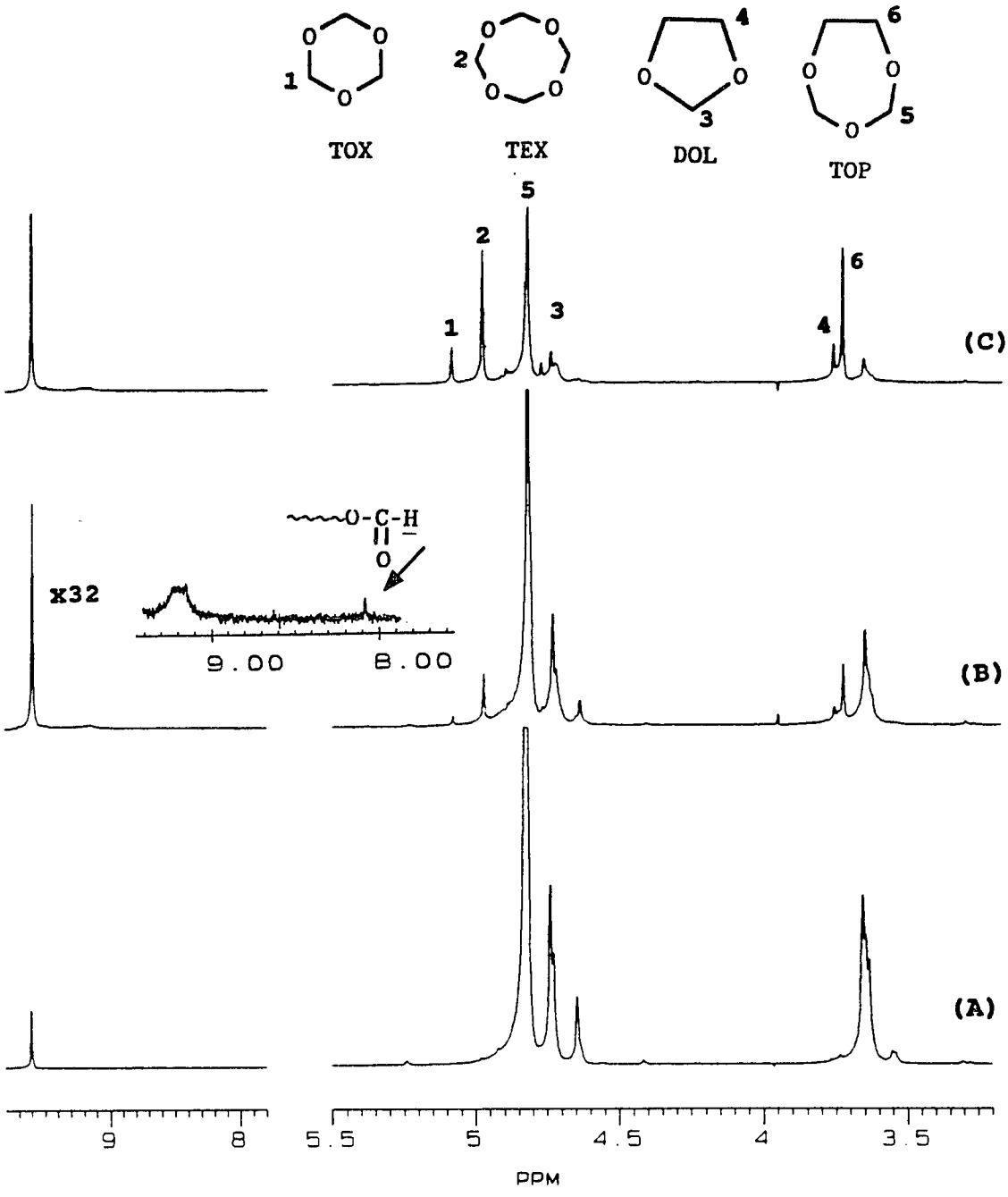

Fig. 2-1 ^{1}H NMR Spectra of degraded TOX-DOL copolymer in DMSO-d_6 solution at 120 °C initiated by addition of 2.4 X 10^{-2} M of trifluoroacetic acid. (A) before addition of trifluoroacetic acid (B) 8 min and (C) 24 min after addition of trifluoroacetic acid

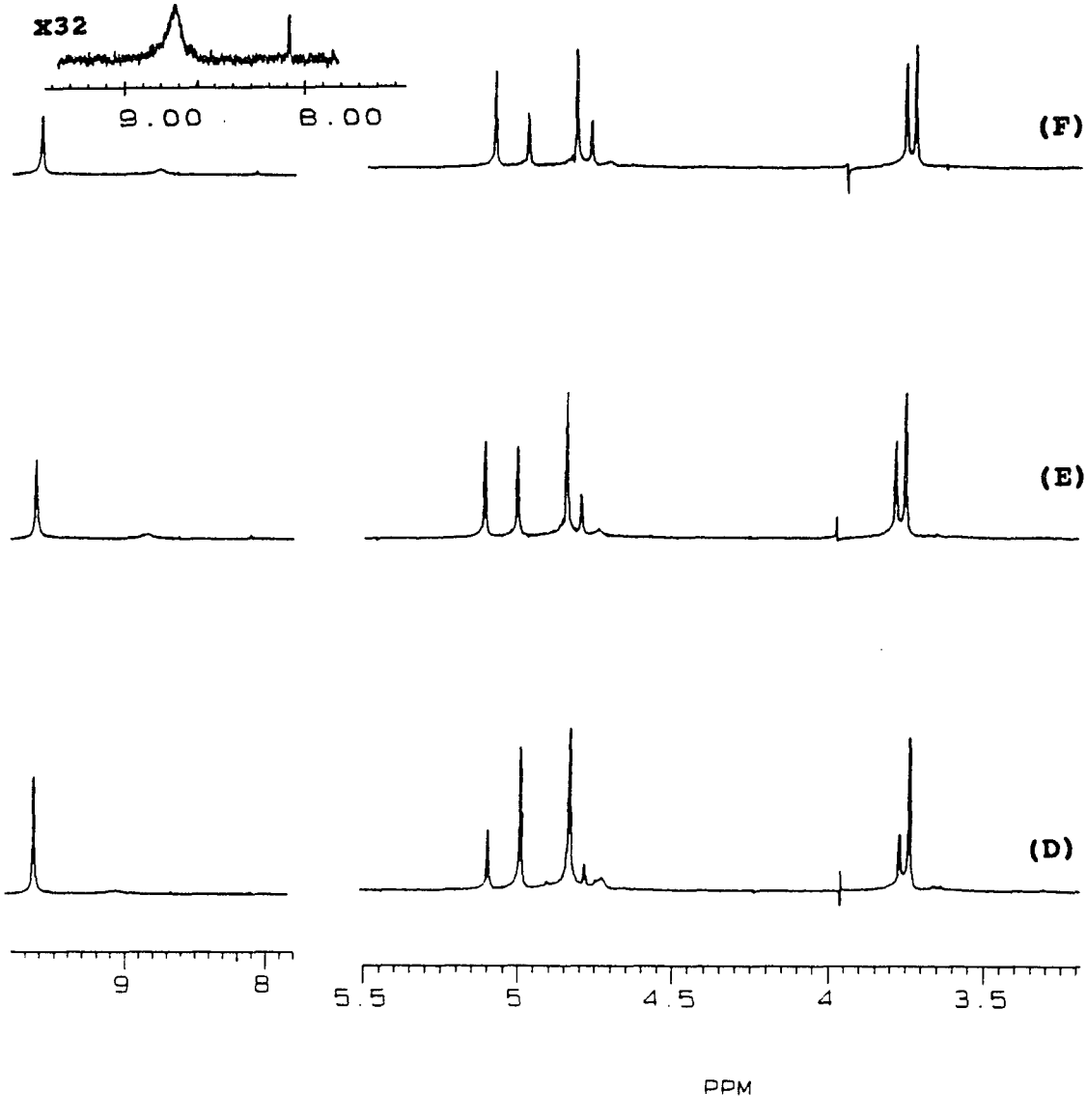

Fig. 2-1 ^{1}H NMR Spectra of degraded TOX-DOL copolymer in DMSO-d_6 solution at 120 °C initiated by addition of 2.4 X 10^{-2} M of trifluoroacetic acid. (D) 37 min, (E) 69 min and (F) 74 min after addition of trifluoroacetic acid

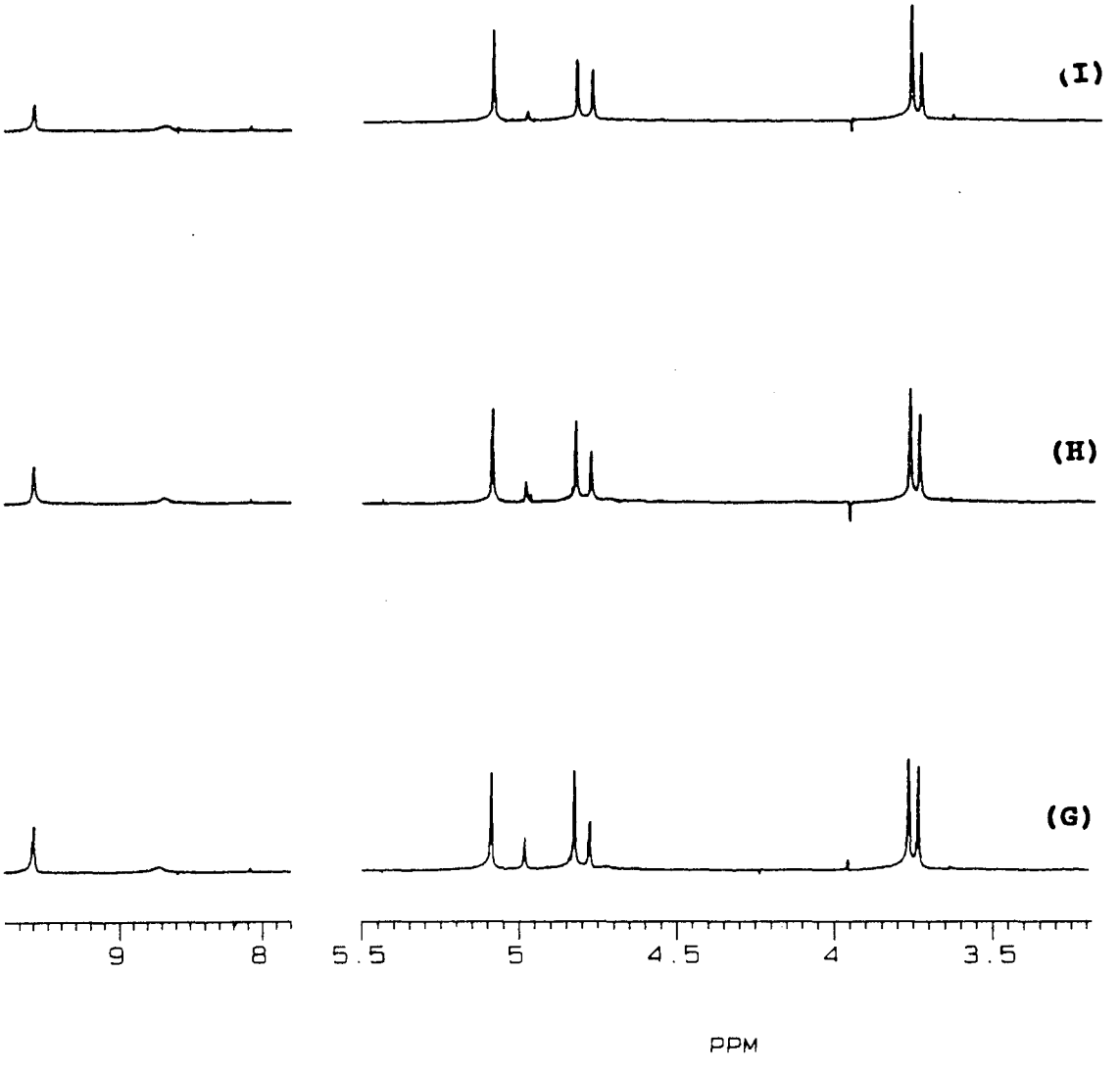

Fig. 2-1 ^{1}H NMR Spectra of degraded TOX-DOL copolymer in DMSO-d_6 solution at 120 °C initiated by addition of 2.4 X 10^{-2} M of trifluoroacetic acid. (G) 90 min, (H) 116 min and (I) 138 min after addition of trifluoroacetic acid

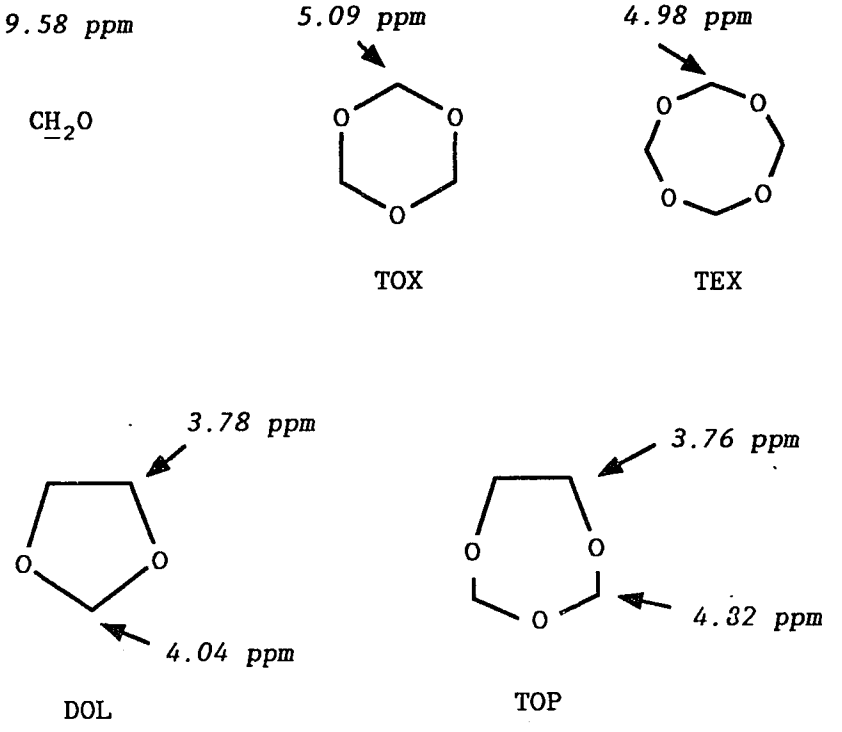

Scheme 2–3

~ 15 minutes and then decreases continuously, indicating polymerization of formaldehyde to paraformaldehyde above the solution. The white solid was collected from the wall of NMR tube above the solution at the end of the degradation process and analyzed by ^1H NMR in DMSO-d_6 solution. In the ^1H NMR spectrum, a single resonance at 4.82 ppm due to -CH_2O- units was observed. The fast polymerization of formaldehyde evolved from the degrading polymer solution contributed to a

rapid decrease in the concentration of formaldehyde.

The formation of cyclic acetals have been attributed to chain end backbiting on oxygen atoms of it's own chain (4). For example, the formation of TOX through backbiting can be depicted as follows:

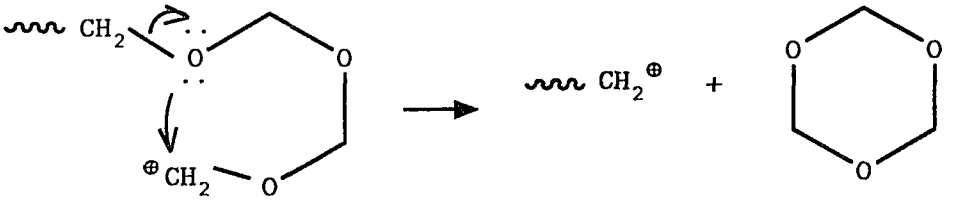

It appears that in the early stage of the degradation process, the growth rate of TEX is higher than TOX and similarly, it is higher for TOP than DOL. These results can be explained by lower positive free energy change for the formation of larger cyclic rings having lower ring strain. This is supported by estimated lower positive free energy change for formation of TEX (+ 4.44 kJ/mol) than TOX (+ 6.12 kJ/mol). These values were calculated based on reported ΔH and ΔS values in the polymerization of TOX or TEX (5). The reported values for polymerization in nitrobenzene at 74 °C are as follows: ΔH and ΔS for TOX, -8.4 (kJ/mol), -5.8 (J/mol·K); and for TEX, -9.2 (kJ/mol), -12.1 (J/mol·K), respectively. The backbiting reaction is in the reverse direction of the polymerization; opposite sign of ΔH and ΔS

values were used for the calculation of degradation. The entropic factor favors the formation of larger ring. At 120 °C, ΔG for formation of TEX is lower than TOX by 1.68 (kJ/mol).

ii. Formate End Groups

The peak at 8.08 ppm (Fig. 2-1 (B)) was considered to be due to either protons of formate (O=C<u>H</u>-OR) end groups resulting from chain transfer reactions, or proton of formic acid (<u>H</u>CO-OH) which can be formed from the oxidation of formaldehyde.

The proton NMR spectra of a model compounds, ethyl formate, (O=C<u>H</u>-OCH_2CH_3, 8.12 ppm) and formic acid (<u>H</u>CO-OH, 8.08 ppm) were obtained at 80 °C in the DMSO-d_6 solution (Fig. 2-2 (A) and (B)). The two chemical shifts are very close to each other. In order to identify this absorption peak, model reactions with an amine were carried out to differentiate formate from formic acid.

The ^1H NMR spectrum of formic acid reacting with tris-(hydroxymethyl)aminomethane was obtained at 80 °C after 10 minutes reaction time at pH=9 on addition of an excess amount of tris(hydroxymethyl)aminomethane to formic acid DMSO-d_6 solution. The ^1H NMR spectrum is given in Fig. 2-3.

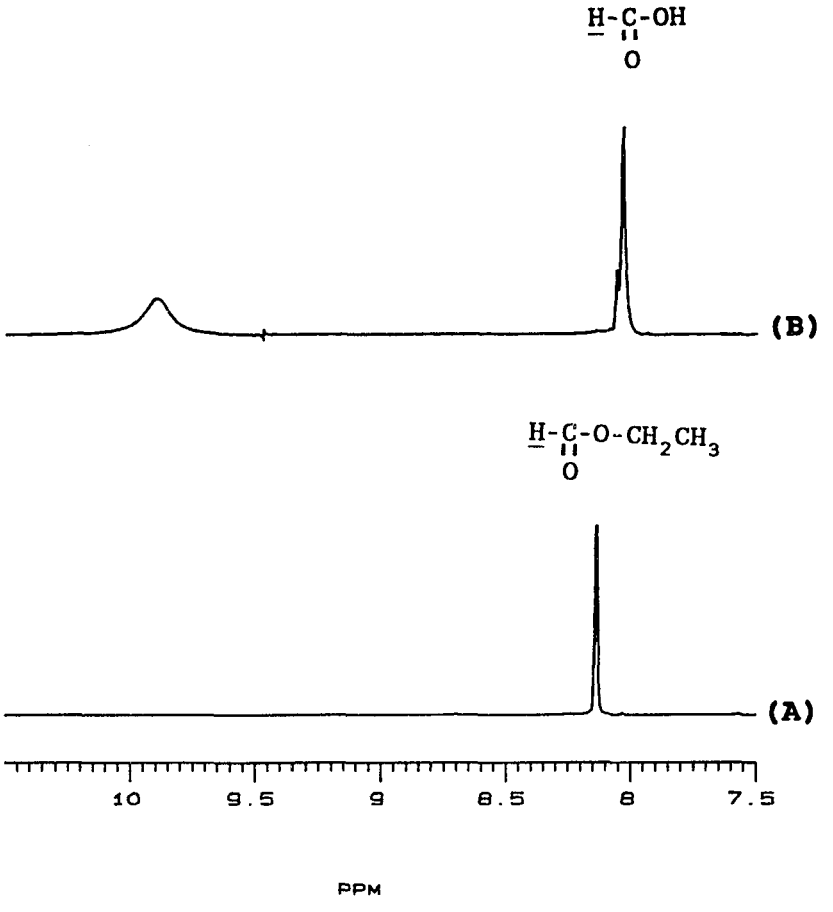

Fig. 2-2 ^{1}H NMR Spectra of (A) ethyl formate and (B) formic acid in DMSO-d_6 solution at 80 °C

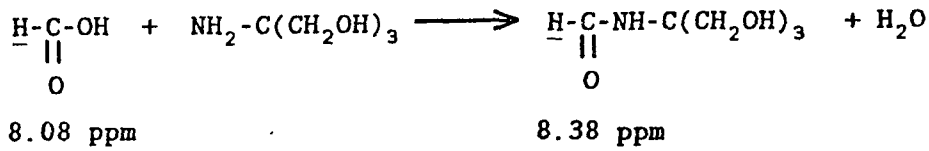

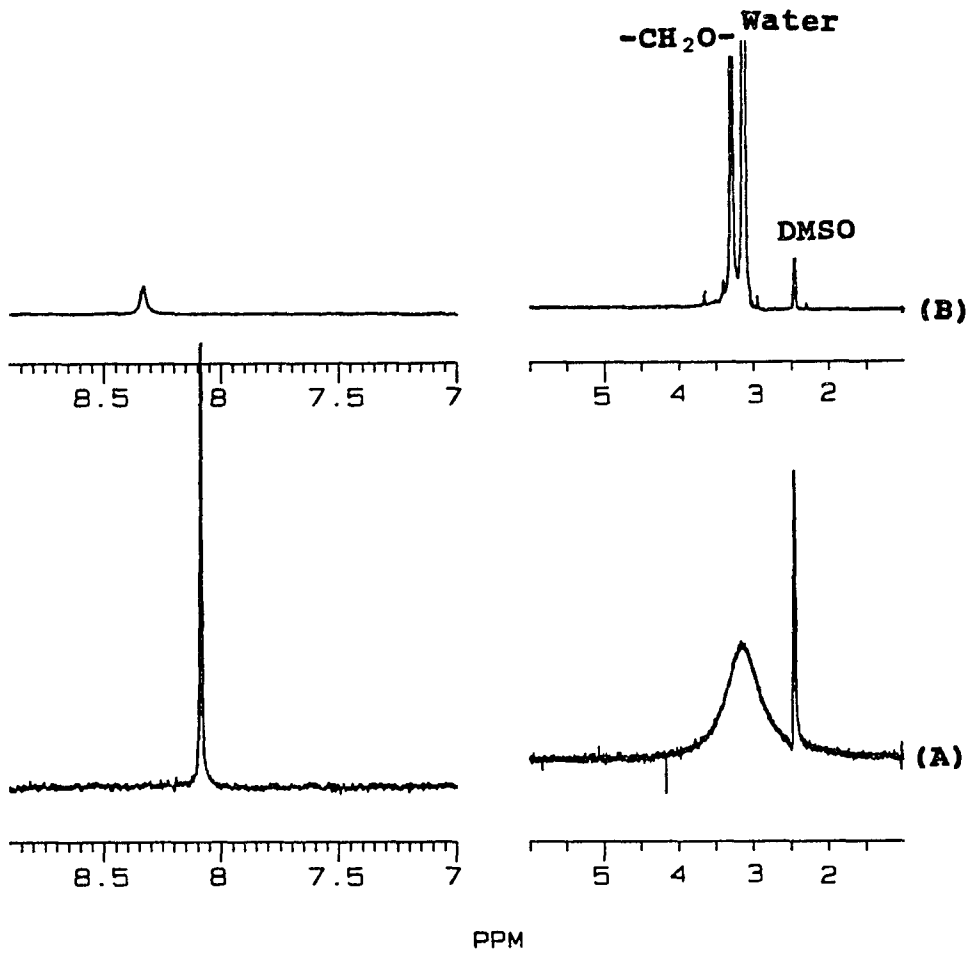

Fig. 2-3 ^{1}H NMR Spectra of formic acid in DMSO-d_6 at 80 °C
(A) before addition of tris(hydroxymethyl)aminomethane
(B) after addition of tris(hydroxymethyl)aminomethane

After 10 minutes reaction time on addition of tris-(hydroxymethyl)aminomethane, the peak at 8.08 ppm shifted to 8.38 ppm by the amino de-hydroxylation reaction, i.e. amide formation:

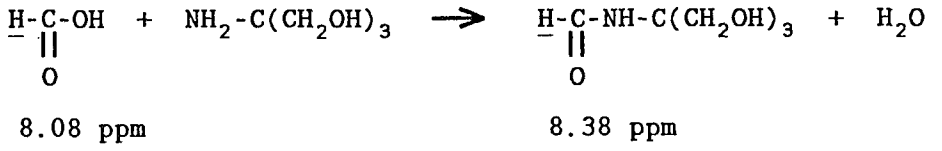

In the ^1H NMR spectrum (Fig. 2-4) of ethyl formate reacting with tris(hydroxymethyl)aminomethane, under the same reaction conditions as for formic acid reaction, the peak at 8.08 ppm was observed to remain unchanged.

^1H NMR spectrum of the degraded polymer solution at pH=9 was obtained at 120 °C after 10 minutes reaction time on addition of a sufficient amount of tris-(hydroxymethyl) -aminomethane. The ^1H NMR spectra of degraded polymer solutions before (Fig. 2-5 (A)) and after (Fig. 2-5 (B)) addition of tris-(hydroxymethyl)-amino methane show no effect on the peak at 8.08 ppm. Thus, the proton peak at 8.08 ppm is most likely due to the protons of formate end groups, O=C<u>H</u>-O-R.

iii. Free Acid and Hydroxyl Chain Ends

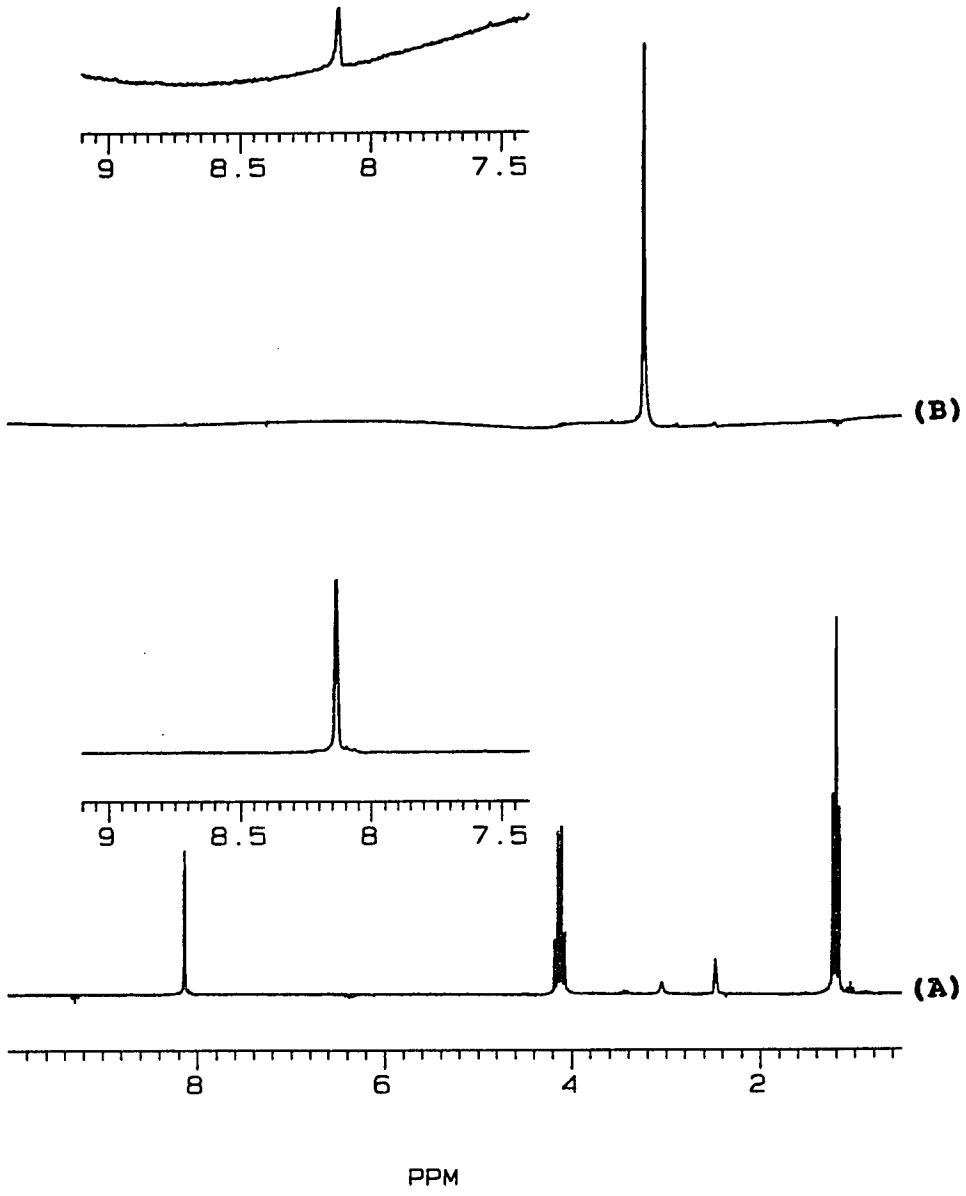

Fig. 2-4 ^{1}H NMR Spectra of ethyl formate in DMSO-d_6 solution at 80 °C. (A) before addition of tris(hydroxymethyl)aminomethane (B) after addition of tris(hydroxymethyl)aminomethane

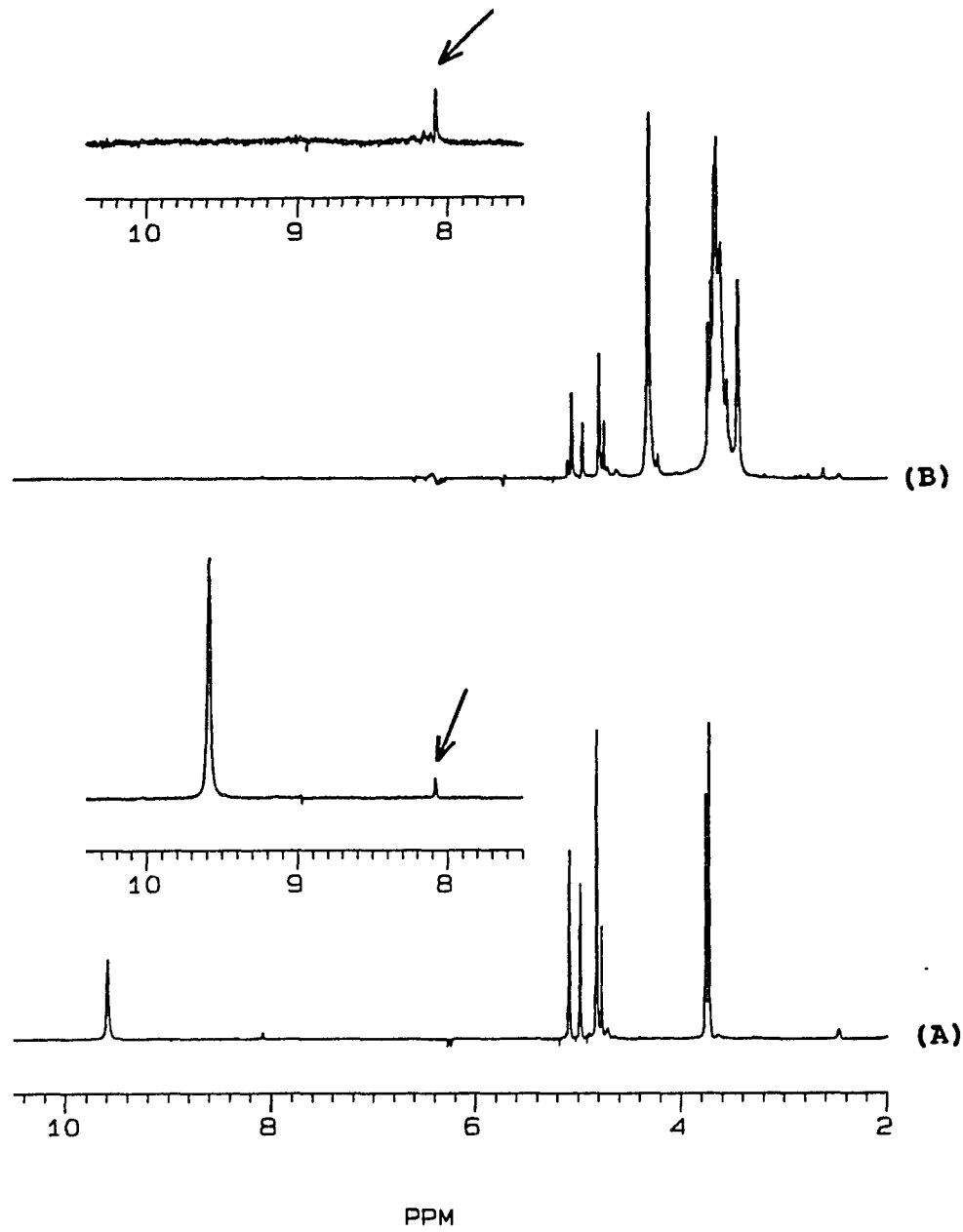

Fig. 2-5 ^{1}H NMR Spectra of the degraded TOX-DOL copolymer in DMSO-d_6 solution at 120 °C initiated by trifluoroacetic acid. (A) before addition of tris(hydroxymethyl)aminomethane (B) after addition of tris(hydroxymethyl)aminomethane

A broad peak further down field in the range of 12.7 ppm to 8.7 ppm (at 9.2 ppm in Fig. 2-1 (B)) may be due to exchangeable protons, oxonium ions, and hydroxyl end groups. This broad peak was always observed at low field region of ^1H NMR spectra from the initial stage of acidic degradation to the final stage. The peak was confirmed based on D_2O exchange experiment as well as the peak intensity of varing concentration of added acid as the degrading agent.

The ^1H NMR spectra in DMSO-d_6 at 120 °C before and after addition of 5 µl of D_2O (98 % deuterated, 9.2×10^{-2} M) are shown in Fig. 2-6 (A) and (B), respectively. The broad peak at 11.2 ppm disappeared through deuterium exchange. The broad peak at 9.6 ppm is probably due to reaction of formaldehyde with D_2O.

The effect of added acid on this broad peak was examined using two concentrations of trifluoroacetic acid and the relationship between solution acidity and the peak intensity was observed. For the initial concentration of trifluoroacetic acid at 2.4×10^{-2} M, the peak appeared at 9.2 ppm at 8 minutes reaction time, and then shifted to upfield at 8.8 ppm at 74 minutes, maintaining the same intensity throughout the whole degradation process (Fig. 2-7 (A)).

With the initial concentration of trifluoroacetic acid doubled to 4.8×10^{-2} M, the absorption at 12.6 ppm at 8

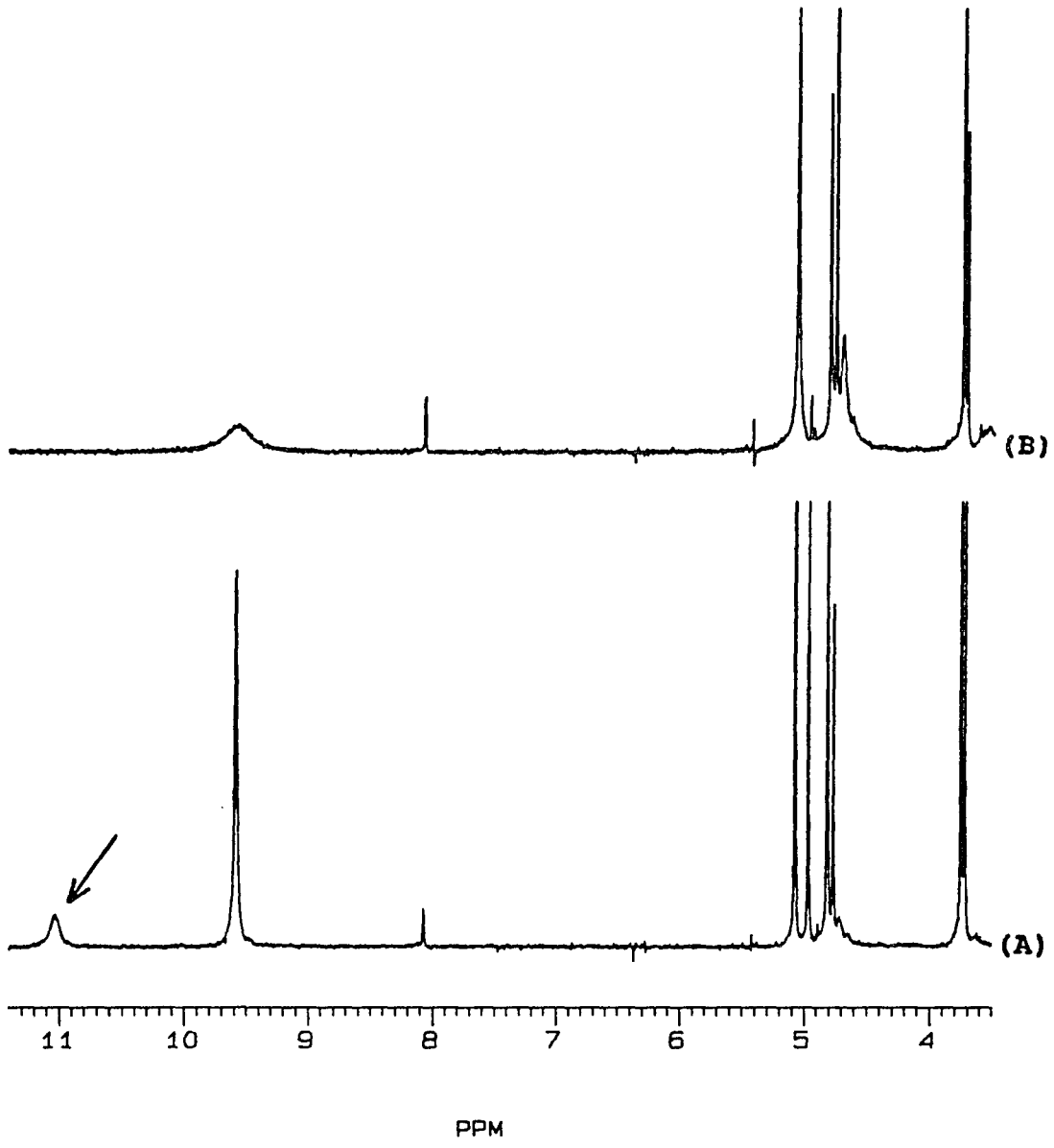

Fig. 2-6 ^{1}H NMR Spectra of degraded TOX-DOL copolymer in DMSO-d_6 solution at 120 °C initiated by addition of 2.4 X 10^{-2} M of trifluoroacetic acid. (A) before addition of D_2O (B) after addition of D_2O

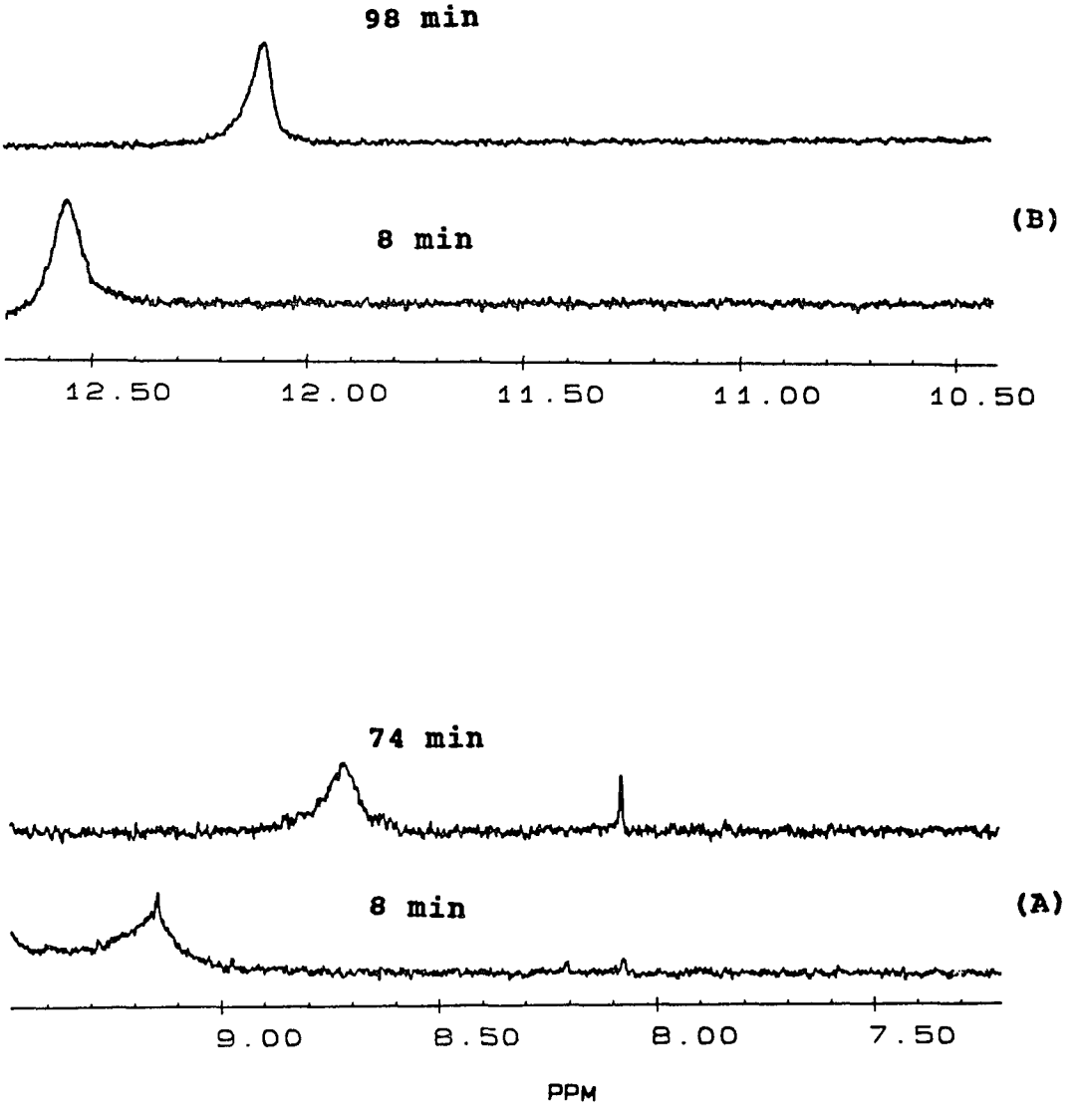

Fig. 2-7 Low field regions of ^{1}H NMR spectra for degraded TOX-DOL copolymer in DMSO-d_6 solution at 120 °C. (A) initiated by addition of 2.4 X 10^{-2} M of trifluoroacetic acid (B) initiated by addition of 4.8 X 10^{-2} M of trifluoroacetic acid

minutes and shifted to 12.1 ppm at 98 minutes (Fig. 2-7 (B)). The intensity was twice of that for the case using 2.4 x 10^{-2} M of trifluoroacetic acid. Thus, the intensity of the broad peak is proportional to the added acid concentration. In the initial stage of degradation process, the broad peak is mostly due to free acid from dissociation of trifluoroacetic acid. The free acid concentration calculated from the broad peak intensity agree with the added concentrations of trifluoroacetic acid within 10 %.

Based on an accepted general mechanism of acidic formal hydrolysis, the acidic hydrolysis of acetal polymer can be illustrated using the following Scheme 2-4 (6):

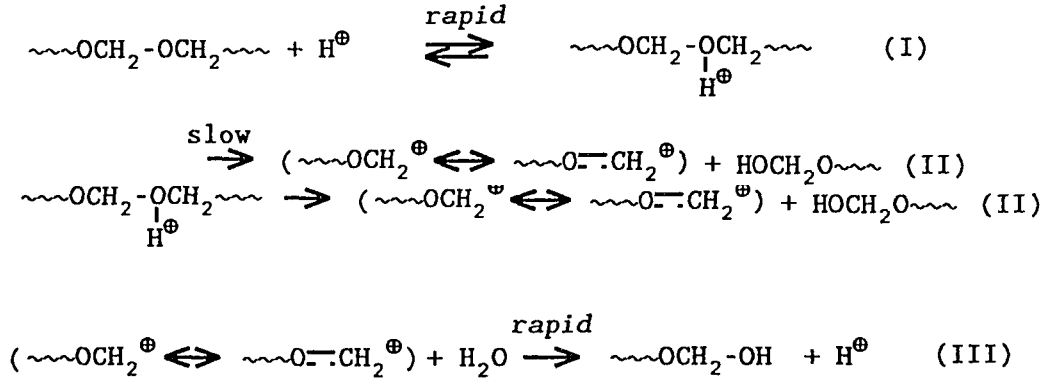

Scheme 2–4

The first step of the mechanism involves rapid proton hydrogen ion addition to oxygen in the polymer chain. The second is the rate determining step of the decomposition of the protonated polymer chain. The third step is a hydrolysis reaction. The second and third steps produce unstable hemiacetal chain ends. Each step in the mechanism involves exchangeable protons so that the amount of exchangeable protons does not change during the degradation process.

From the observations on the ^1H NMR spectra both from the D_2O exchange experiment and variation of added acidity, as well as the proposed general mechanism of acetal hydrolysis, it is suggested that the broad peak appearing at low field is due to exchangeable protons of acid, secondary oxonium ions and the hydroxyl end groups.

A similar broad peak has been observed in acidic polymerization of five-membered cyclic ethers (7). Pruckmayr and Wu claimed that a broad peak in the range of 16.6 ppm to 11.0 ppm is due to exchangeable protons of free acid, secondary oxonium ions, and hydroxyl end groups. The mechanism has been illustrated as follows:

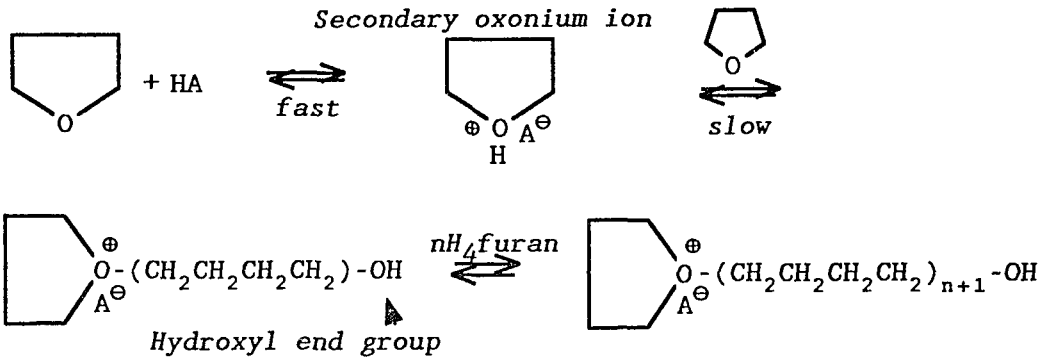

They used the peak to monitor the progress of the polymerization.

(b) ^{1}H NMR Analysis of Degradation Products and Degraded Chain Sequences

The kinetic variation of the degradation products in three experiments are profiled in Figures 2-8, 2-9 and 2-10. The general trends for each product from different runs agree with one another reasonably well. Formaldehyde reached a maximum concentration in the range of 0.057 ~ 0.07 (mol/L) within 15 minutes. The degradation process is divided into the two stages: i) the early stage where the concentrations of all the degradation products increase with time except formaldehyde, and ii) the later stage where the concentrations of TEX and TOP decrease slowly but the concentrations of TOX, DOL, and formate end groups increase.

Fig. 2-8 Kinetics of products formed during acidic degradation of TOX-DOL copolymer

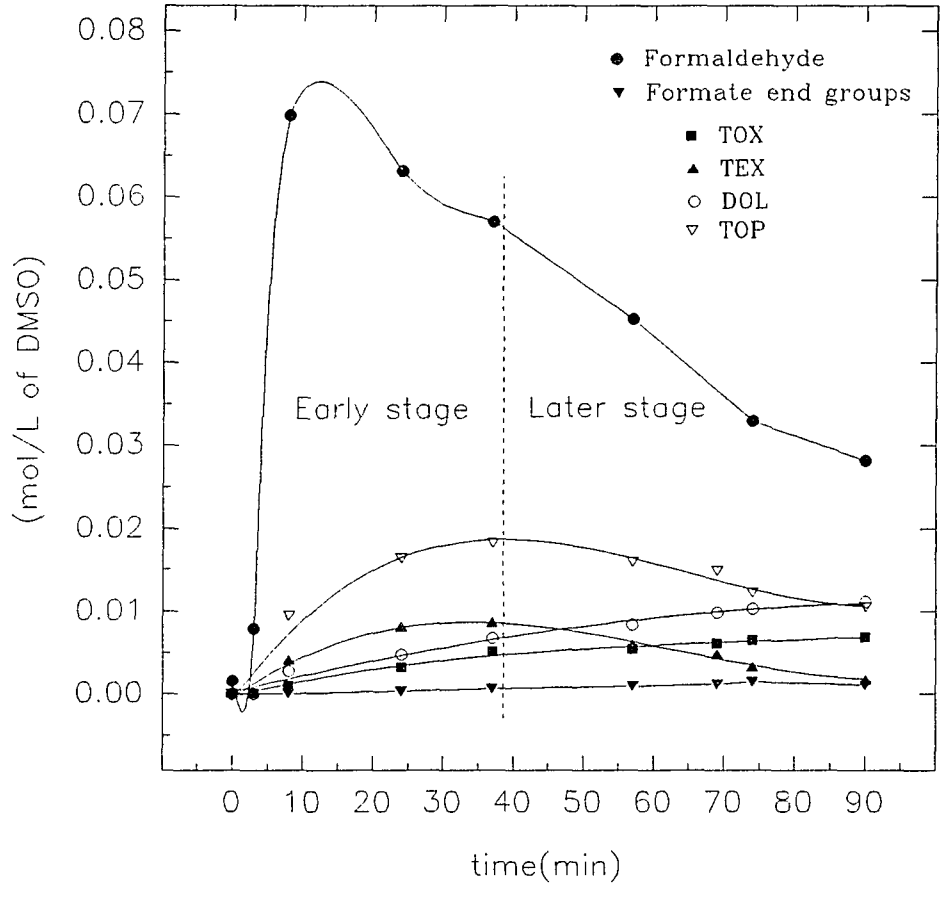

Initiated by CF_3COOH at 2.4 x 10^{-2} (mol/L)

Fig. 2-9 Kinetics of products formed during acidic degradation of TOX-DOL copolymer

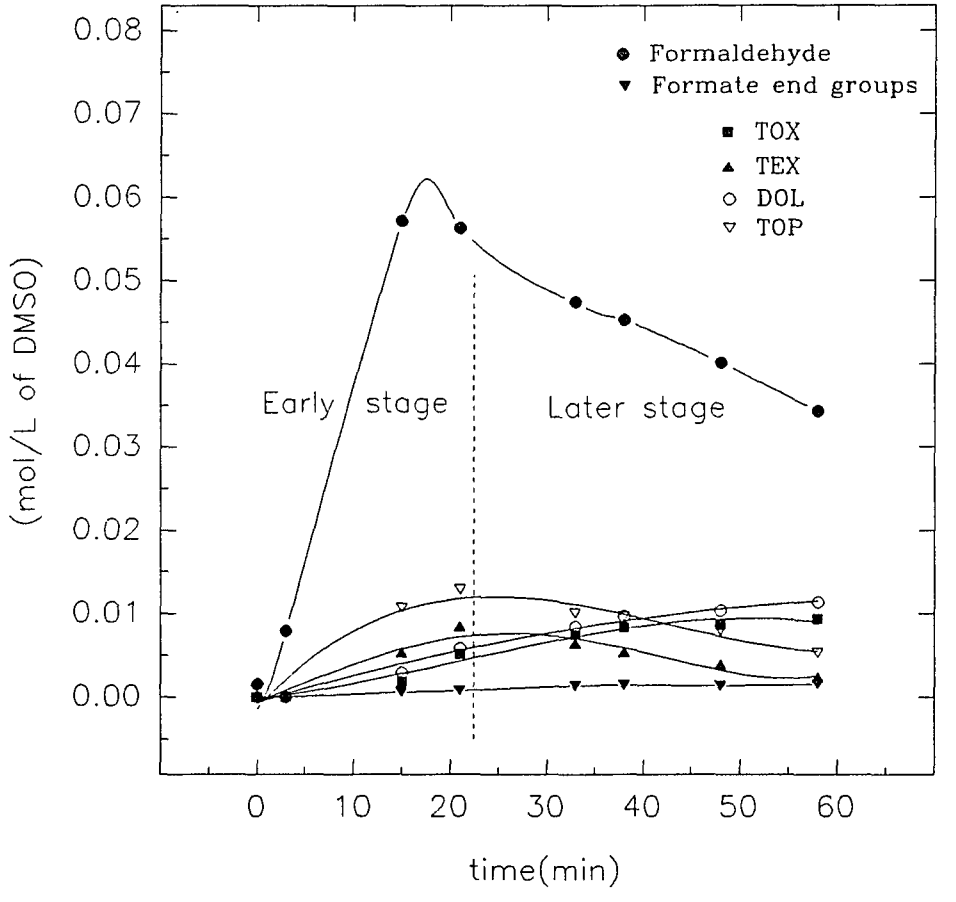

Initiated by CF_3COOH at 2.4 x 10^{-2} (mol/L)

Fig. 2-10 Kinetics of products formed during acidic degradation of TOX-DOL copolymer

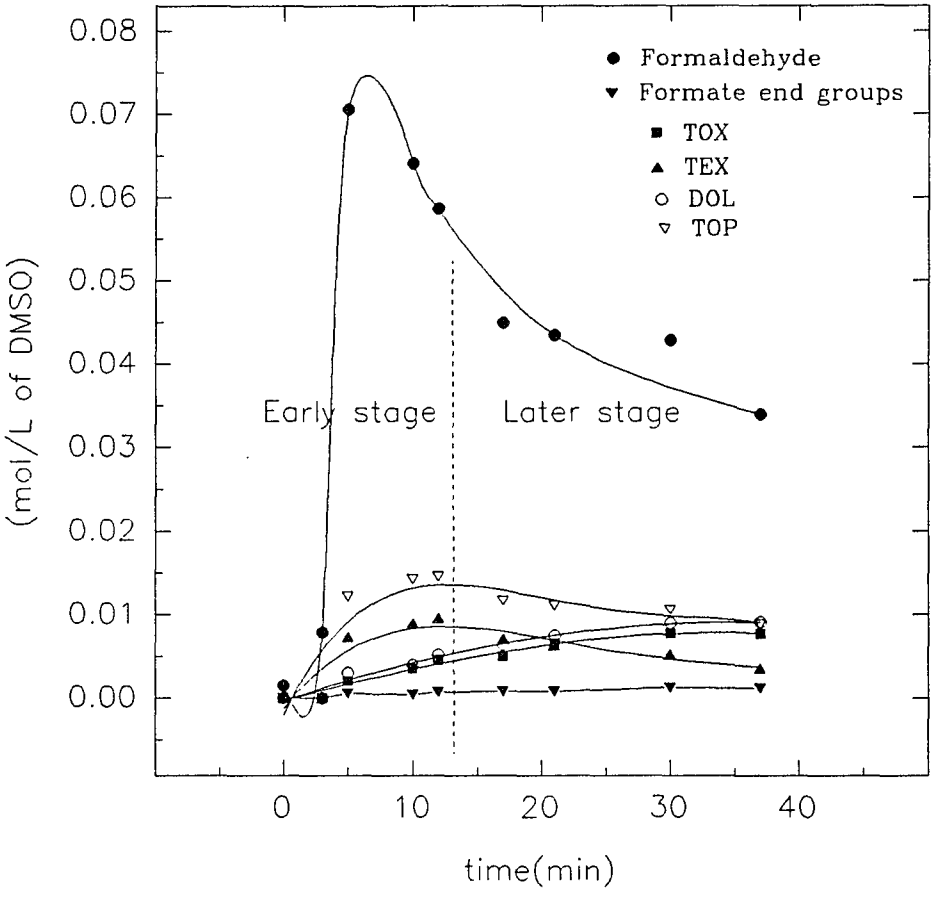

Initiated by CF_3COOH at 2.4 x 10^{-2} (mol/L)

At the early stage, the yields of the degradation products increase in the following order: formate end groups < TOX < DOL < TEX < TOP < formaldehyde. The formation rate of TOP was much higher than TEX and, similarly, DOL higher than TOX (Fig. 2-11). This may be explained by faster β scission of methylene oxide units than the backbiting reaction. The phenomena observed in the later stage of degradation process can be explained by equilibria between TEX with TOX, and TOP and DOL. It will be discussed later (section 2.3.1.(c) iii).

Intensities of the proton peaks for the degradation products were measured and analyzed to determine the amounts quantitatively. The value of each peak was determined by its intensity relative to the absolute intensity of DMSO-d_6 solvent peak. The peak intensity for TOX and TEX from methylene oxide (2 H's), and DOL and TOP from ethylene oxide (4 H's) were used in the analysis. The degradation products were calculated in molar concentration (mol/L of DMSO solution). A set of data for yields of the degradation products is presented in Table 2-1. At 8 minutes, the rate of formations for formaldehyde and cyclic acetals were calculated. The determined values indicate that formaldehyde is generated at least ten times faster than cyclic acetals.

An enlarged ^{1}H NMR spectrum of Fig. 2-1 is shown in Fig. 2-12 for closer examination in the particular regions

Fig. 2-11 Kinetics of cyclic acetals formed during acidic degradation of TOX-DOL copolymer at the early stage

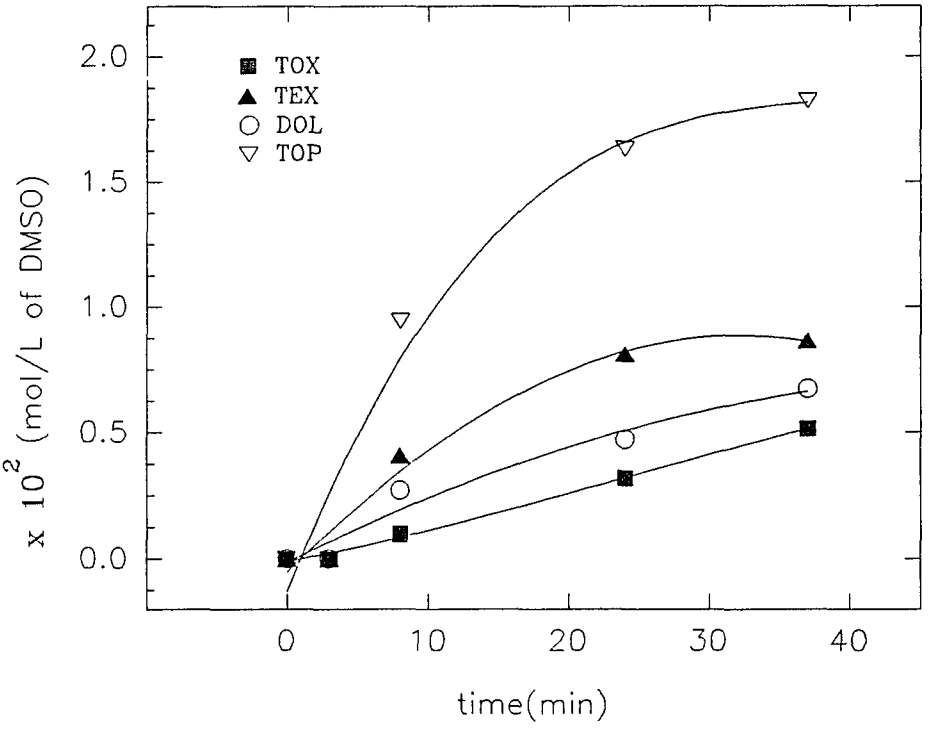

Initiated by CF_3COOH at 2.4 x 10^{-2} (mol/L)

Table 2-1 Yields of products formed during acidic degradation of TOX-DOL copolymer initiated by trifluoroacetic acid at 2.4 x 10^{-2} (mole/L of DMSO)

x 10^{2} (mol/L)

time (min)	[FD]	[FT]	[TOX]	[TEX]	[DOL]	[TOP]	[MX]
0	0.15	0.00	0.00	0.00	0.00	0.00	0.21
3	0.79	0.00	0.00	0.00	0.00	0.00	0.16
*8	6.98	0.00	0.10	0.41	0.27	0.94	0.21
24	6.32	0.03	0.32	0.81	0.47	1.63	0.13
37	5.70	0.06	0.51	0.87	0.67	1.82	0.10
57	4.52	0.09	0.54	0.59	0.84	1.59	0.21
69	4.13	0.11	0.61	0.48	0.98	1.48	0.11
74	3.29	0.14	0.65	0.33	1.03	1.22	0.17
90	2.81	0.10	0.69	0.17	1.11	1.05	0.13

[FD] = Formaldehyde [FT] = Formate end groups

[MX] = Methoxy end groups

* Rate of formaldehyde formation at 8 min.= (6.98 x 10^{-2}) M/ (8 x 60) sec

= 1.5 x 10^{-4} (M/sec)

Rate of cyclic acetals formation at 8 min = (0.1 + 0.41 + 0.27 + 0.94) x 10^{-2} M / (8x 60) sec = 3.6 x 10^{-5} (M/sec)

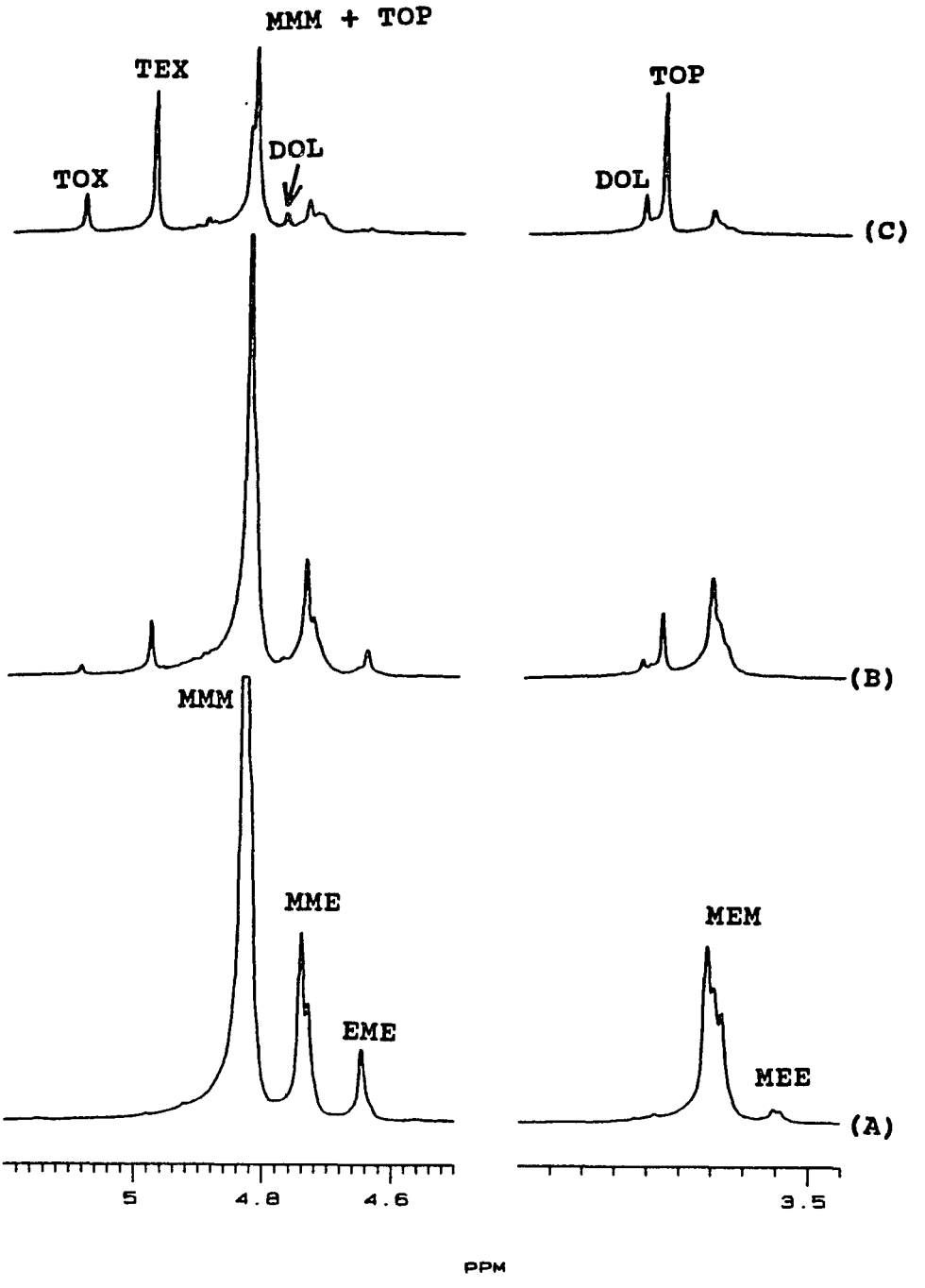

Fig. 2-12 Methylene oxide and ethylene oxide regions for ^{1}H NMR spectra of degraded TOX-DOL copolymer initiated by trifluoroacetic acid at 2.4 X 10^{-2} M. (A) before addition of trifluoroacetic acid (B) 8 min (C) 24 min after addition of trifluoroacetic acid

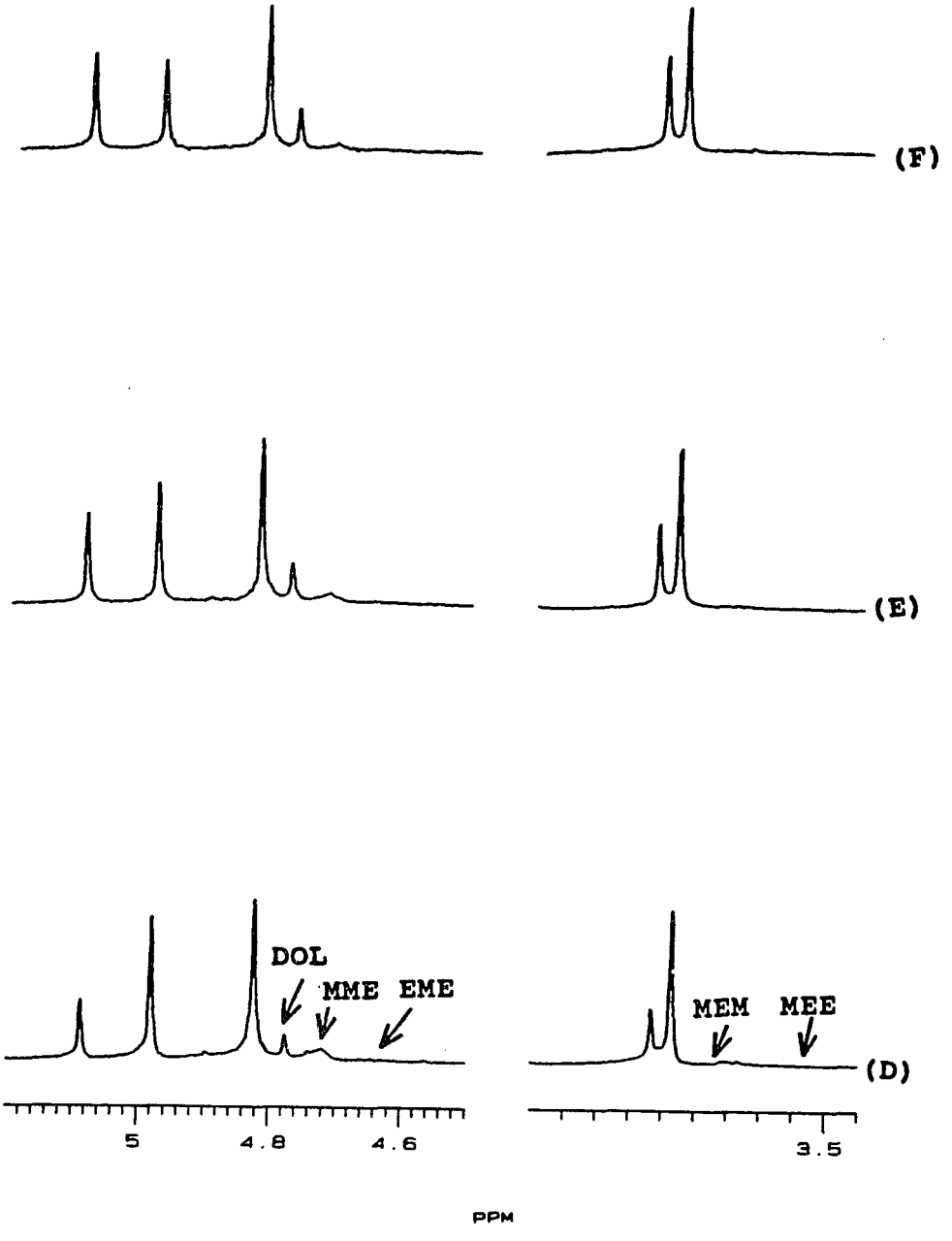

Fig. 2-12 Methylene oxide and ethylene oxide regions for ^{1}H NMR spectra of degraded TOX-DOL copolymer initiated by addition of trifluoroacetic acid at 2.4 X 10^{-2} M. (D) 37 min (E) 54 min (F) 69 min after addition of trifluoroacetic acid

of interest. The three peaks for the methylene oxide units (M) and the two peaks for the ethylene oxide units (E) were observed for different triad sequences of TOX-DOL copolymer chain (Fig. 2-12 (A)).

The microstructure of TOX-DOL copolymer have been investigated by several researchers. Yamashita et al., reported the chemical shift values of three kinds of methylene oxide centered triad sequences and one ethylene oxide which were obtained from the ^{1}H NMR spectra at 60°C in chloroform (8). The chemical shift values were reported as follows: MMM at 4.88 ppm, MME at 4.80 ppm, EME at 4.73 ppm and E at 3.73 ppm. A typical ^{1}H NMR spectrum showing five triad structures with their assignments have been presented by Ishigaki et al. (9). Three triad sequences of methylene oxide units and two triad sequences of ethylene oxide units were assigned by Flescher and Schulz from the ^{1}H NMR spectrum of TOX-DOL copolymer in chloroform solution (10). The ^{1}H NMR chemical shift values of triads reported by Flescher and Schulz and our values in the present degradation study are shown in Scheme 2-5.

The peak of MMM sequence at 4.83 ppm overlaps with methylene oxide peak of TOP at 4.82 ppm and they could not be separated by peak deconvolution. The peak intensity of 4 H's of methylene oxide with 4 H's of ethylene oxide in TOP

Triad structures	*Chemical shifts (δ)*	
	(in $CDCl_3$)	*(in DMSO-d_6)*
~~CH_2O-$\underline{CH_2O}$-CH_2O~~~ MMM	*4.89 ppm*	*4.82 ppm*
~~CH_2O-$\underline{CH_2O}$-CH_2CH_2O~~~ MME	*4.83 ppm*	*4.73 ppm*
~~CH_2CH_2O-$\underline{CH_2O}$-CH_2CH_2O~~~ EME	*4.77 ppm*	*4.64 ppm*
~~CH_2O-$\underline{CH_2CH_2O}$-CH_2O~~~ MEM	*3.73 ppm*	*3.75 ppm*
~~CH_2O-$\underline{CH_2CH_2O}$-CH_2CH_2O~~~ MEE	*3.68 ppm*	*3.54 ppm*

Scheme 2–5

should be same. Therefore the peak intensity for MMM sequence was obtained by subtracting the intensity of 4 H's of ethylene oxide units of TOP from the intensity of overlapped peaks.

The molar concentrations of triad sequences during the course of degradation are calculated and summarized in Table 2-2. The fraction of these peaks remaining was obtained as a function of reaction time (Fig. 2-13). As shown in Table 2-2, for methylene oxide units, the peak due to EME vanished before MME and MMM. The peaks due to MEE of ethylene oxide

Table 2-2 Concentrations for triad sequences of TOX-DOL copolymer during acidic degradation initiated by trifluoroacetic acid at 2.4 x 10^{-2} (mole/L of DMSO)

x 10^{1} (mol/L)

time (min)	Methylene oxide units			Ethylene oxide units	
	[MMM]	[MME]	[EME]	[MEM]	[MEE]
0	3.365	0.850	0.265	0.381	0.029
8	1.654	0.484	0.099	0.266	0
24	0.474	0.210	0.045	0.077	
37	0.178	0.105	0	0.031	
52	0.071	0.096		0	
69	0.049	0.046			
74	0.046	0.034			
90	0.043	0.016			
116	0	0			

Temperature = 120 °C

Concentration of methylene oxide = 0.45 (mol/L)

Concentration of ethylene oxide = 0.04 (mol/L)

Fig. 2-13 Fractional consumption for triad sequences of TOX-DOL copolymer during acidic degradation

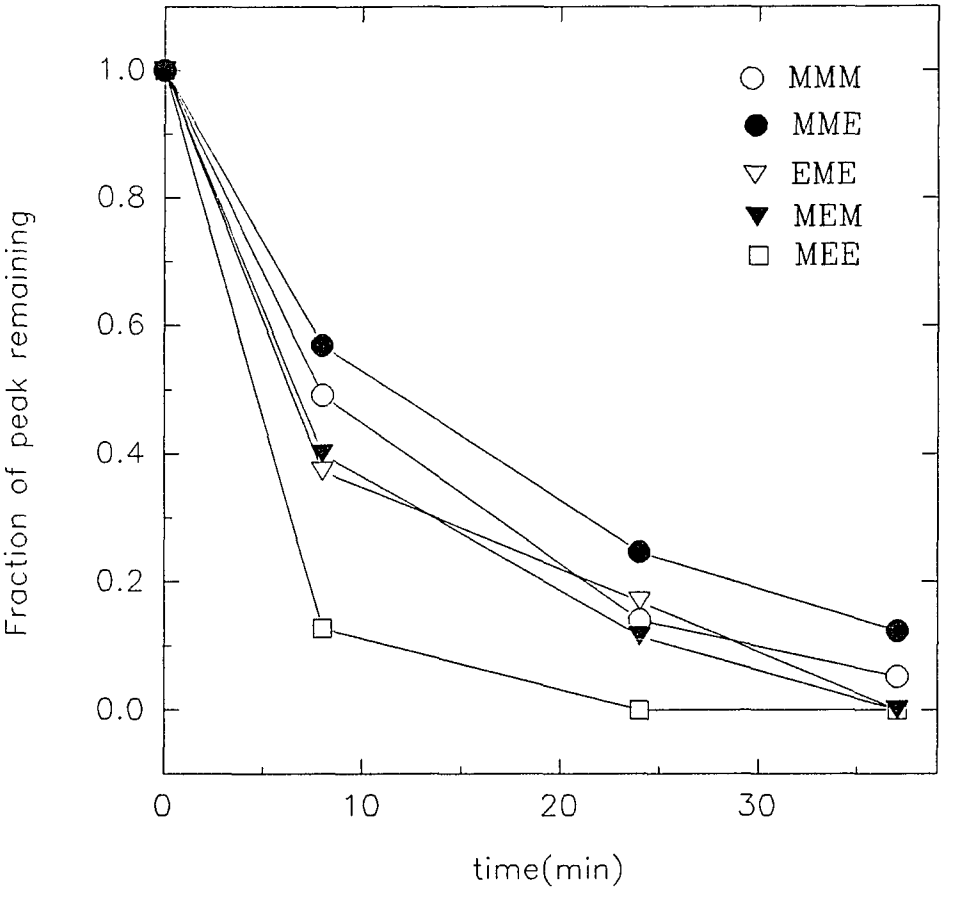

Initiated by CF_3COOH at 2.4 x 10^{-2} (mol/L)

units appeared to be very reactive in the degradation process, showing a 90 % of degradation within 8 minutes (Fig. 2-13). At the same span of time, the peaks due to EME and MEM showed only about 62 % and 60 % degradation, respectively.

These results indicate that the oxygen atom connected to ethylene units are highly susceptible to acid attack. Therefore it is concluded that the main repeat units ($-CH_2O-$) next to ethylene oxide units ($-CH_2CH_2O-$) are most unstable in the acidic degradation.

(c) Degradation Mechanism

From the ^1H NMR observations on kinetic behaviors of degraded copolymer sequences and the degradation products, a degradation mechanism of TOX-DOL copolymer in acidic solution can be proposed. This mechanism involves three areas of consideration: i. β-scission and backbiting reactions; ii. hydride transfer reaction; iii. equilibria between TEX and TOX, and between TOP and DOL.

i. β-Scission and Backbiting Reactions

The initiation of acidic degradation of TOX-DOL copolymer involves protonation of both symmetrical sites and nonsymmetrical sites. The initiation starting at symmetrical sites proceeds as follows:

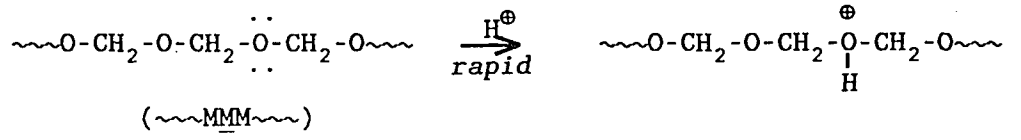

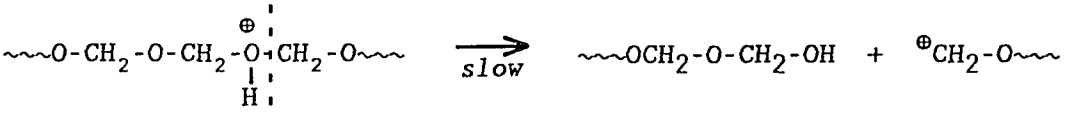

Protonation and decomposition of the resulting macrocation yields unstable hemiacetal, ~~~OCH_2OH, and $\oplus CH_2$-O~~~, cationic chain end.

For nonsymmetrical sites, which connect methylene oxide and ethylene oxide, two different types of chain cleavage are possible: (Scheme 2-6). The oxygens located at between methylene and ethylene are more nucleophilic toward hydrogen ion than the oxygen connecting two methylene units. Therefore, protonation on more nucleophilic oxygens of unsymmetrical sites are favored over oxygens of symmetrical sites. Experimental results show faster initial degradation rate of the E units than M units (Fig. 2-14).

In the chain cleavage step following the protonation, the following reactions are possible: bond scission of C-O

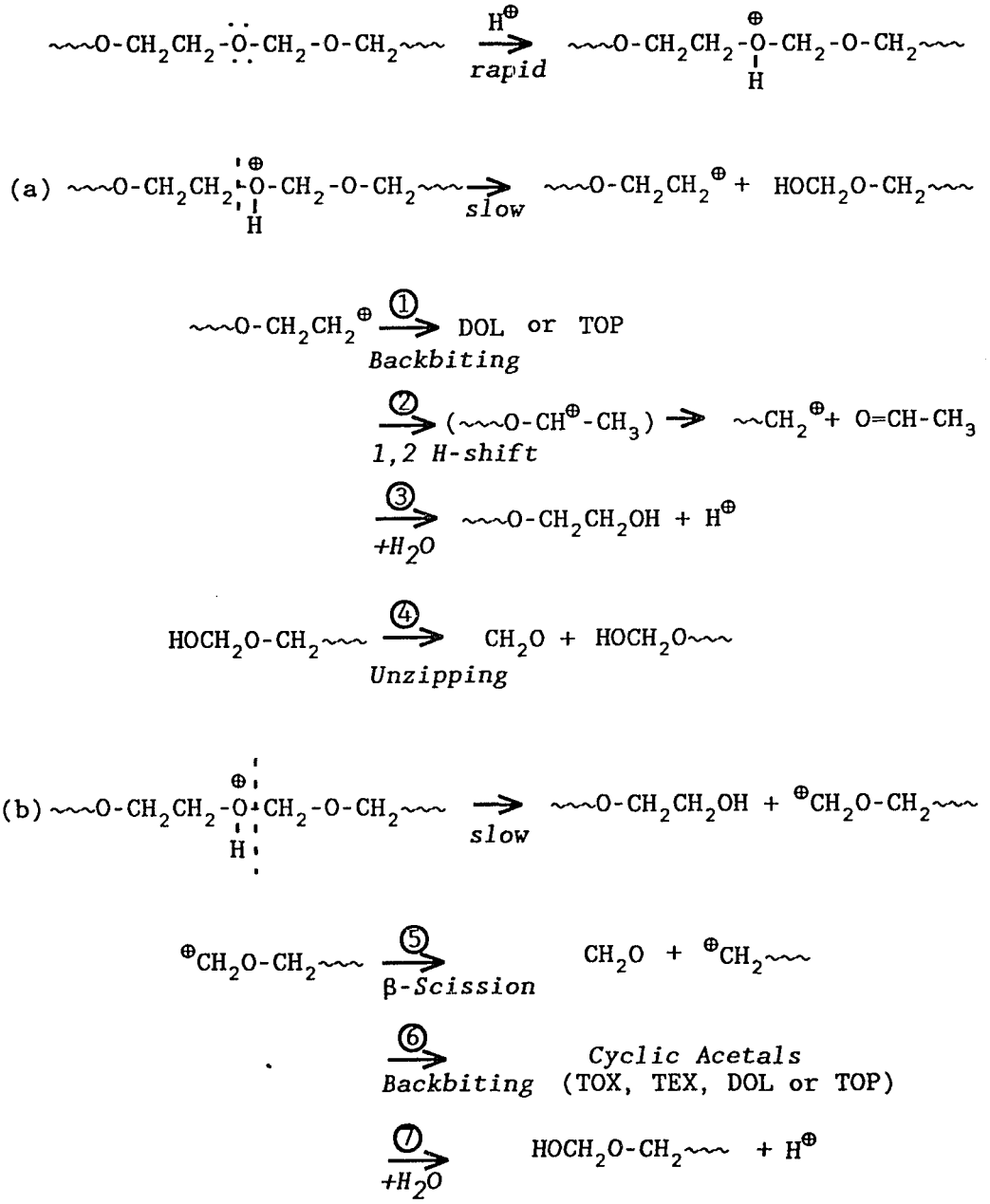
~~O-CH2CH2-O-CH2-O-CH2~~
H⊕
rapid
~~O-CH2CH2-O(H)-CH2-O-CH2~~
(a)
slow
~~O-CH2CH2⊕ + HOCH2O-CH2~~
~~O-CH2CH2⊕
①
DOL or TOP
Backbiting
②
(~~O-CH⊕-CH3)
~~CH2⊕+ O=CH-CH3
1,2 H-shift
③
~~O-CH2CH2OH + H⊕
+H2O
HOCH2O-CH2~~
④
CH2O + HOCH2O~~
Unzipping
(b)
slow
~~O-CH2CH2OH + ⊕CH2O-CH2~~
⊕CH2O-CH2~~
⑤
CH2O + ⊕CH2~~
β-Scission
⑥
Cyclic Acetals
Backbiting
(TOX, TEX, DOL or TOP)
⑦
HOCH2O-CH2~~ + H⊕
+H2O

Scheme 2–6

Fig. 2-14 Fractional consumption for M and E units of TOX-DOL copolymer during acidic degradation

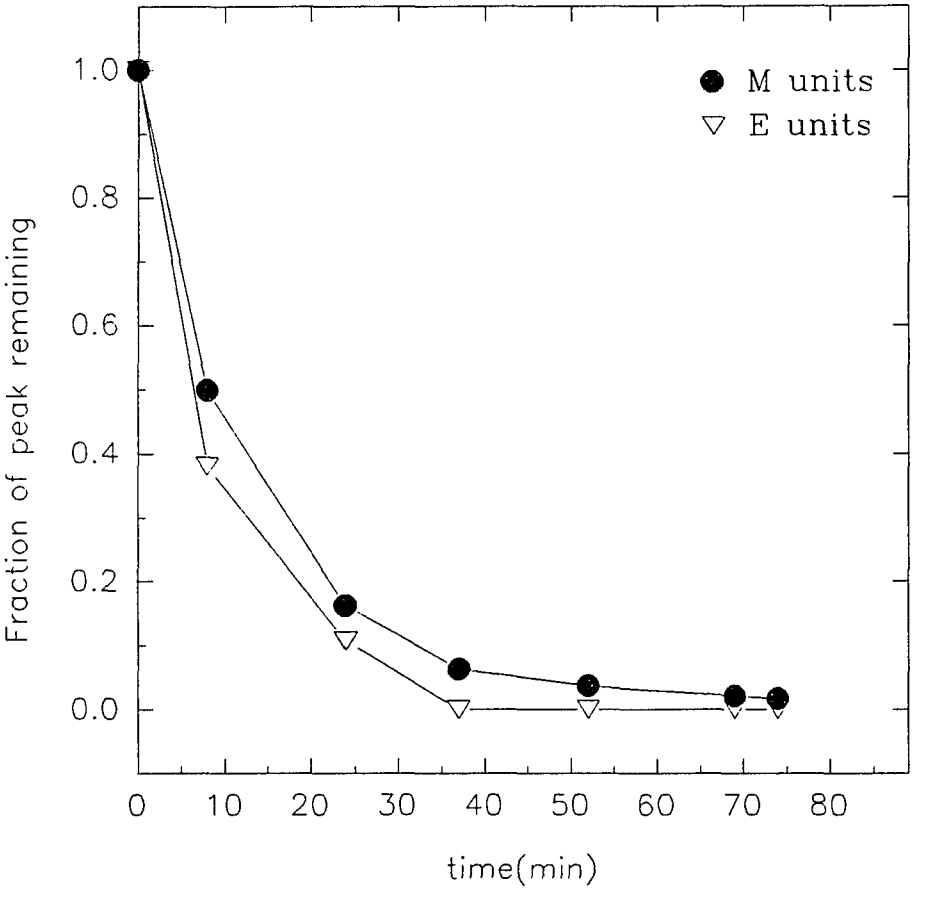

Initiated by CF_3COOH at 2.4 x 10^{-2} (mol/L)

reaction in (a) or (b). Reaction (a) yields a chain end, ~~~$OCH_2CH_2^{\oplus}$, and a chain with an unstable hemiacetal end, $HOCH_2OCH_2$~~~. The chain end, ~~~$OCH_2CH_2^{\oplus}$ may form DOL or TOP through the backbiting: ① . The formation of DOL or TOP by backbiting reactions is illustrated as follows:

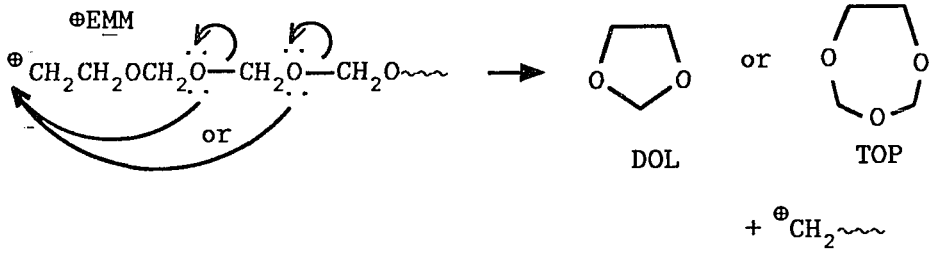

Other route of TOP formation have been reported in the literature. For example, TOP has been considered as being formed from the interaction of DOL with TOX in the presence of acid in the electro-initiated copolymerization of 1,3-dioxolane with trioxane (11). The mechanism involving formaldehyde insertion is shown below.

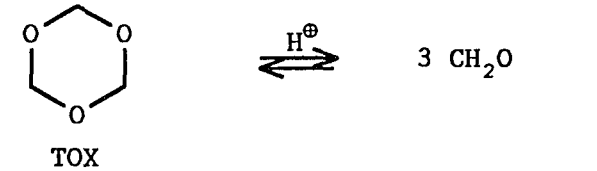

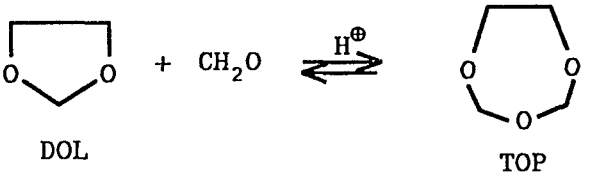

The stoichiometry for formation of TOP was obtained from the

slope of kinetic plots for TOX and DOL consumptions during the copolymerization at 10 minutes reaction in following rate: $-d[DOL]/dt\ -(1/3)d[TOX]/dt \rightarrow d[TOP]/dt$ (11).

In the early stage of TOX-DOL copolymer degradation initiated by trifluoroacetic acid, (Fig. 2-1 (B)), TOP always appears with faster initial rate than TOX and DOL.

However the chain end, $\sim\sim\sim OCH_2CH_2^{\oplus}$, may undergo 1,2 hydride shift to form secondary macro cations, $\sim\sim\sim OCH^{\oplus}\text{-}CH_3$, i.e. ② or displace hydrogen ion from H_2O and form chain end $\sim\sim\sim OCH_2CH_2OH$, i.e. ③ . 1,2 Hydride shift reaction can lead to the formation of acetaldehyde and a cationic chain end. The formation of acetaldehyde was confirmed by an absorption peak due to CH_3 group at 2.0 ppm. Thus, these ionic reactions are considered to compete with the backbiting reaction and may disturb the formation of DOL or TOP.

Concurrently, a polymer chain with the hemiacetal chain ends, $HOCH_2OCH_2\sim\sim\sim$, formed from reaction (a), continues to degrade by releasing formaldehyde through unzipping process, i.e. ④.

In reaction (b) of Scheme 2-6, the bond scission of C-O leads to a polymer chain with a stable chain end,

~~~OCH_2CH_2OH, and a cationic chain end, $\oplus CH_2OCH_2$~~~. The cationic chain end, $\oplus CH_2OCH_2$~~~, continues to release formaldehyde through β-scission reaction, i.e. ⑤ , or undergo backbiting reaction to produce TOX, TEX, DOL or TOP, i.e. ⑥ . Trioxane or TEX can be formed from the backbiting reaction of the cationic chain end with the sequences of MMM⊕ and MMMM⊕. Dioxolane and TOP are formed from the chain end with EM⊕, and MME⊕ or EMM⊕, respectively. In the presence of water, the cationic chain end, $\oplus CH_2OCH_2$~~~, may displace a hydrogen ion from H_2O and form a hemiacetal chain end, $HOCH_2OCH_2$~~~, i.e. ⑦ . Water at low concentration in the system compared to $\oplus CH_2OCH_2$~~~ should not disturb significantly the β-scission and the backbiting reactions.

Highly favored β-scission, i.e. ⑤ , over backbiting, i.e. ⑥ , of $\oplus CH_2OCH_2$~~~, results in considerably lower concentrations of cyclic acetals compared with formaldehyde at the onset of degradation.

A set of typical experimental data for the yields of formaldehyde and cyclic acetals in the initial stage of the degradation (at 8 min) is shown in Table 2-1. The rates of reactions for β-scission ($R_{\beta-s}$) and backbiting (R_B) were calculated to have the values of 1.5×10^{-4} (M/sec) and 3.6×10^{-5} (M/sec) respectively, i.e. β-scission reaction is faster by a factor of four.
~~~

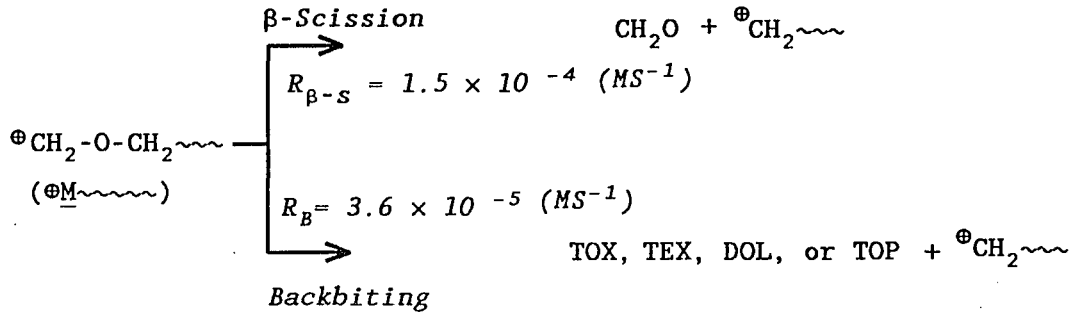

From this relative value of rate of reactions, the difference of free energy of activation between two reactions can be calculated by an Arrhenius equation:

$$R_{\beta-s} / R_B \cong \frac{e^{-\Delta G^{\neq}_{\beta-s} / RT}}{e^{-\Delta G^{\neq}_{B} / RT}}$$

where $\Delta G^{\neq}_{\beta-s}$ and $\Delta G^{\neq}_{B}$ are the free energy of activation of β-scission reaction and backbiting reaction respectively. The calculated free energy of activation for backbiting reaction is about 4.5 kJ higher than that of β-scission reaction.

The free energy change of two reactions were compared based on estimated enthalpy changes from bond dissociation energies, and the expected entropy changes. In backbiting reaction, estimated enthalpy change is zero based on the assumption of zero strain in the six-membered ring of TOX:

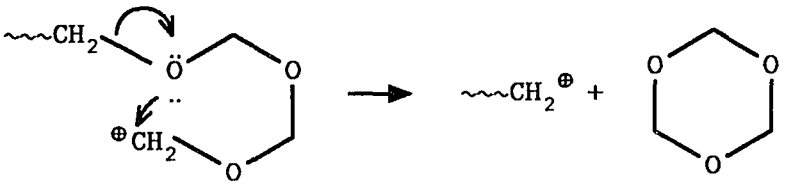

Make C-O σ bond $\Delta H = -351$ *(kJ/mol)*

Break C-O σ bond $\Delta H = +351$ *(kJ/mol)*

$\Delta H = 0$

And favorable entropy change is expected to be associated with the gain of a degree of freedom by the degraded chain upon cleavage to TOX and a chain with shorter length. Therefore backbiting reaction is expected to have negative free energy change ($-\Delta G$) due to favorable change of entropy.

For β-scission reaction, the favorable entropy change is expected to be a little higher than that of the backbiting reaction due to formation of a small molecule, formaldehyde, and a negative enthalpy change is estimated upon break of C-O σ bond and formation of stronger C=O bond (12):

Making C=O from C-O $\Delta H = -(745-351)$ *(kJ/mol)*

Break C-O σ bond $\Delta H = +351$ *(kJ/mol)*

$\Delta H = -43$ *(kJ/mol)*

Δ H for the process was calculated by subtracting bond energy values of C-O σ single bond (351 kJ/mol) from that of

formation of C=O double bond from C-O (394 kJ/mol). Since contribution of entropy is less than that from enthalpy, the free energy change of two reactions mainly are determined by enthalpy term. Therefore the free energy change of β-scission reaction is more negative than that of backbiting reaction. The energy diagram of these reactions are illustrated in Scheme 2-7.

Based on the calculations of activation free energy of transition states and the examinations of enthalpies, it is concluded that β-scission reaction with lower activation free energy and larger negative free energy change (ΔG) is favored over backbiting reaction. Even though the concentration of degraded polymer chain with the sequence of MMM⊕ is higher than those with the end sequence of EME⊕ or MEM⊕, backbiting reaction of the end sequence of MMM⊕ should be suppressed by the highly favored β-scission reaction. Experimental result showed that in the early stage of degradation, the yield of TOX is lower than that of DOL, and TEX is lower than that of TOP. (Fig. 2-11)

In summary, acidic degradation of TOX-DOL acetal copolymer in solution is initiated as follows:
1. Protonation of oxygen take place preferentially at nonsymmetrical sites, leading to a faster degradation of E

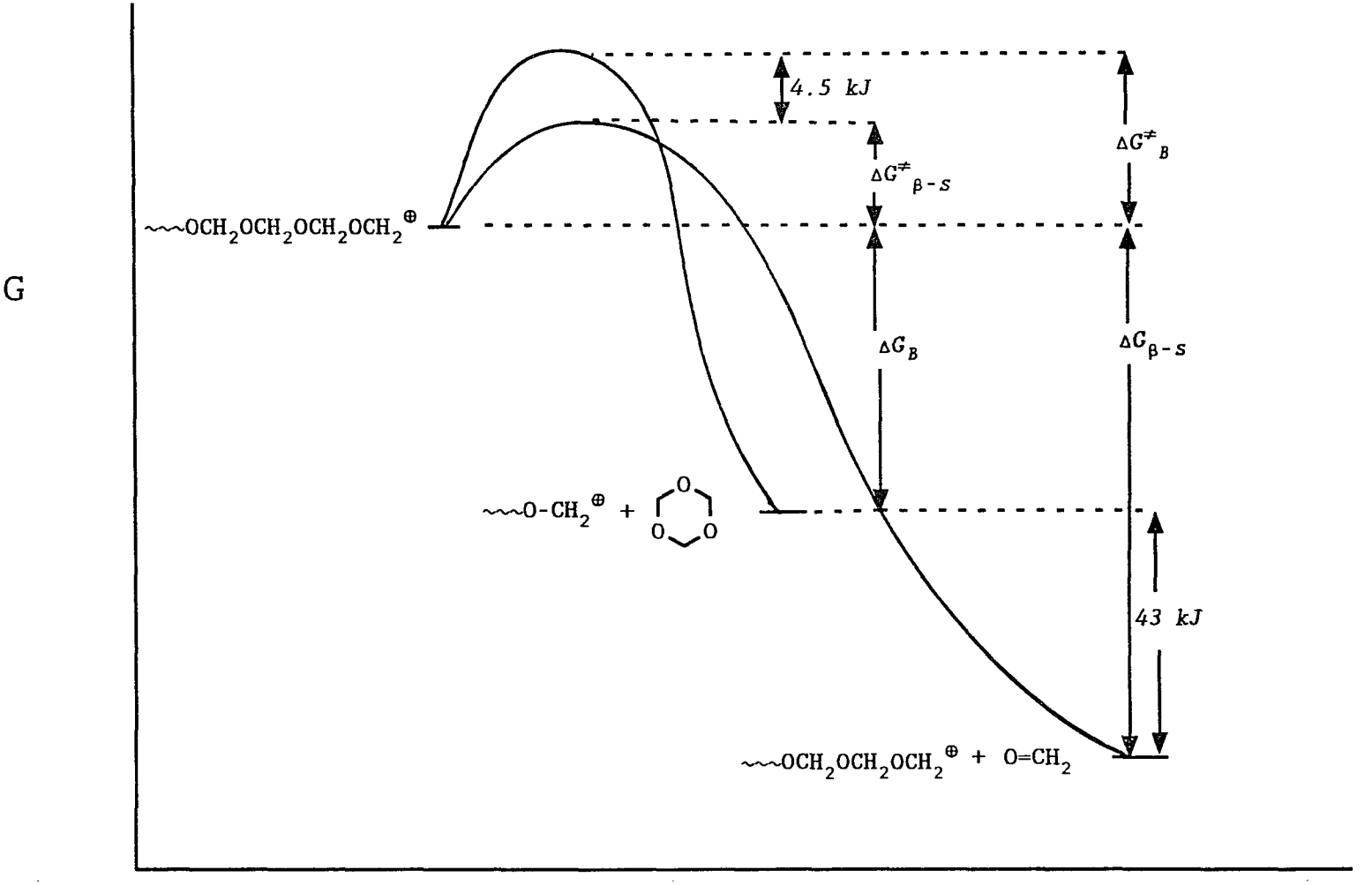
G
4.5 kJ
$\Delta G^{\neq}_{B}$
$\Delta G^{\neq}_{\beta-s}$
~~OCH2OCH2OCH2OCH2⊕
ΔG_{B}
$\Delta G_{\beta-s}$
~~O-CH2⊕ +
43 kJ
~~OCH2OCH2OCH2⊕ + O=CH2
Reaction coordinate

Scheme 2–7

containing units. Experimental rate show that EEM disappears faster than MEM, and EME faster than MMM and MME.

2. The protonations of oxygen of polymer chains and bond scissions yield polymer chains, ~~~$OCH_2CH_2^{\oplus}$ and $^{\oplus}CH_2OCH_2$~~~. The polymer chain, ~~~$OCH_2CH_2^{\oplus}$ mainly undergoes backbiting reactions to give DOL and TOP. Highly competitive β-scission for the macro cation, $^{\oplus}CH_2OCH_2$~~~, is favored over backbiting and leads to the lower rate of formation of TOX than DOL, and TEX lower than TOP.

ii. Hydride Transfer Reaction

The trioxane-dioxolane copolymer contains stable methoxy end groups originating from chain transfer reaction in the polymerization. The methoxy end groups are observed at 3.3 ppm and 3.1 ppm in the ^1H NMR spectrum and they are believed to be two different methoxy groups, ~~~$OCH_2O\underline{H}_3$ and ~~~$OCH_2CH_2O\underline{H}_3$, respectively (13). Oxygens of methoxy end groups are strong nucleophilic sites and the concentration of methoxy end groups should decrease during the degradation process as preferential protonations occur. However, it appears that the concentration of methoxy end groups

fluctuates during the whole process of the degradation (Fig. 2-15), perhaps due to formation of new methoxy end groups.

Concurrently with the formation of new methoxy end groups, formate end groups are formed from the early stage of the degradation process and its concentration was observed to increase continuously during the degradation process. The formation of formate end groups as function of degradation time is shown in Fig. 2-16.

It has been reported that during polymerization of trioxane, formate and new methoxy end groups are formed as a result of hydride shift. The mechanism is shown in Scheme 2-8 (14).

An inter or intramolecular electrophilic attack of C-H bond of methylene group by the macrocation gives a new methoxy end group. The newly formed cation is resonance stabilized and can be cleaved to form formate end group and macro cationic chain end.

Therefore it is believed that hydride transfer reaction taking place in the TOX-DOL copolymer solution leads to the formation of formate and methoxy end groups.

iii. Equilibria between TEX and TOX, and between TOP and DOL

Fig. 2-15 Concentration for methoxy end group of TOX-DOL copolymer during acidic degradation

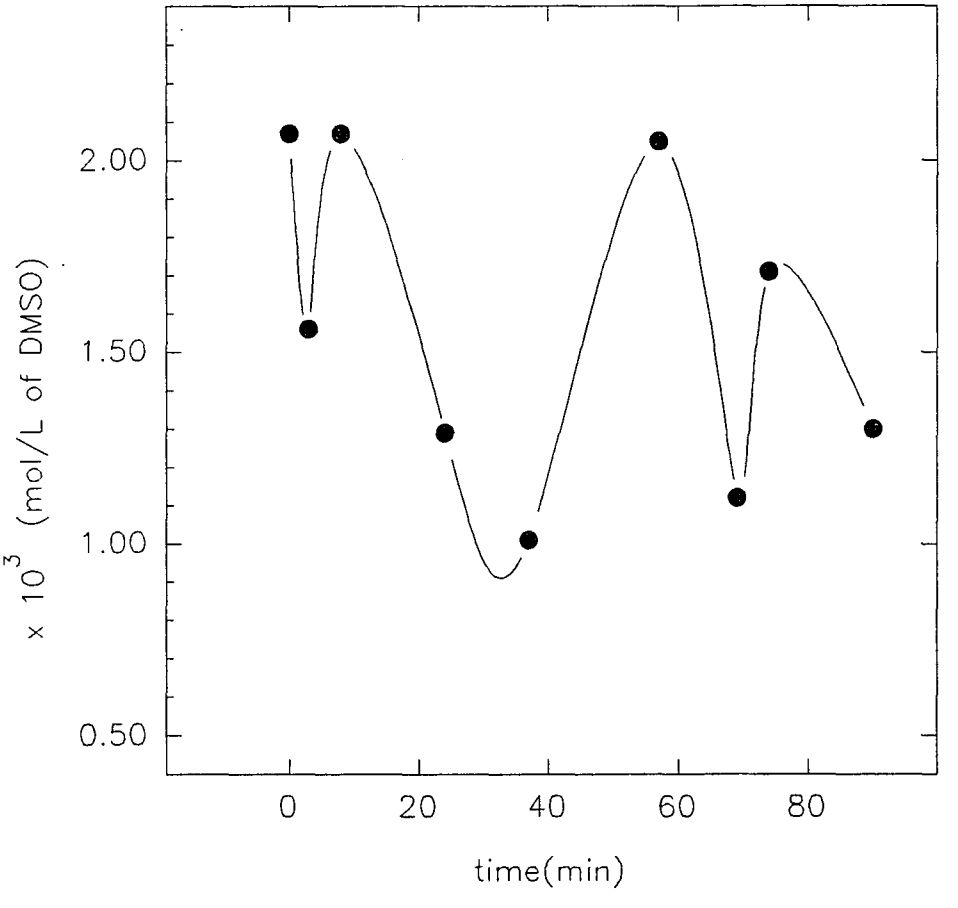

Initiated by $[CF_3COOH]$ at 2.4 x 10^{-2} (mol/L)

Fig. 2-16 Kinetics of formate end groups formed during acidic degradation of TOX-DOL copolymer

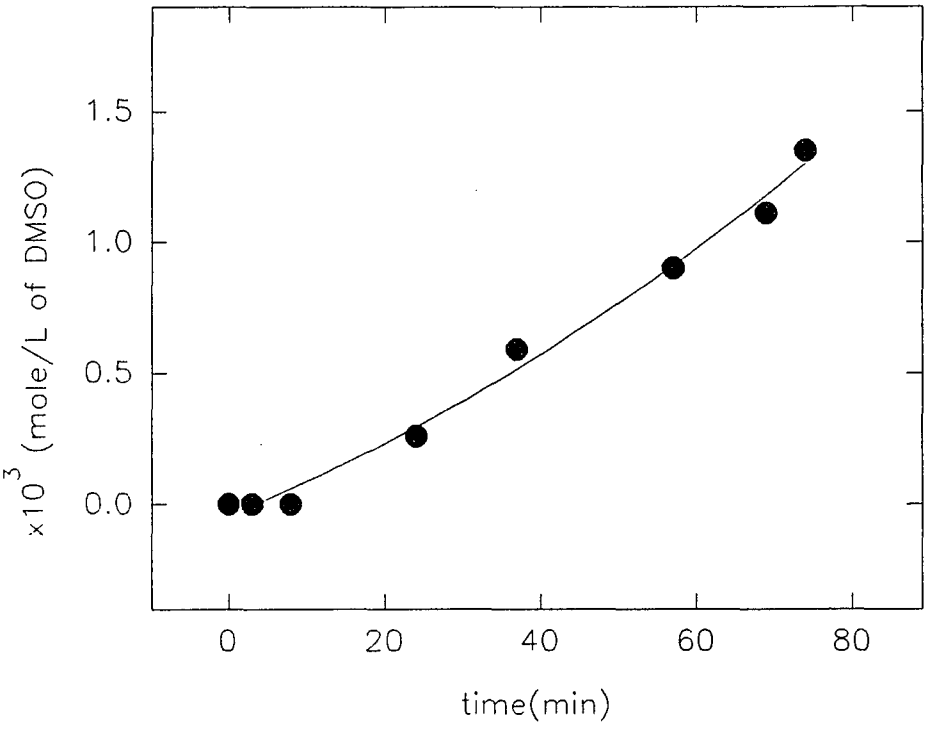

Initiated by $[CF_3COOH]$ at 2.4 x 10^{-2} (mol/L)

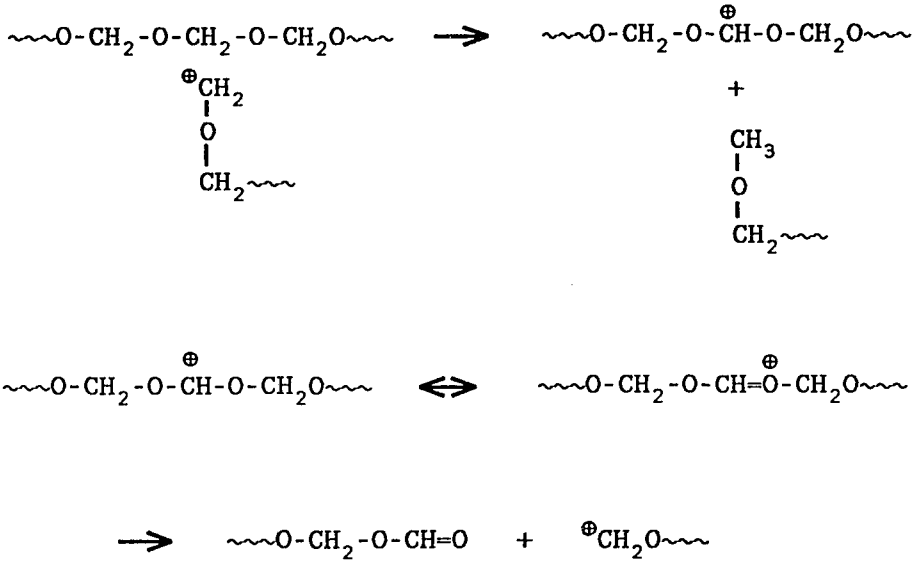

Scheme 2–8

From reference 14

In the early stage of the degradation process, (as shown in Fig. 2-8, 2-9 and 2-10) the concentrations of TOP and TEX increased in the system and reached a maximum. After the maximum, they decreased at a much slower rate compared to the initial growth rate (later stage). This decline of concentration in the later stage of the degradation process is due to lower equilibrium concentration of TEX than TOX, and of TOP than DOL, involving formaldehyde:

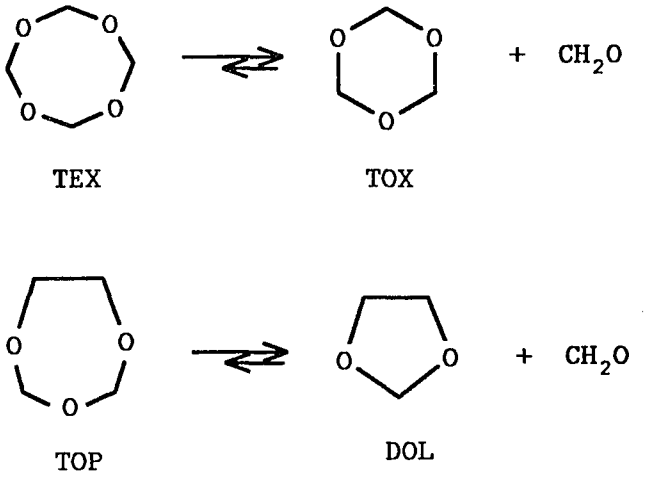

The fast polymerization of formaldehyde evolving from the degrading polymer solution should result in a rapid decrease in the concentration of formaldehyde. This leads to shifting the equilibrium reactions to the right.

The available values of the equilibrium concentrations are somewhat scattered, but a lower value of TEX than that of TOX has been generally reported. In case, the equilibrium concentration of TOX measured from dissolved monomer to dissolved polymer in nitrobenzene at 25 °C and 74 °C, are 1.41 (mol/L) and 0.35 (mol/L), respectively. On the while, the equilibrium concentrations for TEX measured under the same conditions are 0.10 (mol/L) and 0.02 (mol/L), respectively (15).

Similarly, lower equilibrium concentration of TOP (0.68 mol/L) than DOL (3.1 mol/L) was obtained from the

calculation based on reported thermodynamic parameters of the polymerization reaction using the equation (15):

$$ln\ [M]_e = \frac{\Delta H^o}{R\,T_c} - \frac{\Delta S^o}{R}$$

The reported ΔH and ΔS are; -6.6 (kJ/mol) , -18.9 (J/mol·K) for TOP at 25 °C and -15 (kJ/mol), -59 (J/mol·K) for DOL at 30 °C, respectively (15).

iv. Degradation Scheme

Based upon ^1H NMR data analysis of the degraded chain sequences, the degradation products, and the kinetic behaviors discussed above, the mechanism of acidic degradation of TOX-DOL copolymer initiated by addition of trifluoroacetic acid in DMSO-d_6 solution at 120 °C is proposed (Scheme 2-9). The species designated in the boxes are the degradation products observed in the experiments.

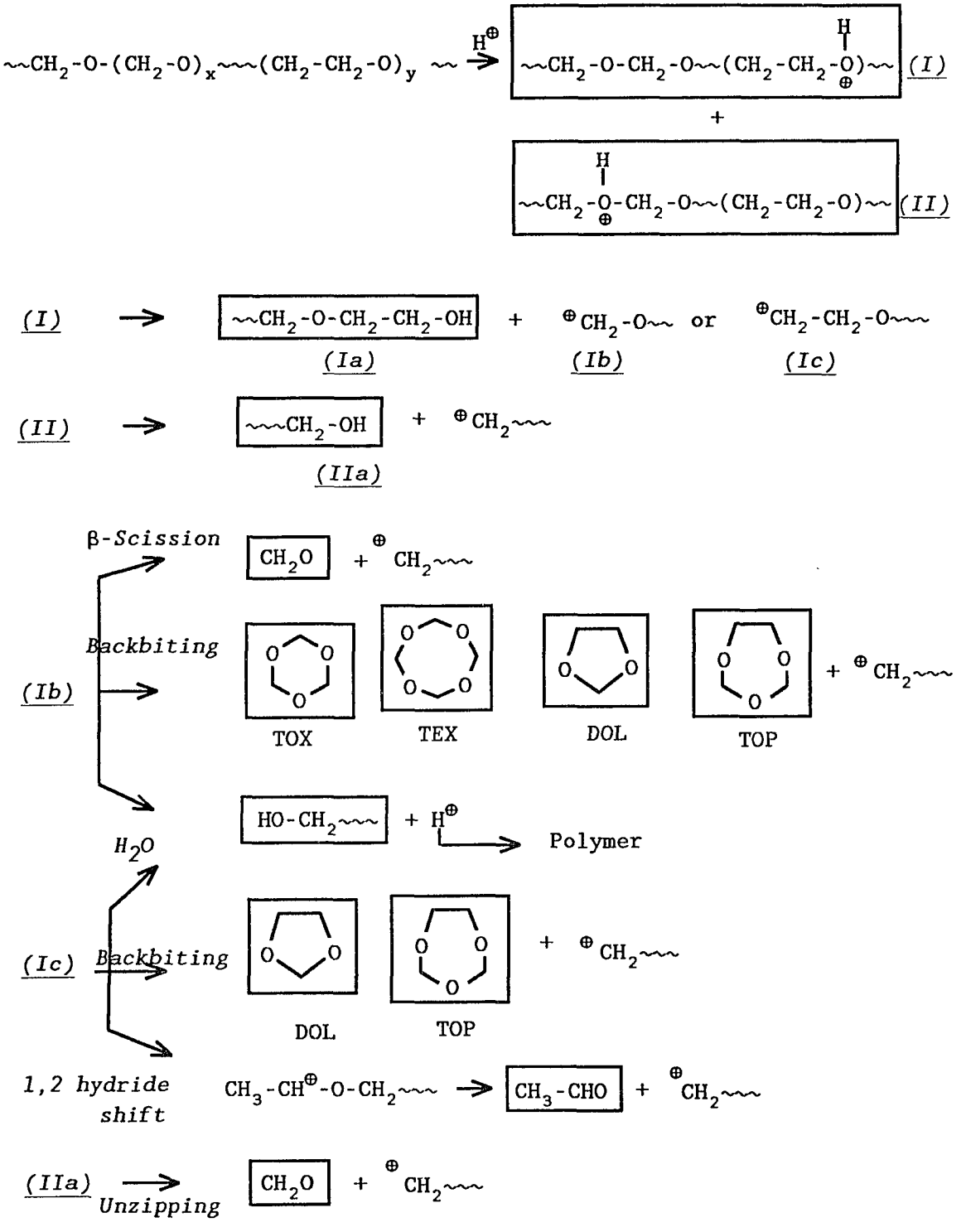
~~CH2-O-(CH2-O)x~~~(CH2-CH2-O)y ~~
H⊕
~~CH2-O-CH2-O~~(CH2-CH2-O)~~
(I)
+
~~CH2-O-CH2-O~~(CH2-CH2-O)~~
(II)
(I)
~~CH2-O-CH2-CH2-OH
(Ia)
+
⊕CH2-O~~
(Ib)
or
⊕CH2-CH2-O~~~
(Ic)
(II)
~~~CH2-OH
(IIa)
+
⊕CH2~~~
β-Scission
CH2O
+
⊕CH2~~~
Backbiting
(Ib)
TOX
TEX
DOL
TOP
+
⊕CH2~~~
HO-CH2~~~
+
H⊕
Polymer
H2O
(Ic)
Backbiting
DOL
TOP
+
⊕CH2~~~
1,2 hydride shift
CH3-CH⊕-O-CH2~~~
CH3-CHO
+
⊕CH2~~~
(IIa)
Unzipping
CH2O
+
⊕CH2~~~

Scheme 2–9
~~~

2.3.2. Radical Degradation

The overall process of radical degradation, initiated by AIBN at initial concentration equal to trifluoroacetic acid, proceeded more slowly compared to the acidic degradation process. The slow rate of radical degradation reaction is mainly due to the slow decomposition rate of AIBN compared to that of the trifluoroacetic acid instaneous dissociation. In the degradation process initiated by radicals, the degrading agent was generated by the homolytic dissociation of an initiator I:

$$I \xrightarrow{k_d} 2\,R^{\bullet}$$

The first order rate law is expressed in terms of the rate constant of initiator decomposition, k_d:

$$-\frac{d\,[I]}{dt} = k_d\,[I]$$

The concentration of radicals $R^{\bullet}$, then can be calculated using the equations below:

$$R^{\bullet} = 2\,(\,I_o - I_t\,)$$

$$I_t = I_o\; e^{-k_d\,t}$$

where I_o and I_t are the concentration of the initiator at initial and at a time t, respectively.

The decomposition rate constant of AIBN under our experimental conditions, at 120 °C in DMSO, was calculated based on the well-known Arrhenius equation using the literature values of k_d = 1.55 x 10 $^{-4}$ (sec^{-1}) at 82 °C in n-butanol and E_a = 30.8 (kcal/mole) (16). The calculated k_d value is 1.53 x 10 $^{-4}$ (sec^{-1}). In order to obtain the concentration of active radicals at a specific time of the degradation process, it was necessary to normalize radical concentration at specified time intervals during the degradation process. The time average concentration of radical at specific time, t, of the degradation process was calculated using the following equation assuming no radical recombination:

$$[\,R^{\bullet}\,] = \frac{\int_0^t 2\,I_0\,(\,1 - e^{-k_d t}\,)\,dt}{\int_0^t dt}$$

(a) ^{1}H NMR Analysis of Degradation Products and Degraded Chain Sequences

^{1}H NMR spectra for AIBN catalyzed degradation of TOX-DOL copolymer covering the entire process were obtained (Fig. 2-17). The identification of degradation products and the analysis of remaining chain sequences were carried out

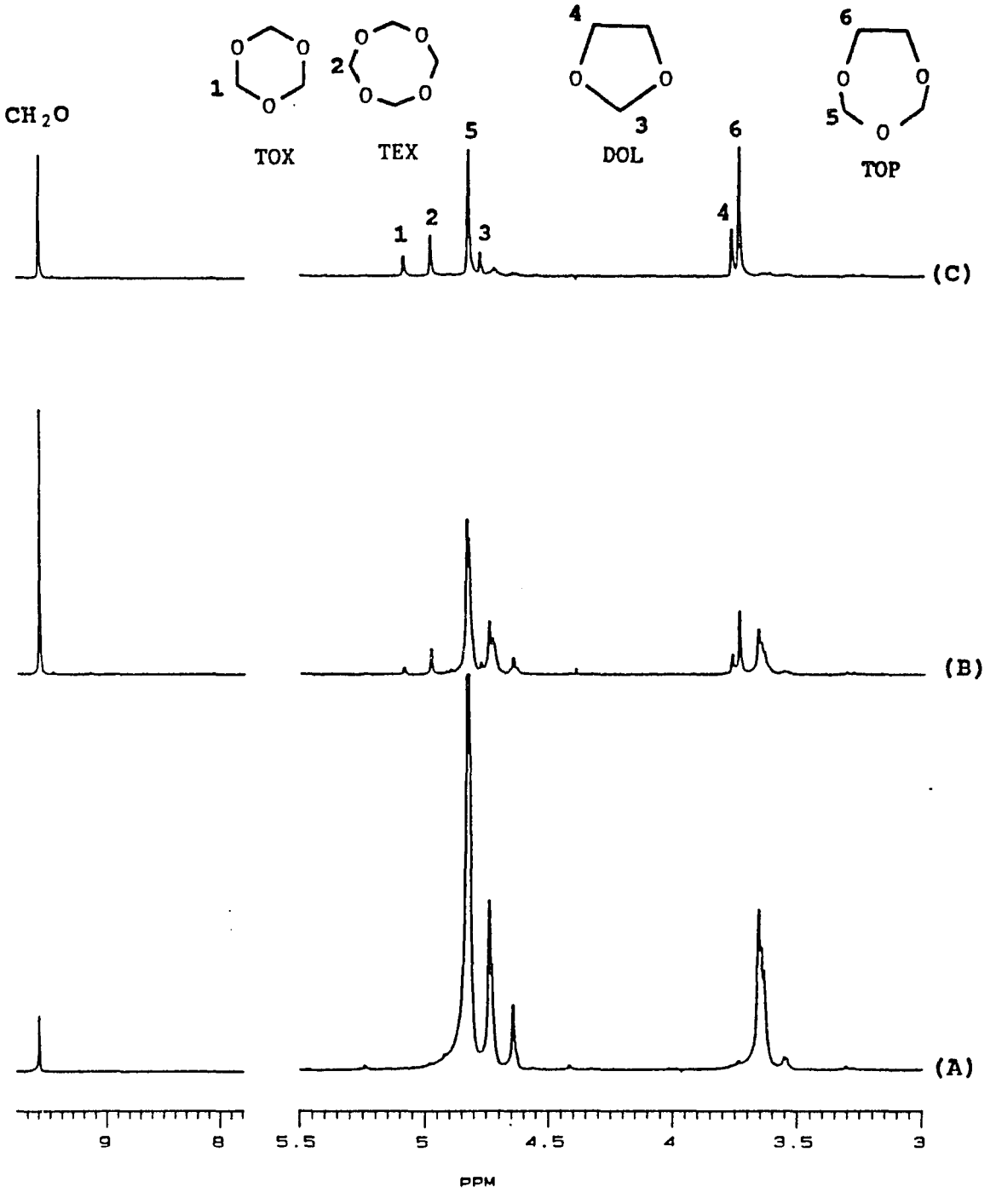

Fig. 2-17 ^{1}H NMR Spectra of degraded TOX-DOL copolymer in DMSO-d_6 solution at 120 °C initiated by addition of 2.4 X 10^{-2} M of AIBN. (A) before addition of AIBN (B) 15 min and (C) 55 min after addition of AIBN

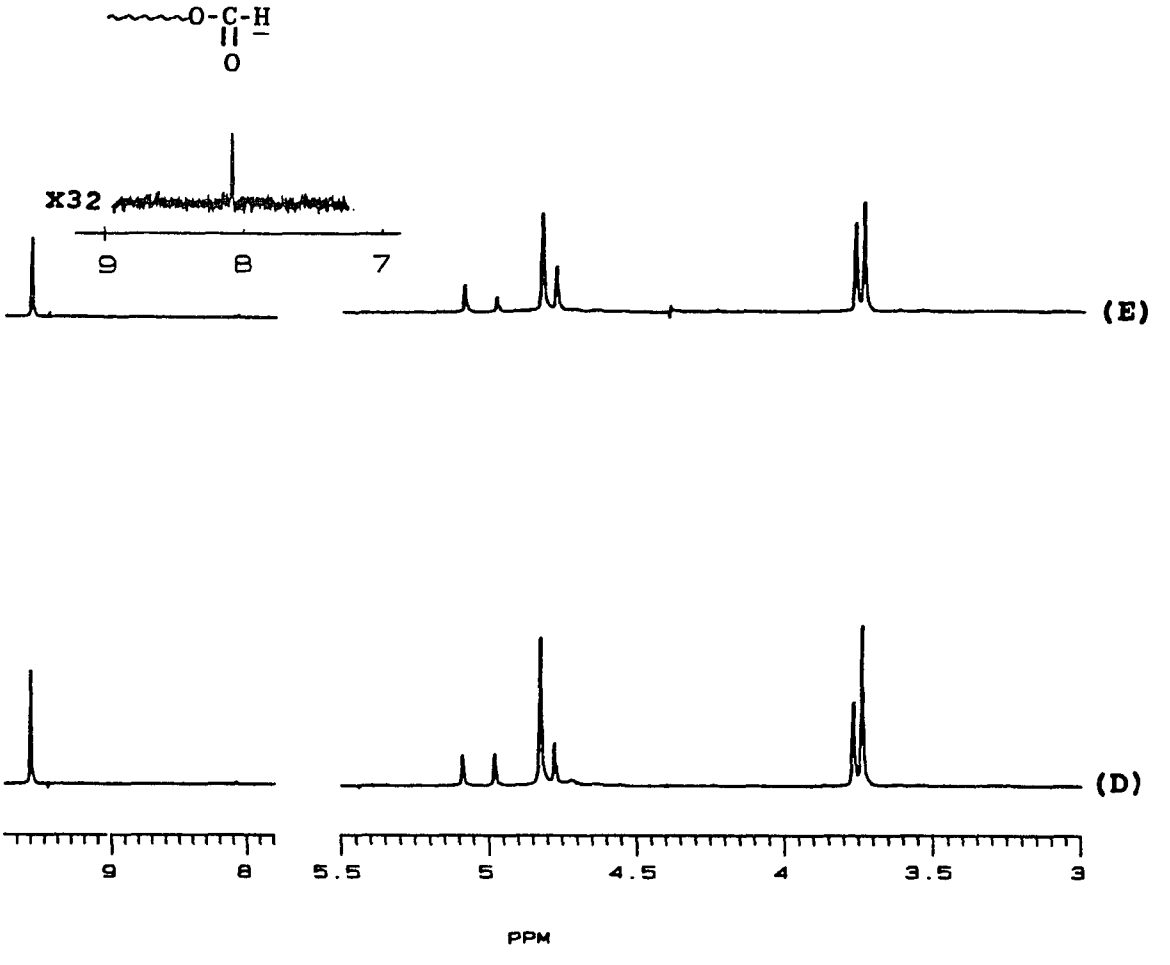

Fig. 2-17 ^{1}H NMR Spectra of degraded TOX-DOL copolymer in DMSO-d_6 solution at 120 °C initiated by addition of 2.4 X 10^{-2} M of AIBN. (D) 85 min, (E) 115 min after addition of AIBN

in a manner similar to the analysis of acidic degradation. The degradation products were identified as formaldehyde, formate end groups, TOX, TEX, DOL and TOP. They include the same species obtained during the acid degradation. The kinetic variations of the degradation products in three experiments are profiled in Fig. 2-18, 2-19 and 2-20. The general features of the degradation products agree with one another reasonably well. Formaldehyde concentration increases with the higher rate and reached a maximum concentration in the range from 0.063 to 0.078 (mol/L). In the early stage, the concentrations of TOX, DOL, TEX and TOP increase. In the later stage, the shifts of equilibria from TEX to TOX, and from TOP to DOL were observed. A representative sample (Fig. 2-18) of the kinetic data for the degradation products are presented in Table 2-3. Initial five minutes of the degradation showed fast formation rate of formaldehyde but the formation rates of TEX, DOL, and TOP were very low. In the degradation time range of 5 ~ 15 minutes, the concentrations of TOP and DOL increase ca. five and nine times, respectively while TOX and TEX increase ca. two and three times, respectively.

A series of ^{1}H NMR spectra depicting radical degradation (Fig. 2-12) enlarged for the methylene oxide and ethylene oxide regions is shown in Fig. 2-21. In this

Fig. 2-18 Kinetics of products formed during radical degradation of TOX-DOL copolymer

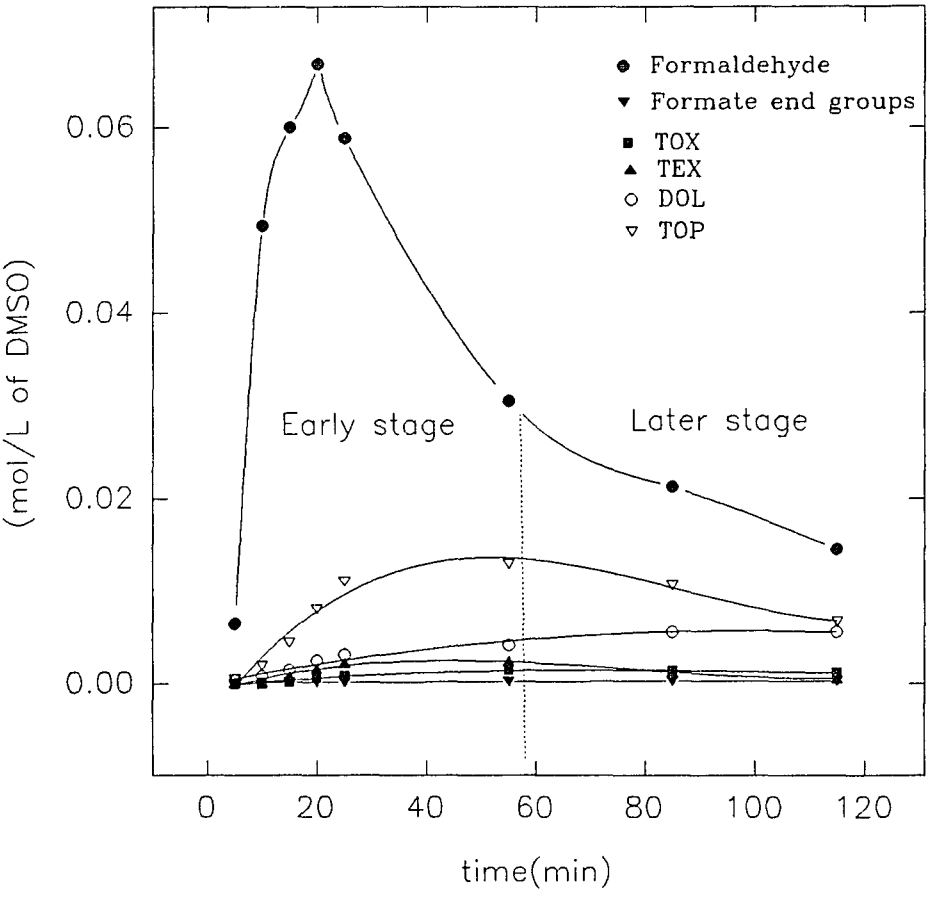

Initiated by [AIBN] at 0.0238 (mol/L)

Fig. 2-19 Kinetics of products formed during radical degradation of TOX-DOL copolymer

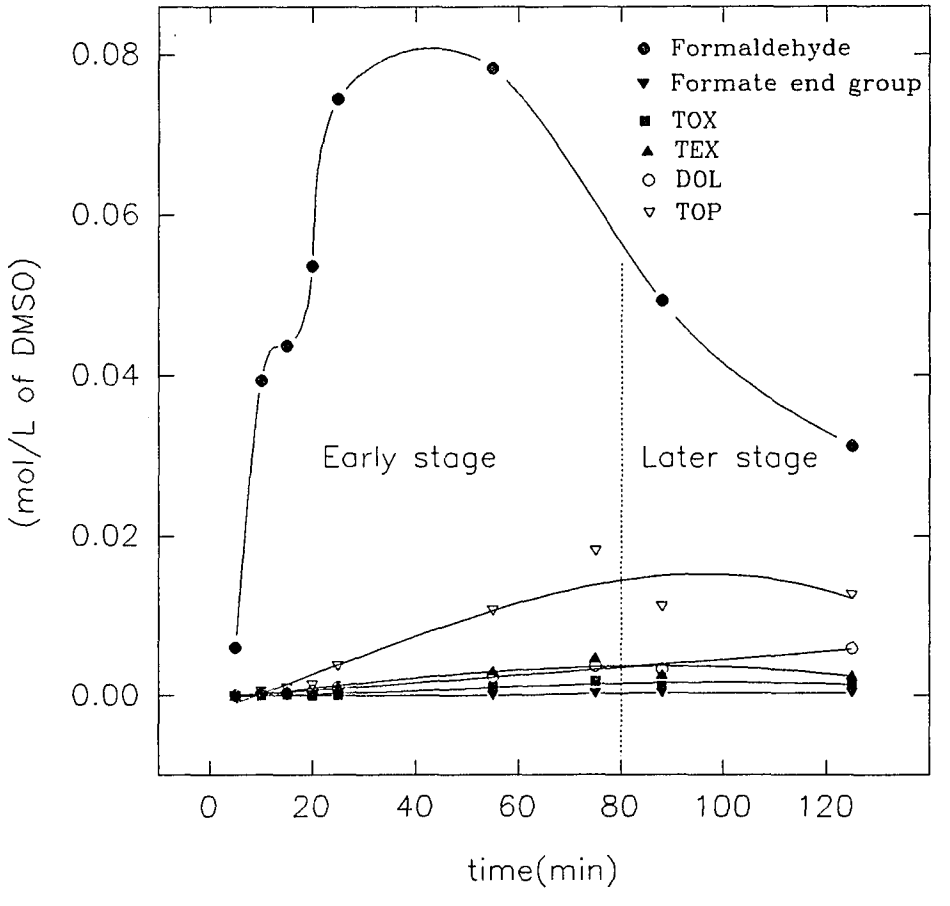

Initiated by [AIBN] at 2.4 x 10^{-2} (mol/L)

Fig. 2-20 Kinetics of products formed during radical degradation of TOX-DOL copolymer

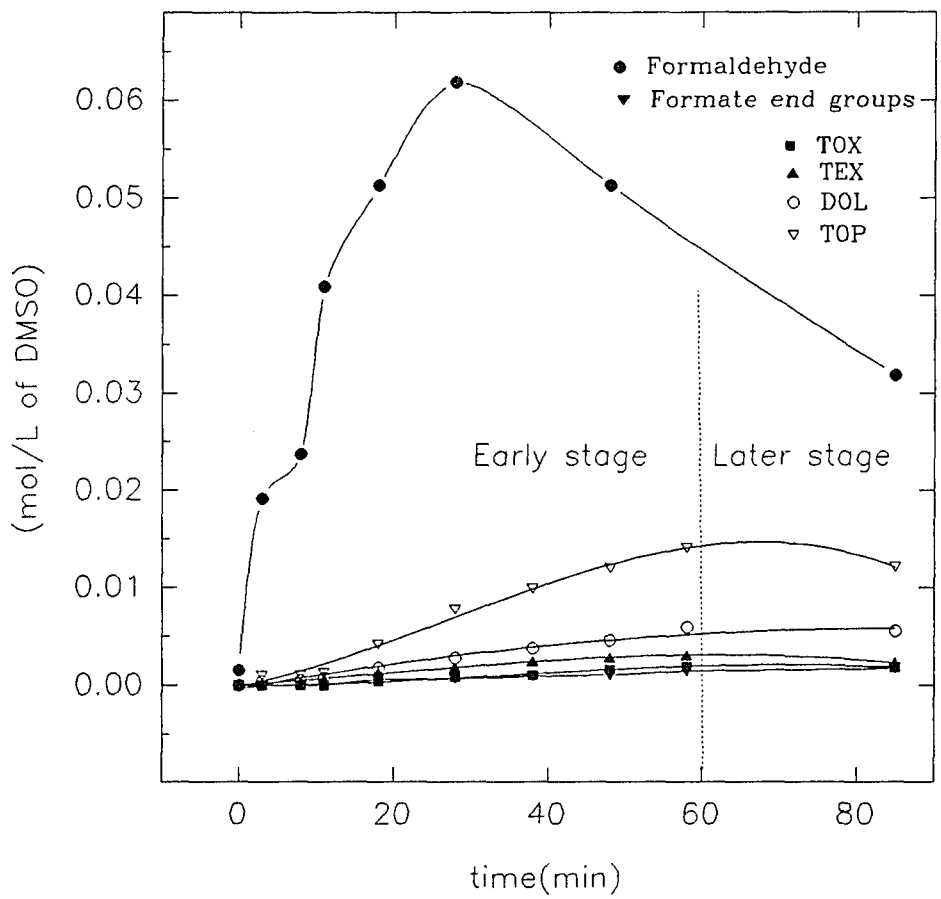

Initiated by [AIBN] at 2.4 x 10^{-2} (mol/L)

Table 2-3 Yields of products formed during radical degradation of TOX-DOL copolymer initiated by AIBN at 2.4 x 10^{-2} (mole/L of DMSO)

x 10^{2} (mol/L)

time (min)	[FD]	[FT]	[TOX]	[TEX]	[DOL]	[TOP]	[MX]
0	0.00	0.00	0.00	0.00	0.00	0.00	0.23
5	0.65	0.00	0.00	0.02	0.03	0.05	0.12
10	4.94	0.01	0.00	0.02	0.08	0.19	0.13
15	6.00	0.01	0.02	0.07	0.15	0.45	0.11
20	6.68	0.02	0.06	0.16	0.25	0.80	0.10
25	5.88	0.01	0.08	0.22	0.31	1.10	0.08
55	3.06	0.02	0.15	0.24	0.41	1.30	0.08
85	2.13	0.03	0.14	0.12	0.56	1.07	0.04
115	1.45	0.03	0.12	0.06	0.56	0.67	0.03
145	1.13	0.03	0.10	0.03	0.61	0.45	0.01
175	0.86	0.03	0.09	0.02	0.29	0.57	0.00
205	0.65	0.03	0.09	0.02	0.55	0.20	0.00

[FD] = Formaldehyde

[FT] = Formate end groups

[MX] = Methoxy end groups

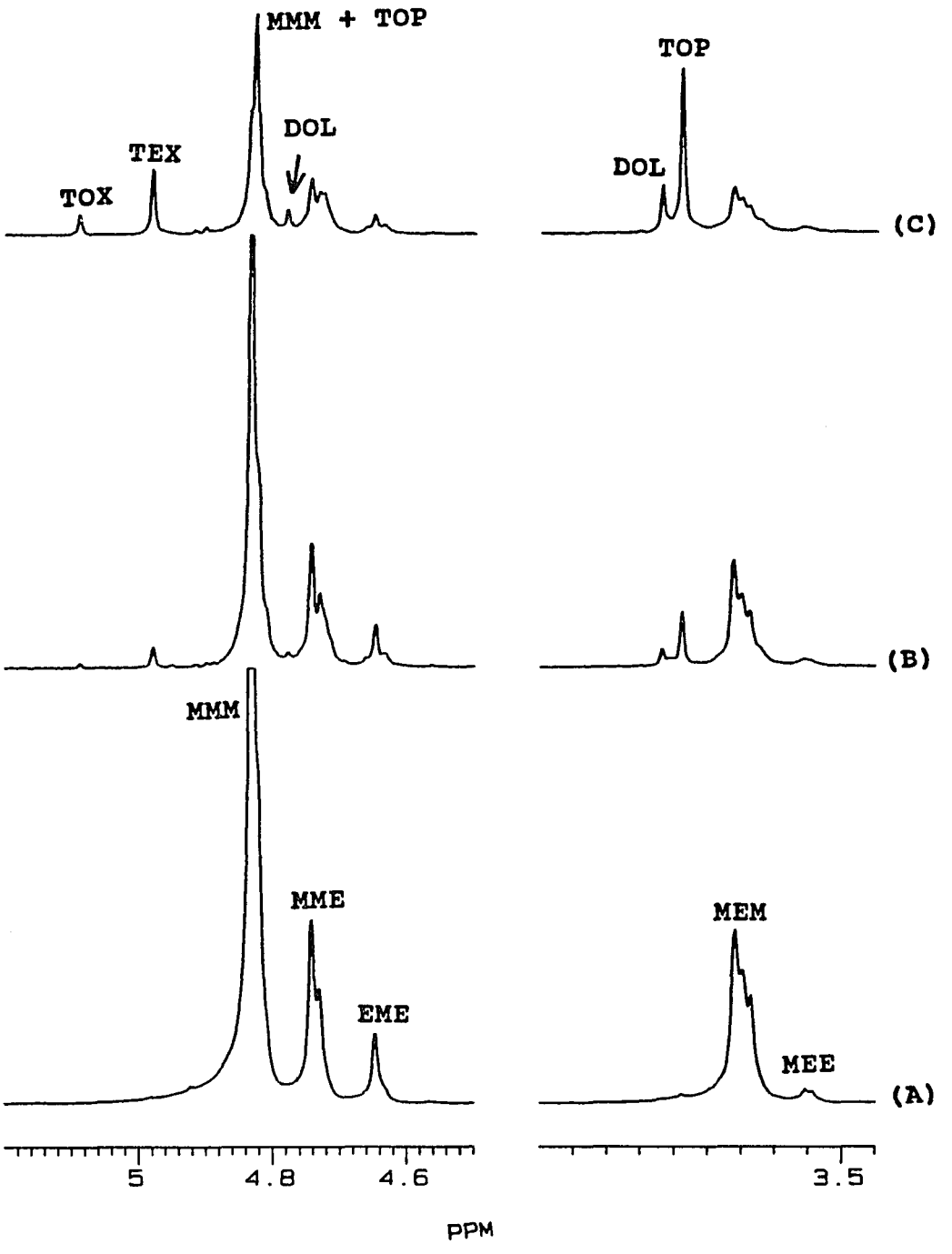

Fig. 2-21 Methylene oxide and ethylene oxide regions in the ^{1}H NMR spectra of degraded TOX-DOL copolymer initiated by addition of AIBN at 2.4 X 10^{-2} M. (A) before addition of AIBN (B) 15 min, and (C) 25 min after addition of AIBN

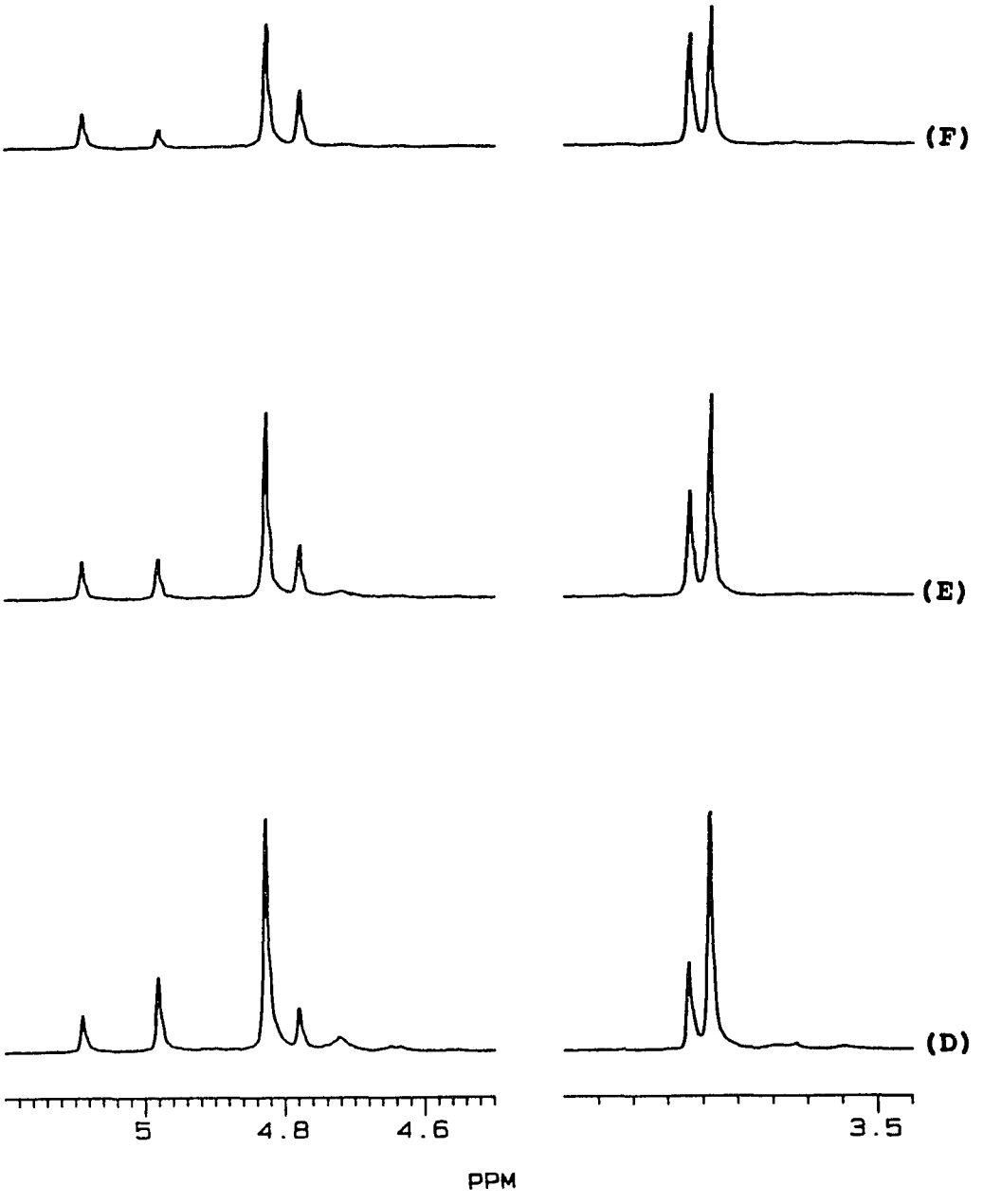

Fig. 2-21 Methylene oxide and ethylene oxide regions in the ^{1}H NMR spectra of degraded TOX-DOL copolymer initiated by addition of AIBN at 2.4 X 10^{-2} M. (D) 55 min (E) 85 min, and (F) 115 min after addition of AIBN

particular regions, one can observe clearly the variation of triad monomer sequences and formations of cyclic acetals during the degradation process. From the ^1H NMR data of one experiment (Fig. 2-18), the molar concentration of triad sequences was calculated and presented in Table 2-4. The remaining fraction of triads was plotted as a function of degradation time (Fig. 2-22). Among the M centered triads, MMM appears to be the most unstable in the radical degradation, showing a 58 % of degradation within 5 minutes. At the same span of time, the peaks due to MME and EME showed about 31 % and 3 % degradation, respectively. Between two of the E centered triads, MEE is more stable than MEM. The triad MEE showed about 7 % degradation while MEM, 39 % degradation. The initial degradation rate of the triad sequences is in the increasing order of EME < MEE < MME < MEM < MMM. The peaks EME and MEE showed 32 % and 35 % of degradation respectively in the period from 5 to 15 minutes.

The degradation rates of these triad sequences within 15 minutes and formations of TOP and DOL at span of time 5 ~ 15 minutes indicate that initially methylene oxide blocks degrade at a faster rate and if the degradation has ceased at ethylene oxide units, then either TOP or DOL is formed.

(b) Degradation Mechanism

Table 2-4 Concentrations for triad sequences of TOX-DOL copolymer during radical degradation initiated by AIBN at 2.4 x 10^{-2} (mole/L of DMSO)

x 10^{1} (mol/L)

time (min)	Methyle oxide units			Ethylene oxide units	
	[MMM]	[MME]	[EME]	[MEM]	[MEE]
0	4.019	0.685	0.176	0.415	0.035
5	1.729	0.468	0.173	0.257	0.030
15	1.249	0.389	0.118	0.186	0.021
25	0.326	0.253	0.065	0.101	0.013
55	0.013	0.069	0.029	0.013	0.006
85	0.005	0.005	0.014	0.003	0.002
115	0	0.003	0	0.002	0.001

Temperature = 120 ^{o}C

Concentration of methylene oxide = 0.45 (mol/L)

Concentration of ethylene oxide = 0.04 (mol/L)

Fig. 2-22 Fractional consumption for triad sequences of TOX-DOL copolymer during radical degradation

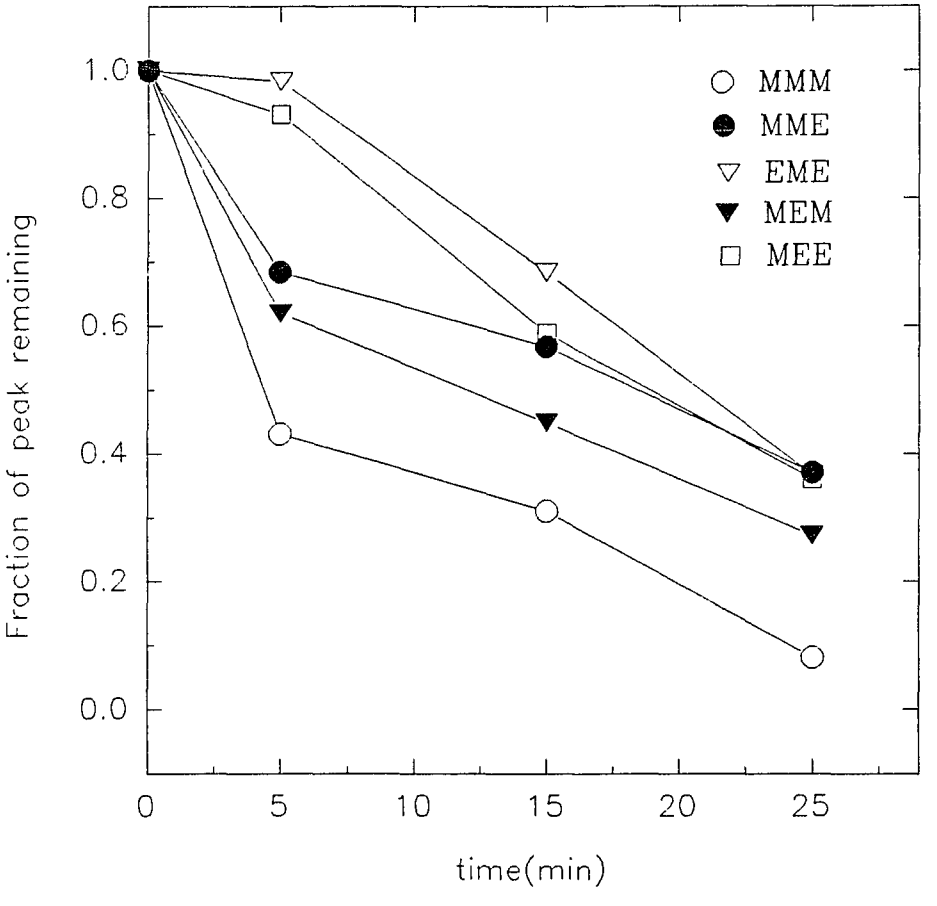

Initiated by AIBN at 2.4 x 10^{-2} (mol/L)

i. β-Scission Reaction

Based on the experimental results, a mechanism for the initiation of radical degradation is proposed (Scheme 2-10). Degradation of polymer is initiated by hydrogen abstraction by free radical, resulting in the formation of polymer backbone radicals *III* and *IV*. The two methylenic hydrogens of methylene oxide units on the polymer are highly reactive toward free radicals due to the doubly labializing effect exerted by their two neighboring oxygen atoms. The polymer back bone radicals (*IV*) are from the hydrogen abstraction on ethylenic units. In the ^{1}H NMR spectra of radically degraded TOX-DOL copolymer, the presence of polymer chain ends with aldehyde (*VIII*) or carbon-carbon double bond (*IX*), which can be generated by the decomposition of ethylenic polymer backbone radicals, were not observed. This may be due to the favored hydrogen abstractions on more labile hydrogens of methylene oxide units over the hydrogens of low concentration ethylene oxide units (1).

The preferred hydrogen abstractions on methylene oxide units is supported by faster initial degradation rate of M units than E units (Fig. 2-23). At 8 minutes, M units and E units showed 35 % and 52 % of degradations respectively. This result clearly verifies the preferred hydrogen

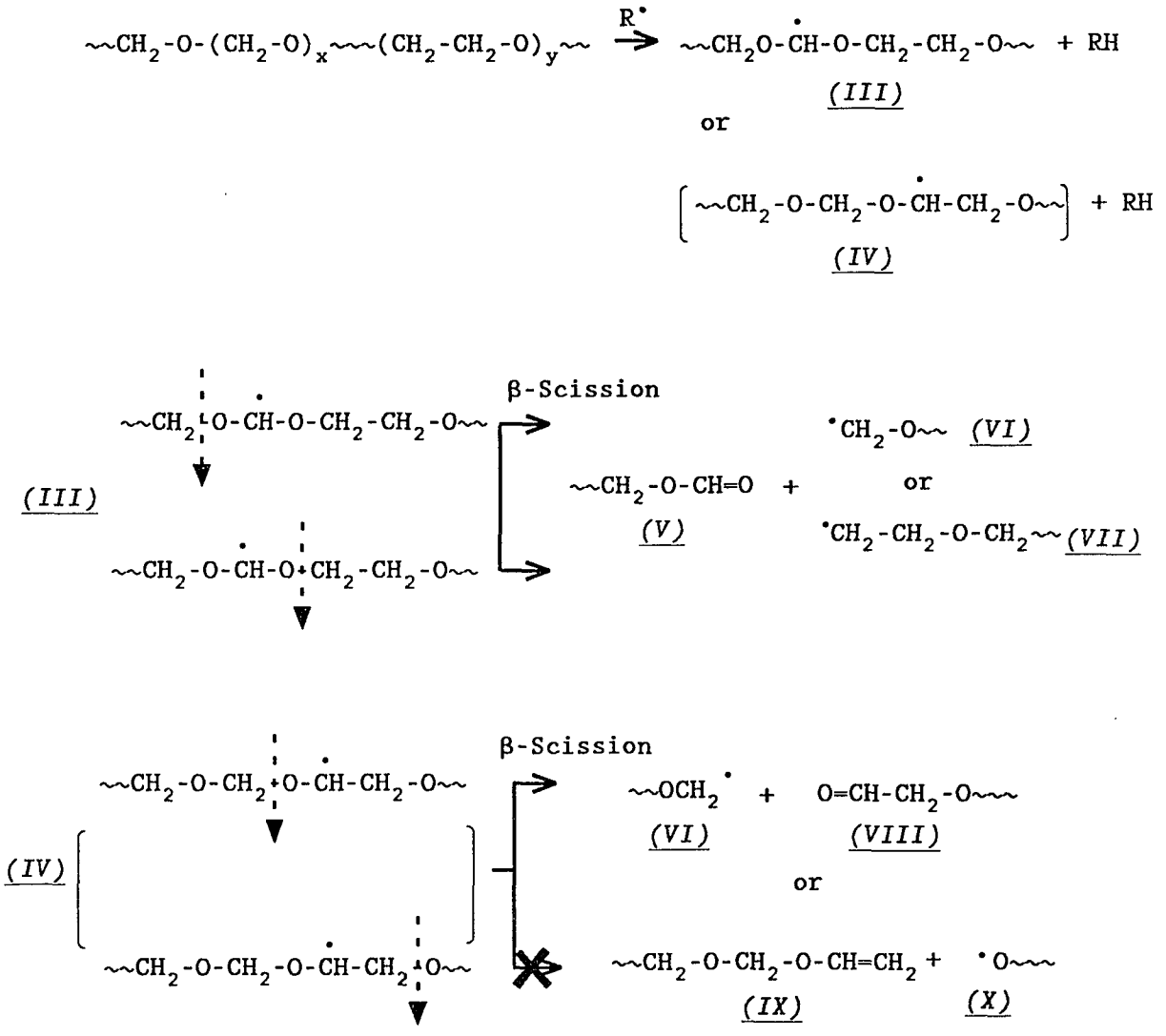
R•
+ RH
(III)
or
(IV)
+ RH
β-Scission
(III)
(V)
+
or
(VI)
(VII)
β-Scission
(IV)
(VI)
+
(VIII)
or
(IX)
+
(X)

Scheme 2–10

Fig. 2-23 Fractional Consumption for M and E units of TOX-DOL copolymer during radical degradation

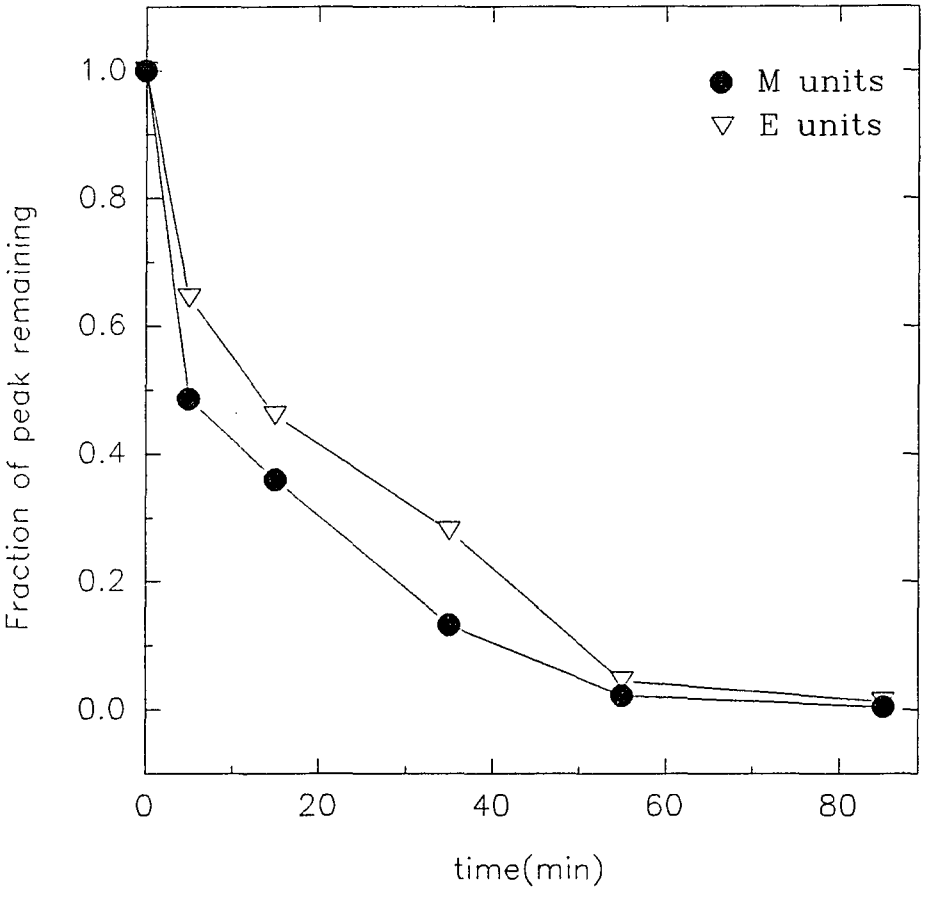

Initiated by AIBN at 2.4 x 10^{-2} (mol/L)

abstraction by free radicals on the methylene oxide units over the ones from the ethylene oxide units.

Higher reactivity of hydrogen for abstraction on the acetal carbon attached to oxygen atoms on both sides than the hydrogen on the carbon connected with one oxygen atom have been reported by Kuhn and Wellman in the reaction of isopropyl acetal with t-butyl peroxide (17):

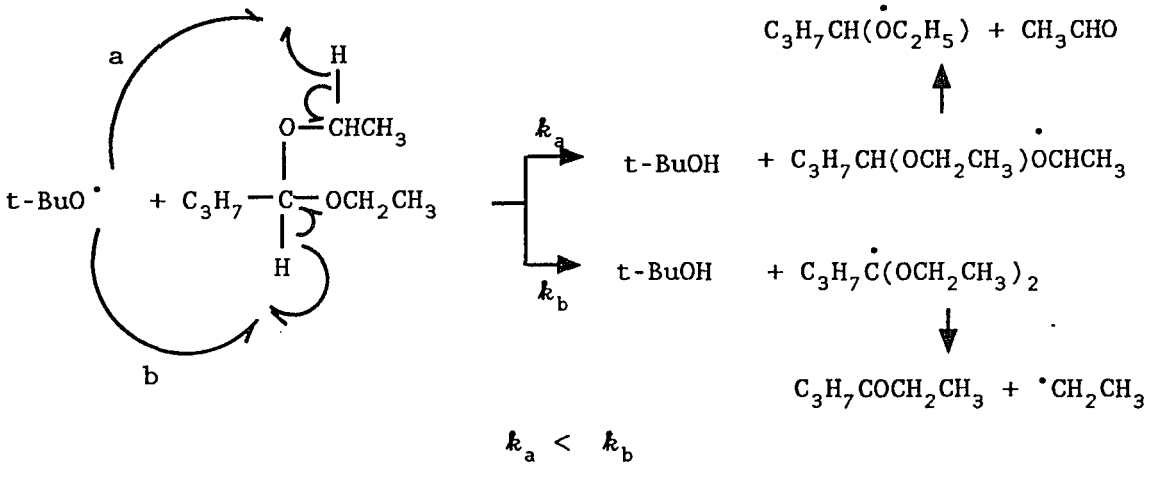

The relative yield of acetaldehyde to ethyl butyrate was 3.3, indicating that the hydrogen on acetal carbon is ca. 17 % more reactive, i.e. 1 - (3.3/4).

The polymer backbone radicals (*III*) formed after abstraction of the methylene hydrogen is highly unstable and can decompose by β-scission to generate two chains, one with

formate end group (*V*) and the other with primary alkyl radical end group (*VI*) or (*VII*).

ii. Intramolecular Radical Substitution and 1,5 Hydrogen Shift Reactions

Based on the analysis of the degraded chain sequences and the degradation products, it is proposed that three competitive radical reactions can occur for the radical chain end with methylene oxide end unit (*VI*), while only radical substitution reaction can take place for the radical chain end with ethylene oxide end unit (*VII*). The proposed mechanism is illustrated in Scheme 2-11. The radical chain end, •MMM~~~, undergoes fast β-scission to cleave formaldehyde. Meanwhile intramolecular radical substitution reaction competes with β-scission reaction to give TOX or TEX:

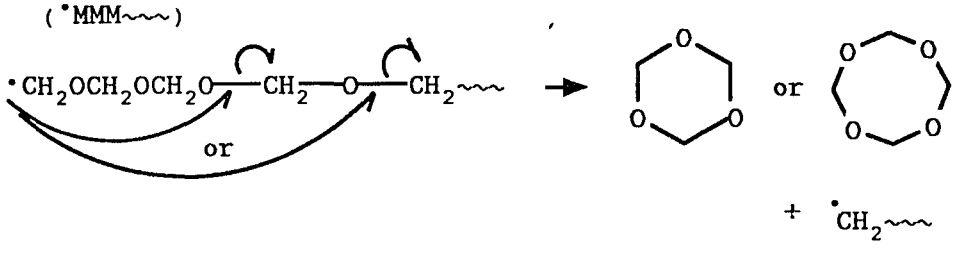

Formations of DOL and TOP also take place through intramolecular radical substitution reactions involving the

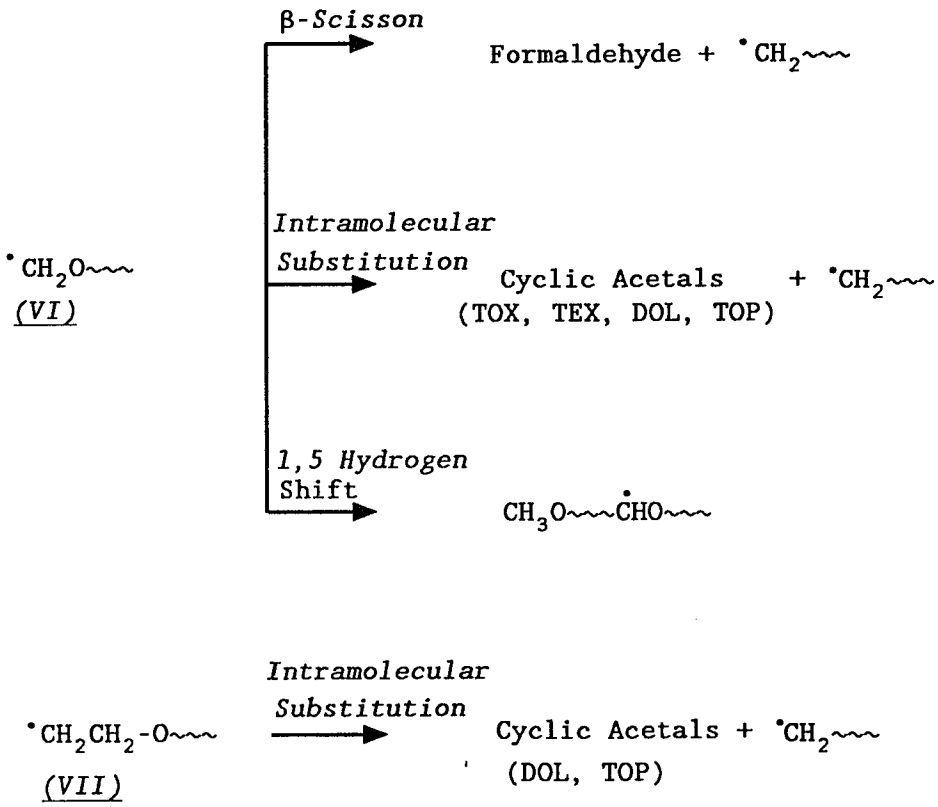
β-Scisson
Formaldehyde + •CH2~~
Intramolecular
Substitution
Cyclic Acetals + •CH2~~
(TOX, TEX, DOL, TOP)
•CH2O~~
(VI)
1,5 Hydrogen
Shift
CH3O~~ĊHO~~
Intramolecular
Substitution
•CH2CH2-O~~
Cyclic Acetals + •CH2~~
(DOL, TOP)
(VII)

Scheme 2–11

attack of a carbon radical on oxygen of its own polymer chain. Intramolecular radical substitution reaction of degraded TOX-DOL copolymer is attributed to sufficient mobility of radical chain ends in solution at high reaction temperature.

An intramolecular substitution reaction, similar to that of degraded TOX-DOL copolymer, has been reported by Menapace and Kuivila (18):

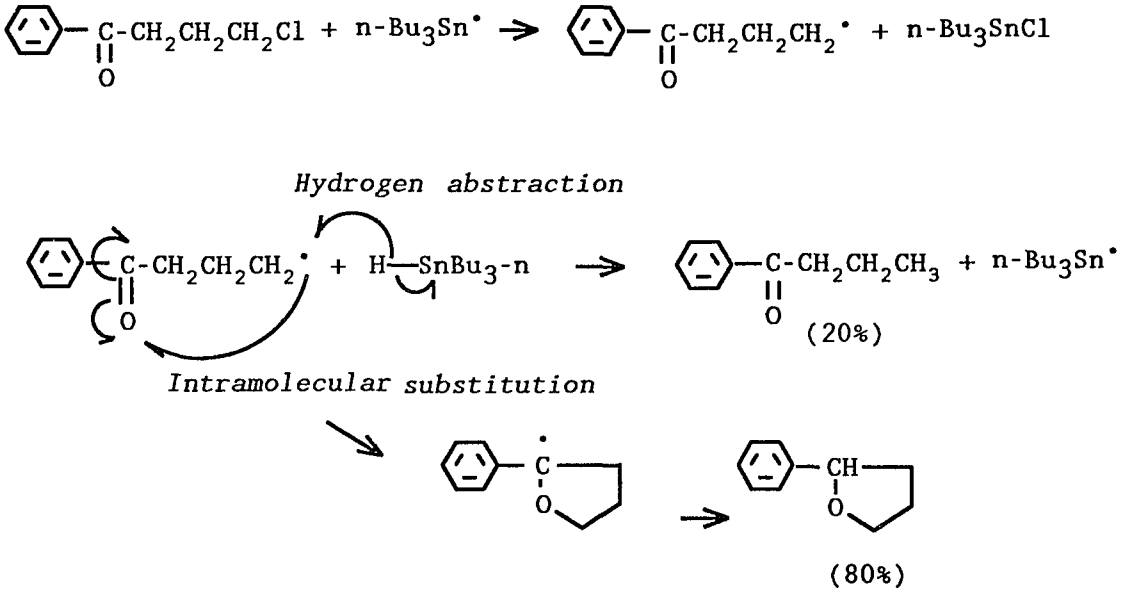

The reaction involves the attack by a carbon radical on carbonyl oxygen, and the reduction of γ-chlorobutyrophenone with tri-n-butyltin hydride at 80 °C provided 65 % of the product containing 80 % of 2-phenyl-tetrahydrofuran and 20 % butyrophenone. The driving force for this intramolecular

substitution at oxygen was considered as formations of the five membered ring α-alkoxy radical.

In another similar radical reaction, decomposition of 4-iodobutyryl peroxide, an intramolecular radical substitution reaction at oxygen lead to 5-membered ring, butyrolactone (19):

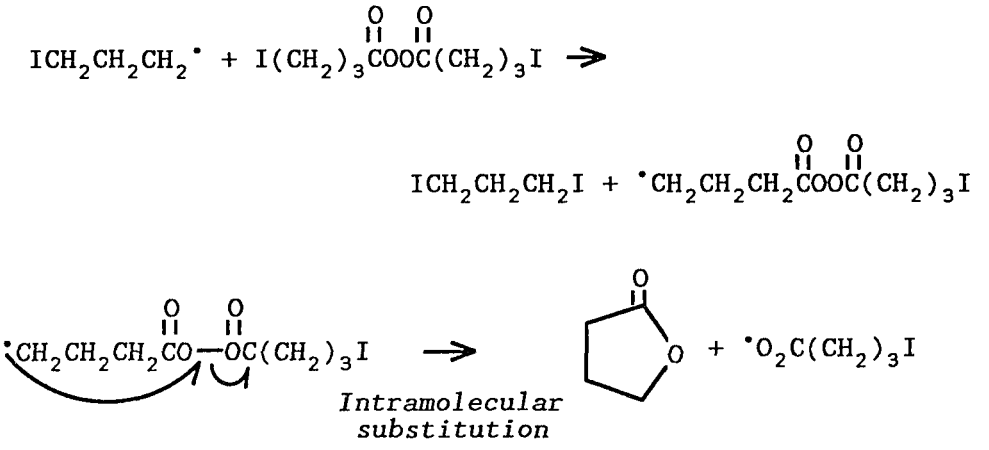

Some of the degraded polymer radical chain ends can satisfy colinearity requirement for the formation of an intermediate state leading 1,5 hydrogen shift:

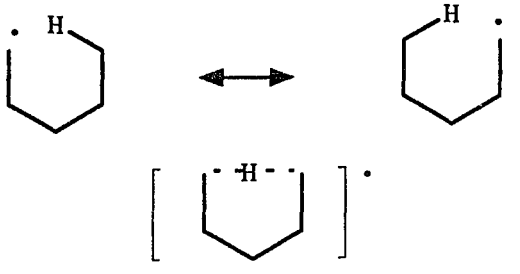

Intermediate with colinearity

The 1,5 hydrogen shift may compete with intramolecular substitution reaction. For long radical chain, hydrogen shift on 1,5 position has been proposed as a favored radical rearrangement reaction (20).

The competition of 1,5 hydrogen shift with intramolecular substitution reaction depends on the various sequences of chain ends as illustrated in Scheme 2-12.

For radical chain end of •MMM~~~ (*VIa*), 1,5 hydrogen shift reaction may compete with intramolecular substitution reaction and form (*VIb*). Thus, this reaction interferes with the formations of TOX and TEX. Two types of bond scission of (*VIb*) yield CH_3OCH_2OCHO (*VIc*) and $\bullet CH_2$~~~, or $CH_3OCH_2\bullet$ and O=CH-O-CH_2~~ (*VId*). Hydrogen abstraction reaction of $CH_3OCH_2\bullet$ from polymer yields methyl ether, CH_3OCH_3, (*VIe*). However the presence of these products was not confirmed. The proton absorption peaks for methoxy and methylene oxide and formates of (*VIc*) and (*VId*) may not be distinguished from absorption peaks due to other process, e.g. β-scission of backbone radical. Methyl ether in low concentration may not be observed due to it's low boiling point, -24.5 °C.

Dioxolane and TOP are generated from intramolecular substitution of chain sequences such as triads •MEM~~~ (*VIf*) and •EMM~~~ (*VIIa*). These sequences do not have methylene hydrogen atom available for 1,5 shift. Therefore, the

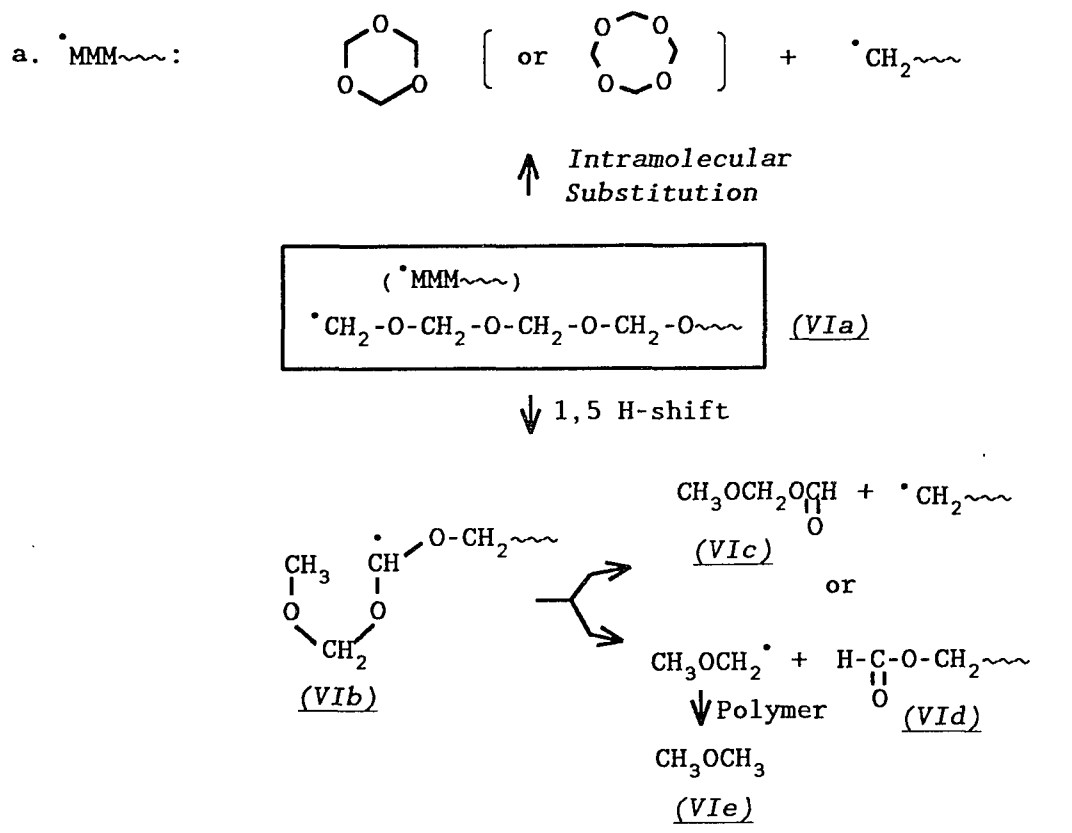
a. •MMM~~:
or
+ •CH2~~
Intramolecular Substitution
(•MMM~~)
•CH2-O-CH2-O-CH2-O-CH2-O~~
(VIa)
1,5 H-shift
O-CH2~~
CH3
CH
O
O
CH2
(VIb)
CH3OCH2OCH
O
+ •CH2~~
(VIc)
or
CH3OCH2•
+ H-C-O-CH2~~
O
Polymer
(VId)
CH3OCH3
(VIe)

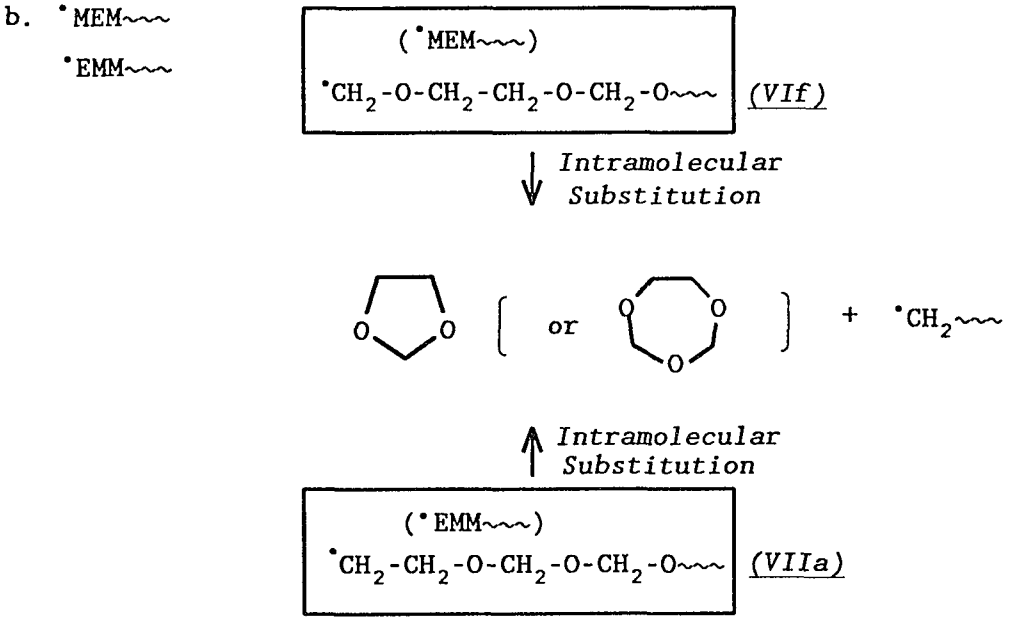
b. •MEM~~
•EMM~~
(•MEM~~)
•CH2-O-CH2-CH2-O-CH2-O~~
(VIf)
Intramolecular Substitution
or
+ •CH2~~
Intramolecular Substitution
(•EMM~~)
•CH2-CH2-O-CH2-O-CH2-O~~
(VIIa)

Scheme 2–12

formations of DOL and TOP should not be disturbed by 1,5 hydrogen rearrangement at all.

From the consideration of lower bond dissociation energy of C-O bond (351 kJ/mol) compared with C-H bond (414 kJ/mol), it is expected that intramolecular substitution reaction should dominate kinetically over 1,5 hydrogen shift (12).

In conclusion, radical degradation of TOX-DOL copolymer caused by the addition of AIBN at 120 °C in solution can be initiated as follows.

1. Preferred hydrogen abstraction occur on the methylenic unit of the polymer chain. Hydrogen abstraction and β-scission reactions lead to the formation of chains with a formate and a radical ends, $^{\bullet}CH_2O\sim\sim\sim$ or $^{\bullet}CH_2CH_2O\sim\sim\sim$.
2. The ethylenic chain end, $^{\bullet}CH_2CH_2O\sim\sim\sim$, mainly undergoes intramolecular radical substitution reaction to form DOL or TOP. The methylenic chain end, $^{\bullet}CH_2O\sim\sim\sim$, undergoes highly favored β-scission reaction over intramolecular substitution reaction. For the degraded chain with MMM end sequence, 1,5 hydrogen shift reaction can compete with the intramolecular substitution reaction and interfere with the formation TOX or TEX. However the 1,5 hydrogen shift reaction could not be verified through products identification using ^1H NMR. The products having formate end groups may not be distinguished

from the other formates. Other product, methyl ether, is volatile under the experimental conditions and was not observed.

iii. Intermolecular Hydrogen Abstraction Reaction

In the course of the analysis for the formation rates of formate end groups and for degradation of methoxy end groups, it was found that the intermolecular hydrogen abstraction reaction is a slow process in the radical degradation process.

The radical chain end, $^{\bullet}CH_2\sim\sim\sim$, can abstract hydrogen from the other polymer chain intermolecularly. This reaction yields a polymer chain with methoxy end group and a polymer backbone radical:

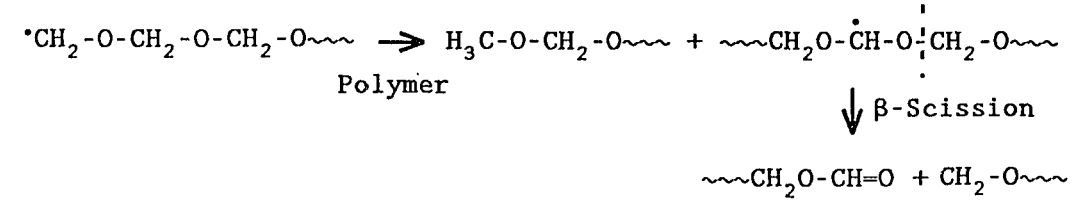

Due to this reaction, the high rate of formation of formate end groups is expected.

A comparison of formation rates for formate end groups (Fig. 2-24) in the radical and acidic degradation processes indicates that the formation rate of formate end groups in the radical degradation is much lower than in acidic degradation by a factor of at least 3. In a comparison of kinetic variations on methoxy end groups (Fig. 2-25) for its two processes, the methoxy end groups in the radical degradation decrease linearly in contrast with their fluctuation in the acidic degradation.

The low formation rate of formate end groups and the trend of methoxy end groups decreasing linearly indicate hydrogen abstraction reaction in the radical degradation process is at a lower rate than hydride transfer in the acidic degradation process.

iv. Degradation Process involving Oxidation

In the radical degradation process of TOX-DOL copolymer initiated by hydroperoxide (Luperox), 2,5-dihydroperoxy-2,5-dimethyhexane, the rate is relatively slow compared with the degradation initiated by AIBN. This is to be expected due to the lower activation energy of decomposition for AIBN compared to Luperox. However, higher yields of formate end groups and hemiacetal hydroxyl group

Fig. 2-24 Rates of formate end groups formed during degradation of TOX-DOL copolymer: Acidic vs. Radical

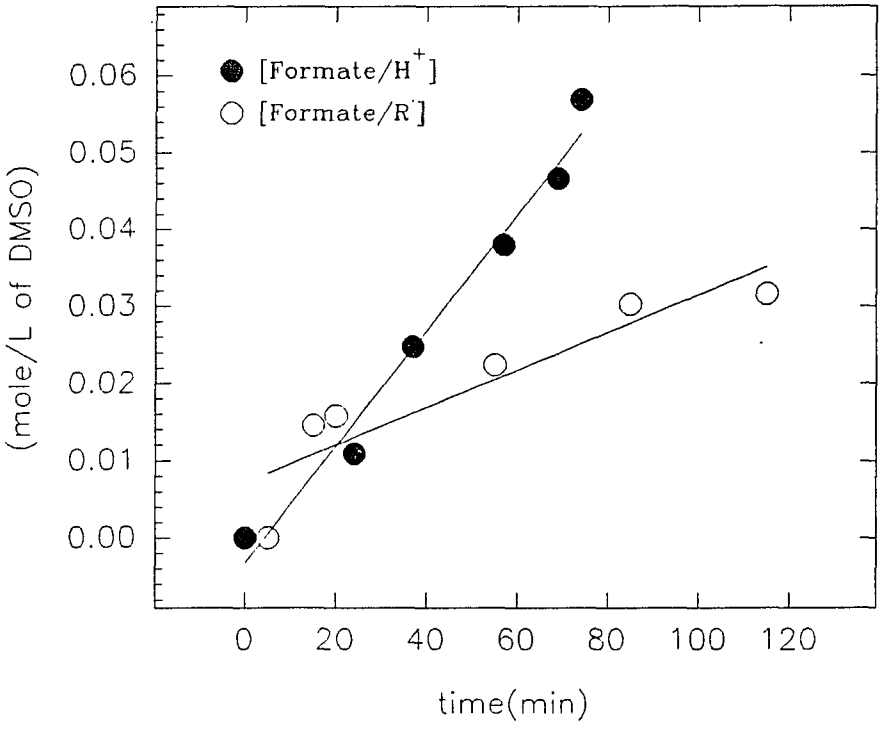

[R·] , time average concentration at time t

● Rate per chain = 1.1 x 10^{-5} (sec^{-1}), initiated by CF_3COOH

○ Rate per chain = 3.3 x 10^{-6} (sec^{-1}), initiated by AIBN

Fig. 2-25 Concentration for methoxy end groups of TOX-DOL copolymer during degradation: Acidic vs. Radical

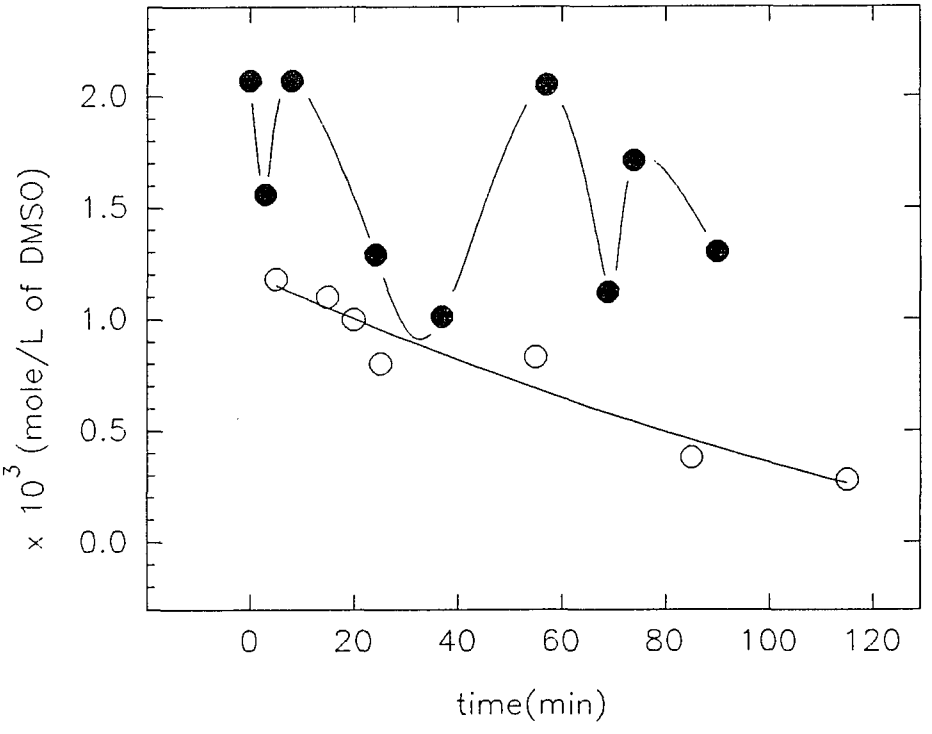

● Acidic Degradation initiated by $[CF_3COOH]$ at 2.4 x 10^{-2} (mol/L)

○ Radical Degradation initiated by [AIBN] at 2.4 x 10^{-2} (mol/L)

were observed. This can be explained by the oxidation process of polymer backbone radicals. The generation of oxygen from Luperox is considered as free radical induced decomposition reactions (21):

$$ROOH \longrightarrow RO^{\bullet} + {}^{\bullet}OH$$

$$ROOH + RO^{\bullet} \longrightarrow R\text{-}OO^{\bullet} + R\text{-}OH$$

$$2\ R\text{-}O\text{-}O^{\bullet} \longrightarrow R\text{-}O\text{-}O\text{-}O\text{-}O\text{-}R \begin{cases} \longrightarrow ROOR + O_2\ (10 \sim 20\ \%) \\ \longrightarrow 2\ RO^{\bullet} + O_2\ (90 \sim 80\ \%) \end{cases}$$

A comparison of ^1H NMR spectra of degraded TOX-DOL copolymer initiated with AIBN (Fig. 2-26 (A)) and Luperox (Fig. 2-26 (B)) reveals that in the degradation process initiated by Luperox, a much higher concentration of formate end groups and a broad peak at 6.8 ppm was observed even at lower level of degradation. The broad peak usually emerged at 6.0 ppm and shifted to 6.8 in the final stage of the degradation.

The mechanism for formation of formate end groups at high concentration can be illustrated as follows (Scheme 2-13):

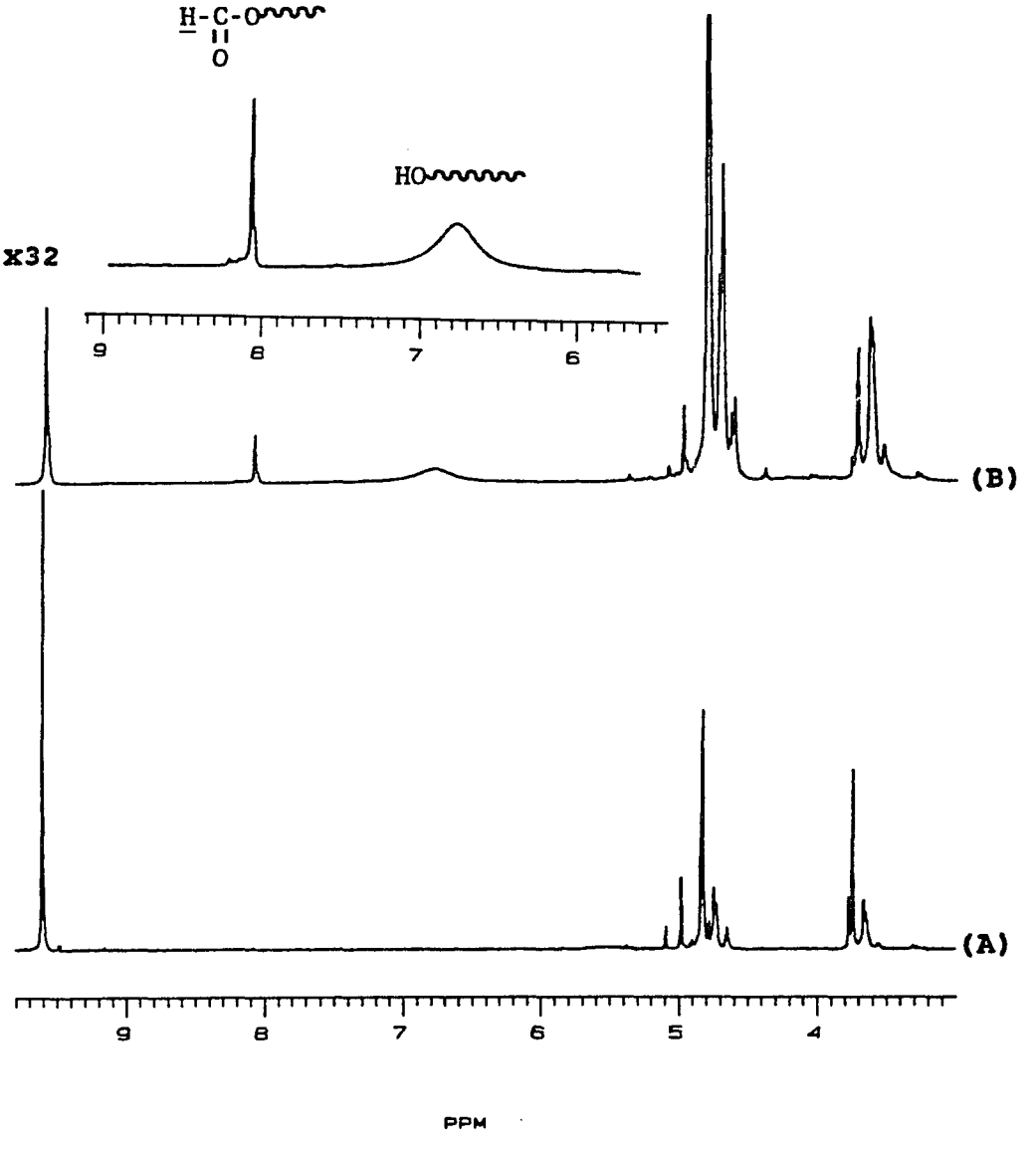

Fig. 2-26 ^{1}H NMR Spectra of degraded TOX-DOL copolymer in DMSO-d_6 solution at 120 °C. (A) 35 min after initiation by addition of 2.4 X 10^{-2} M of AIBN (B) 196 min after initiation by addition of 2.4 X 10^{-2} M of Luperox

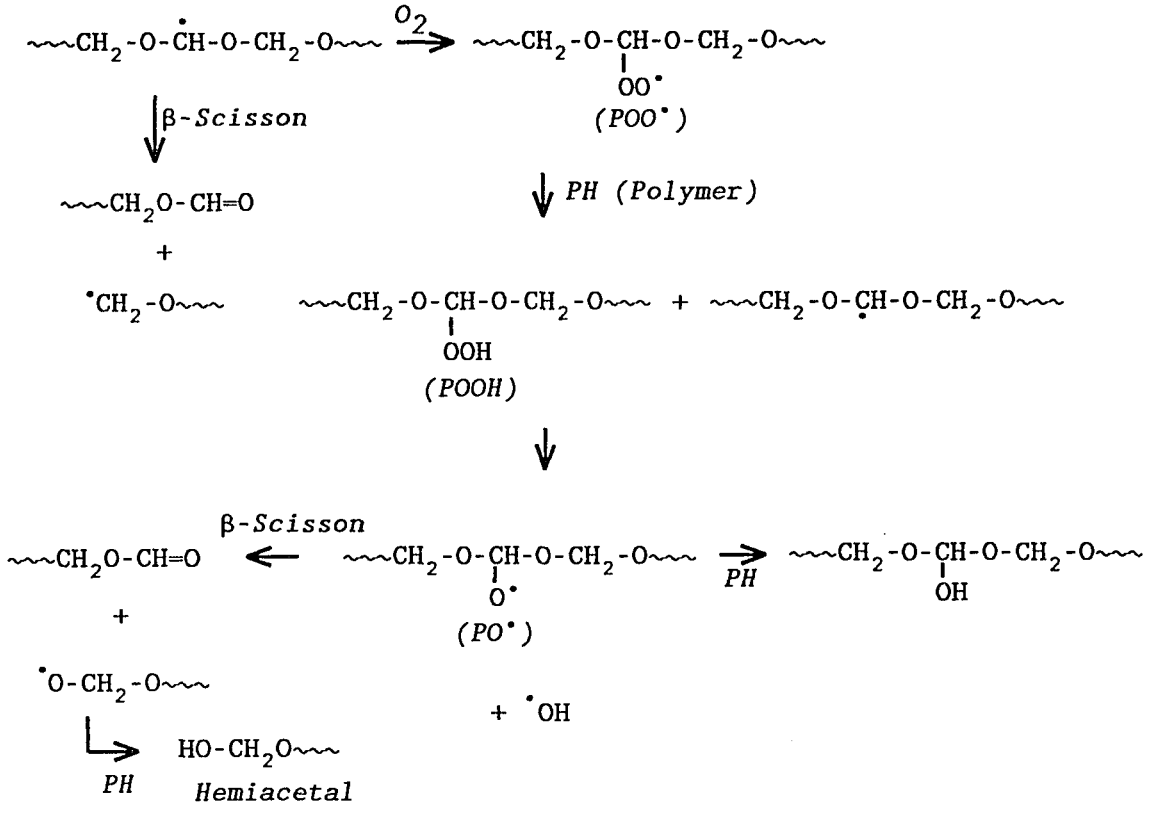

Scheme 2–13

The secondary alkoxyperoxy radicals, *POO•*, formed from peroxidation of the backbone radicals, can readily abstract a hydrogen atom from the polymer chain to form polymer hydroperoxide, POOH. The polymer hydroperoxide can decompose to primary alkoxy *PO•* radicals. Formate end groups can be formed from the β-scissions of *PO•* radicals and the backbone radicals. The hydroxyl groups can be generated by hydrogen

abstraction reaction of alkoxy radicals (*PO*• or •O-CH_2-O~~~) from polymer. The broad peak observed at about 6.7 ppm of ^1H NMR spectrum (Fig. 2-26 (B)) can be attributed to -OH groups generated in the hydrogen abstraction reaction of *PO*• radicals from polymer.

Formation of formates has been reported from the favored β-scission of *PO*• radicals in the oxidation of polyethylene oxide (22):

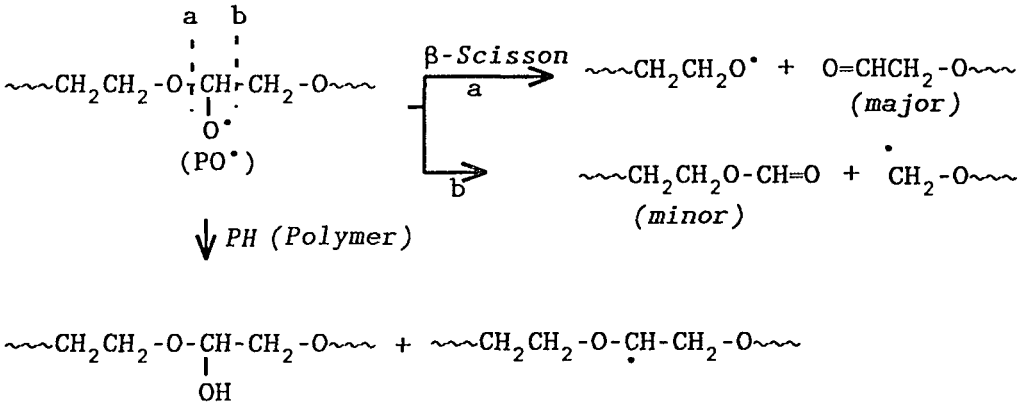

Formate end groups as well as carbonate groups have been detected by IR spectroscopy in the photo-oxidation degradation process of polyacetal copolymer film (3). The author proposed that the β-scission reaction and cage reaction of the alkoxy radical yield formate end groups and carbonate groups, respectively:

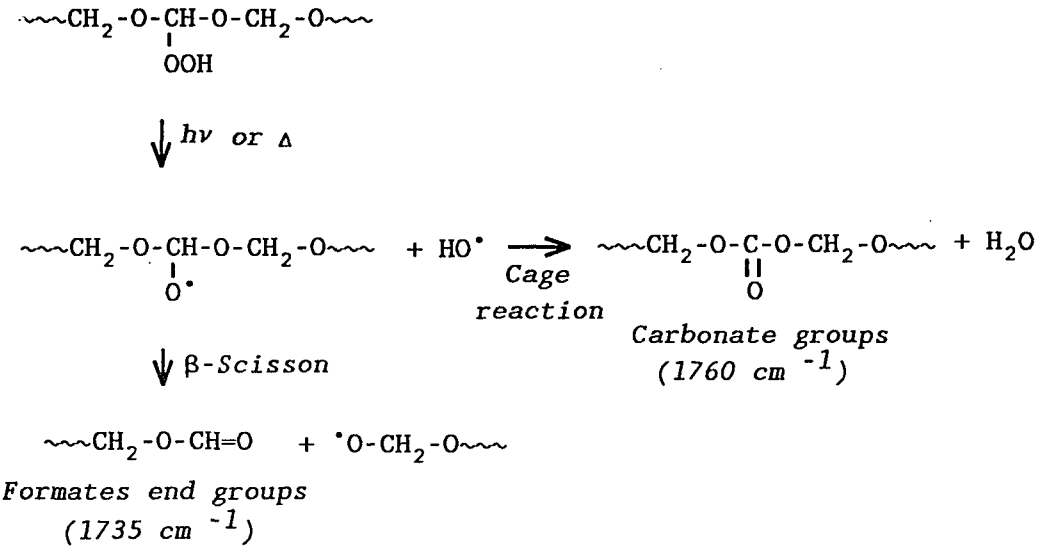

Carbonyl stretching of formate group was detected at 1735 cm $^{-1}$, while that for carbonate was observed at 1760 cm $^{-1}$.

v. Degradation Scheme

Based upon ^{1}H NMR data analysis of the degraded chain sequences, the degradation products and the kinetic behaviors discussed above, a mechanism of radically degraded TOX-DOL copolymer initiated by AIBN at 120 °C in DMSO-d_6 solution is proposed (Scheme 2-14):

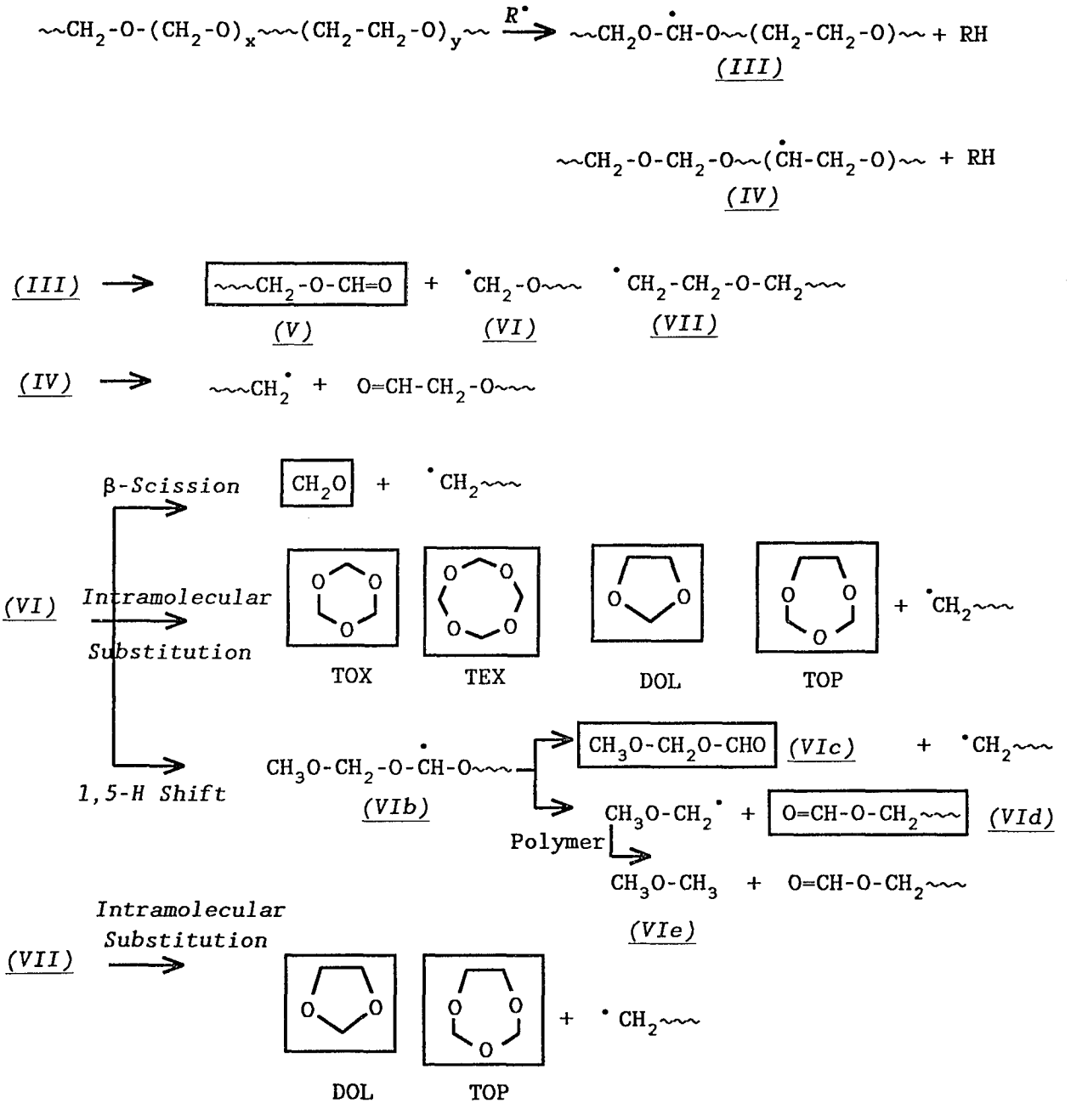
~~CH2-O-(CH2-O)x~~~(CH2-CH2-O)y~~ R•
~~CH2O-CH-O~~(CH2-CH2-O)~~ + RH
(III)
~~CH2-O-CH2-O~~(CH-CH2-O)~~ + RH
(IV)
(III)
~~~CH2-O-CH=O
(V)
•CH2-O~~~
(VI)
•CH2-CH2-O-CH2~~~
(VII)
(IV)
~~~CH2•
O=CH-CH2-O~~~
β-Scission
CH2O
•CH2~~~
(VI)
Intramolecular Substitution
TOX
TEX
DOL
TOP
•CH2~~~
1,5-H Shift
CH3O-CH2-O-CH-O~~~
(VIb)
CH3O-CH2O-CHO
(VIc)
•CH2~~~
CH3O-CH2•
O=CH-O-CH2~~~
(VId)
Polymer
CH3O-CH3
O=CH-O-CH2~~~
(VIe)
Intramolecular Substitution
(VII)
DOL
TOP
•CH2~~~

Scheme 2–14

2.3. Comparison of two Degradation Processes of TOX-DOL Copolymer, Acidic vs. Radical

It has been seen that radical degradation system in using of Luperox as radical initiator involves oxidation of polymer backbone radicals due to generation of oxygen from decomposition of hydroperoxide. Also this system must include oxidation of formaldehyde to formic acid which can initiate the acidic route of degradation. Exclusion of acidic route of degradation process was achieved by use of AIBN as initiator for the radical degradation study of TOX-DOL copolymer. In this system, AIBN decompose to mostly alkyl radicals:

$$(CH_3)_2\underset{CN}{\overset{|}{C}}\text{-N=N-}\underset{CN}{\overset{|}{C}}(CH_2)_3 \rightarrow 2(CH_3)_2\underset{CN}{\overset{|}{C}}{}^{\bullet} + N_2$$

without the generation of oxygen during the degradation process. A fair comparison for two routes of degradation processes, acidic and radical, is now possible based on the acidic degradation initiated by trifluoroacetic acid and the radical degradation initiated by AIBN.

The comparison between two processes includes the comonomer stability, facility of β-scission reaction, backbiting reaction vs. radical substitution reaction, and the relative degradation rates of active chain ends in terms

of the rate for elimination of monomer units. These comparisons revealed the following results. The most unstable triad sequence of polymer chain by acid attack is EME while MMM is the most unstable one toward radical attack. β-Scission reaction of the radical chain end is at a faster rate than of the cationic chain end by a factor of 10. Formation rates of DOL and TOP are slightly slower but formation rates of TOX and TEX are slightly faster in the acidic process than that in the radical process. The difference of activation energy between β-scission and backbiting of cationic chain end is lower than the case for radical chain end. On the basis of per chain end, the radical chain end degrades more than eight times faster than the cationic one.

(a) Stability of Comonomer Sequences

A comparison of ^{1}H NMR spectra between radical degradation and acidic degradation at a comparable stage of degradation reveals a significant difference in the relative intensity of the triad peaks (Fig. 2-27). At 25 minutes of radical degradation (Fig. 2-27 (A)), the absorption peaks EME, MEE still persisted in the radical process while they had almost vanished at 24 minutes in the acidic degradation

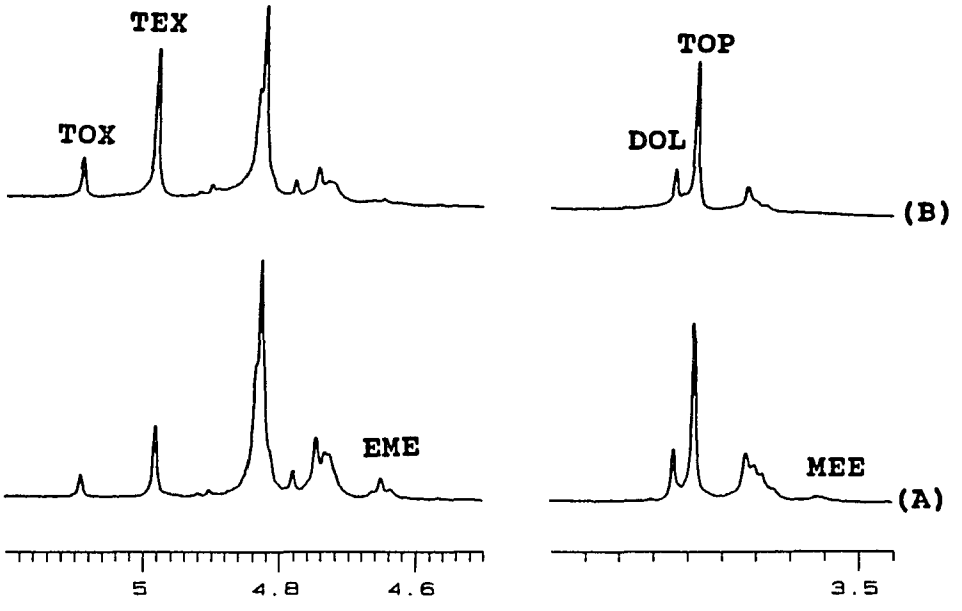

Fig. 2-27 ^{1}H NMR Spectra of degraded TOX-DOL copolymer in DMSO-d_6 solution at 120 °C. (A) 25 min after initiation by addition of 2.4 X 10^{-2} M of AIBN (B) 24 min after initiation by addition of 2.4 X 10^{-2} M of trifluoroacetic acid

(Fig. 2-27 (B)).

This comparison demonstrates the stabilities of comonomer sequences in two routes of degradation process. The most unstable methylene oxide unit is EME in the acidic process and the most unstable methylene oxide unit is MMM in the radical process. This can be clearly illustrated by the ratio of remaining fraction of EME to MMM. For acidic degradation, this ratio is 1, while for radical degradation, a high ratio of 4 is obtained (Fig. 2-27).

(b) β-Scission Reaction

The formation of formaldehyde in both of the degradation processes is illustrated in Scheme 2-15.

In the acidic degradation, formaldehyde is produced by β-scission of cationic chain ends as well as through unzipping process of hemiacetal chain ends (23). However, the concentration of hemiacetal chain ends is much lower than that of cationic ends. Consequently, unzipping process turned out to be less important and β-scission is considered as a main reaction to produce formaldehyde.

In the radical degradation process, formaldehyde is formed only from β scission reaction of radical chain end.

In Acidic Degradation

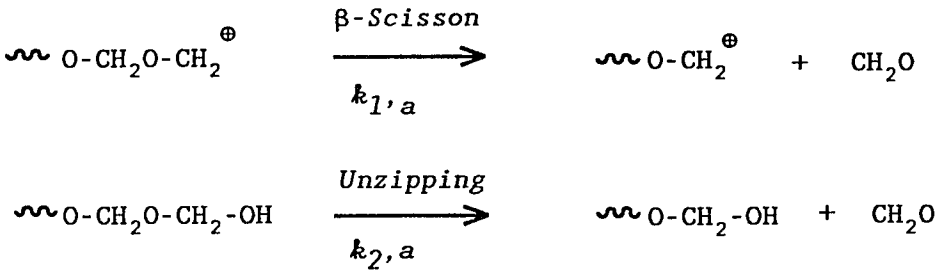

In Radical Degradation

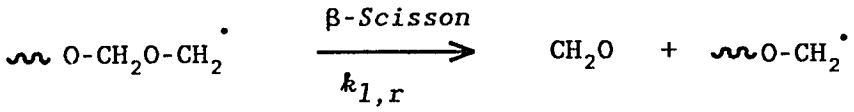

Scheme 2–15

A comparison of the initial rate of formaldehyde formation for both degradation processes is given in Table 2-5. This rate per active chain was calculated from the maximum slope of the time curve (e.g. Fig. 2-9, Fig 2-19) in the region where formation of cyclic acetals are still slow, and the polymer degradation is less than 50 %. The values, $\mathcal{R}$, formation rates of formaldehyde, were obtained by dividing the formation rate with concentration of $[H^{\oplus}]$ or the time average radical concentration, $[R^{\bullet}]$, at degradation time t.

These results indicate that formaldehyde is generated faster per active chain end in the radical degradation process than in the acidic degradation processes at least by a factor of 10, i.e. β-scission reaction is much more efficient from the radical chain end than from the cationic chain end. If correction for hemiacetal unzipping in the acidic degradation was made, the factor would be even higher.

(c) Backbiting Reaction vs. Intramolecular Substitution Reaction

Comparisons of the formations for cyclic acetals in

Table 2-5 Comparison for initial rate of formaldehyde generation during degradation of TOX-DOL copolymer: Acidic vs. Radical

	Formation rate per chain R (sec^{-1})
Acidic Degradation*	3.9×10^{-3}
Radical Degradation**	3.3×10^{-2}

* $[H^+] = 2.4 \times 10^{-2}$ (mol/L) during the degradation process

** $[R\cdot] = 2.1 \times 10^{-3}$ (mol/L) at 10 min, a time average value.

both degradation processes reveal the kinetic reactivity of degraded chain ends. The comparison of formation for TOX in both processes indicate that backbiting of cationic chain ends, ~~~$OCH_2^{\oplus}$, competes better than intramolecular substitution of radical chain ends, ~~~$OCH_2^{\bullet}$, with β-scission.

The ^1H NMR spectra (Fig. 2-27) for the early stage of the two degradation processes with comparable concentrations of TOP and DOL show large difference in the concentrations of TOX and TEX. The concentrations of TOX and TEX relative to TOP and DOL in the radical degradation are much lower than that in the acidic degradation.

The formation rates of cyclic acetals in the early stage of degradation were calculated from the kinetic data (Table 2-6). The formation rates are average of duplicate experiments. For comparison of the formation rates of cyclic acetals between two processes, the formation rates were divided by the concentration of $[H^{\oplus}]$ or $[R^{\bullet}]$ to obtain rate per active chain (Table 2-7). The concentration of $[R^{\bullet}]$ is a time averaged value.

These results show that during the early stage of degradation, the formation rates per chain to give DOL and TOP in the acidic process are slightly slower than that in the radical process but the formation rate of TOX and TEX are slightly faster in the acidic process than that in the

Table 2-6 Kinetic data of cyclic acetals formed in the early stage degradation of TOX-DOL copolymer: Acidic vs. Radical

x 10^{2} (mol/L)

time (min)	[TOX]	[TEX]	[DOL]	[TOP]
		Acidic Degradation *		
37	0.51	0.87	0.67	1.82
21	0.51	0.84	0.58	1.30
17	0.50	0.70	0.64	1.15
		Radical Degradation **		
28	0.08	0.18	0.28	0.77
25	0.01	0.12	0.11	0.37
25	0.08	0.22	0.31	1.10

* $[H^{+}]$ = 2.4 x 10^{-2} (mol/L) during the degradation process

** $[R\cdot]$ = 5.1 x 10^{-3} (mol/L) at 25 min, a time average value

5.7 x 10^{-3} (mol/L) at 28 min, a time average value

Table 2-7 Comparison for initial rate of cyclic acetals formed during degradation of TOX-DOL copolymer: Acidic vs. Radical

Formation rate per chain (sec^{-1})			
R_{TOX}	R_{TEX}	R_{DOL}	R_{TOP}
Acidic Degradation			
2.1×10^{-4}	3.8×10^{-4}	2.5×10^{-4}	6.6×10^{-4}
Radical Degradation			
7.0×10^{-5}	2.1×10^{-4}	2.8×10^{-4}	9.1×10^{-4}

radical process. The lower rate of formation for DOL and TOP in the acidic process can be attributed to the higher reactivity of chain ends, ~~~MME$^{\oplus}$, to participate in ionic side reactions competing with backbiting:

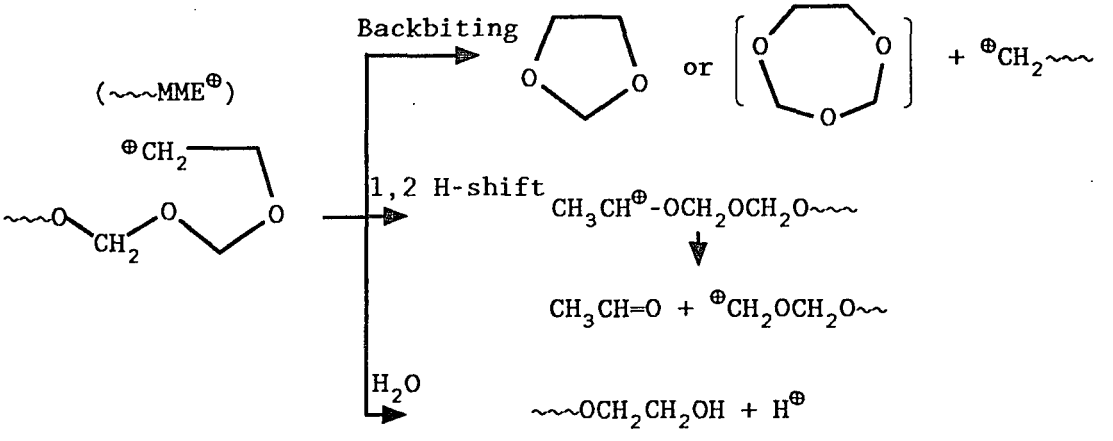

On the other hand, radical side reactions such as 1,2 hydrogen shift reaction of the radical chain ends, ~~~MME$^{\bullet}$, is known to require a much higher activation energy (26). Thus intramolecular substitution of these radical chain ends to form DOL or TOP is favored. Since radical β-scission is more efficient, the concentration of ~~~$OCH_2CH_2^{\bullet}$ is expected to be higher than the concentration of ~~~$OCH_2CH_2^{\oplus}$.

For the formation of TOX and TEX, the chain ends involved are ~~~MMM$^{\bullet}$ and ~~~MMM$^{\oplus}$. Formations of TOX and TEX at slightly lower rates in the radical process are mainly

due to the much faster rate of β-scission. With a rate of generation of formaldehyde ten time faster in the radical process, the radical chain end with at least three M units would be at a much lower concentration. Also, 1,5 hydrogen shift reaction of radical chain ends, ~~~MMM•, may disturb the formation of TOX:

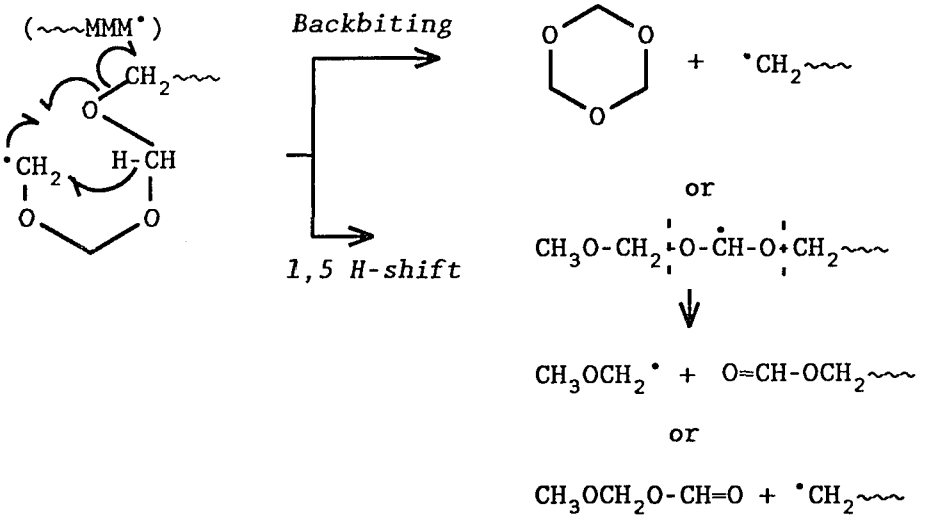

On the other hand, backbiting reaction of cationic chain ends, ~~~MMM$^{\oplus}$, is expected to be favored over 1,5 hydride shift, due to the stability of tertiary oxonium intermediate involved:

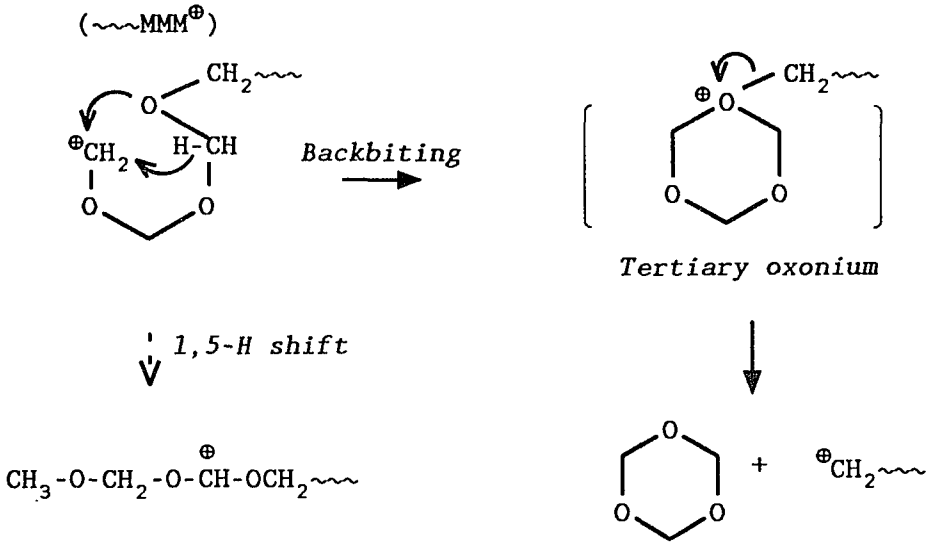

The stability of tertiary oxonium ion is well known. For example, in the polymerization of DOL and other cyclic acetals, the two cations depicted below are considered to play important roles (27,28):

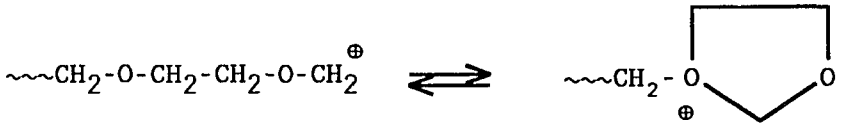

(d) Relative Degradation Rates

The 1,2 hydride shift in acidic degradation and 1,5 hydrogen shift in radical degradation are considered as

minor reactions compared to β-scission, backbiting, and intramolecular substitution reactions. Thus the competition of two unimolecular reactions of the degraded chain ends with M unit become the main consideration: (Scheme 2-16). The competition of β-scission with backbiting for the cationic chain end, and β-scission with intramolecular substitution in the radical chain end can be evaluated based on the relative yields of the formaldehyde to cyclic acetals produced in the degradation processes. The data for the formation of formaldehyde and cyclic acetals and the calculated ratio of formaldehyde to cyclic acetals, ([CH_2O] / ([TOX] + [TEX] + [DOL] + [TOP]), are presented in Table 2-8. This ratio in the radical process is greater than that in the acidic degradation at least by a factor of six, i.e. $(k_{1,r}/ k_{2,}) \cong 6\ (k_{1,a}/ k_{2,})$.

This finding supports the conclusions in sections 2.3.3.(b) and (c): β-scission of radical chain end, ~~~MMM$^{\bullet}$, to give formaldehyde is a more efficient process than that of cationic chain end, ~~~MMM$^{\oplus}$; and the backbiting of cationic chain end, ~~~MMM$^{\oplus}$, is more efficient than the intramolecular substitution of radical chain, ~~~MMM$^{\bullet}$.

From the averaged ratio of 18.1 for [CH_2O] / [Cyclic Acetals] in radical degradation process, the difference of activation energy between β-scission and intramolecular

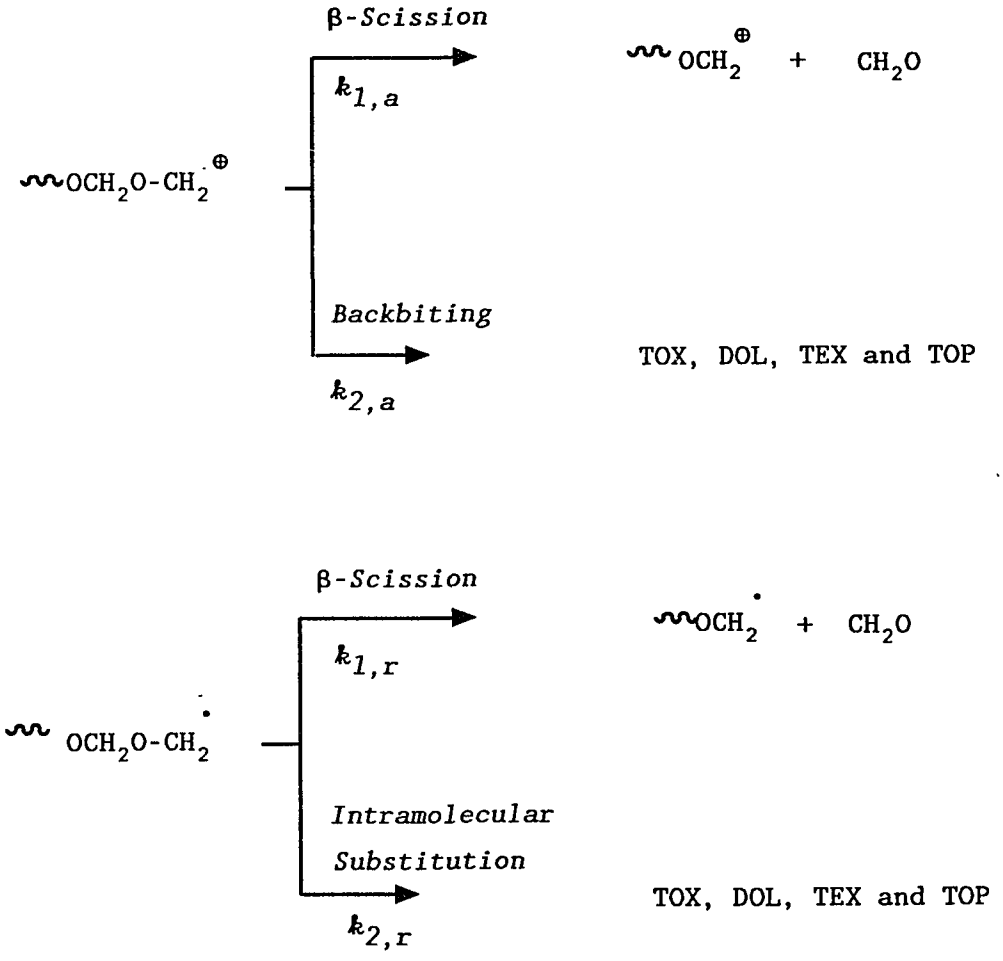
β-Scission
$k_{1,a}$
$\sim\sim OCH_2^{\oplus}$ + CH_2O
$\sim\sim OCH_2O\text{-}CH_2^{\cdot\oplus}$
Backbiting
$k_{2,a}$
TOX, DOL, TEX and TOP
β-Scission
$k_{1,r}$
$\sim\sim OCH_2^{\cdot}$ + CH_2O
$\sim\sim OCH_2O\text{-}CH_2^{\cdot}$
Intramolecular
Substitution
$k_{2,r}$
TOX, DOL, TEX and TOP

Scheme 2–16

Table 2-8 Data for formation of formaldehyde, cyclic acetals and their ratio during degradation of TOX-DOL copolymer at the early stage: Acidic vs. Radical

x 10^{2} (mol/L)

time (min)	[FD]	[TOX]	[TEX]	[DOL]	[TOP]	Ratio*
		Acidic Degradation initiated by CF_3COOH				
8	6.98	0.1	0.41	0.27	0.94	4.06
10	6.41	0.35	0.70	0.39	1.42	2.09
5	7.06	0.20	0.73	0.30	1.22	2.90
						3.01**
		Radical Degradation initiated by AIBN				
11	4.09	0	0.06	0.07	0.12	16.4
10	4.94	0	0.02	0.08	0.19	17.0
15	4.37	0.02	0.06	0.04	0.09	20.9
						18.1**

[FD] = Formaldehyde

*Ratio = [FD]/([TOX]+ [TEX] + [DOL] + [TOP])

**Average ratio

substitution reactions was calculated in the same manner as given in section 2.3.1.(c) and was found to be 9.4 (kJ/mol). The difference of activation energy between β-scission and backbiting reaction has been determined to be 4.5 (kJ/mol) in the acidic degradation (section 2.3.1.(c)). Thus, the difference of activation energy between β-scission and backbiting reaction of cationic chain end is at least two times lower than that of activation energy between β-scission and substitution of radical chain end.

The lower difference of free energy of activation in the cationic process can be explained in terms of involvement of the tertiary oxonium ion structure of the chain ends:

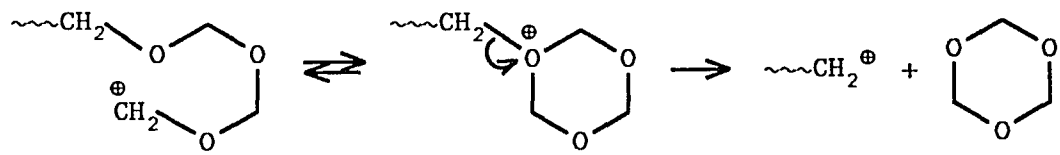

Tertiary oxonium

On the other hand, higher activation energy should be required for β-scission of cationic chain end than β-scission of radical chain end. The former process involves heterolysis of C-O bond with shift of two electrons from the same bond, while the latter, homolysis of C-O bond with shift of only one electron:

β-Scission of Cationic Chain End

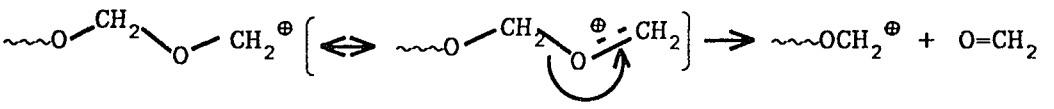

β-Scission of Radical Chain End

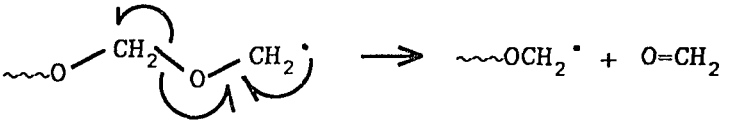

Based on the calculated difference of activation energies and the discussion above, the difference of activation energy for formations of formaldehyde and cyclic acetals in two process is illustrated in Scheme 2-17.

In conclusion, with lower free energy of activation, the β-scission of radical chain end is more efficient than that of cationic chain end, and the backbiting of cationic chain end is more efficient than the intramolecular substitution of radical one.

The net degradation rate of chain end in both degradation processes can be evaluated in terms of the rate for elimination of monomer units M or E. The rate for elimination of monomer units were calculated from the sum of the formation rate for formaldehyde and cyclic acetals. These values (Table 2-9) indicate that on the basis of per

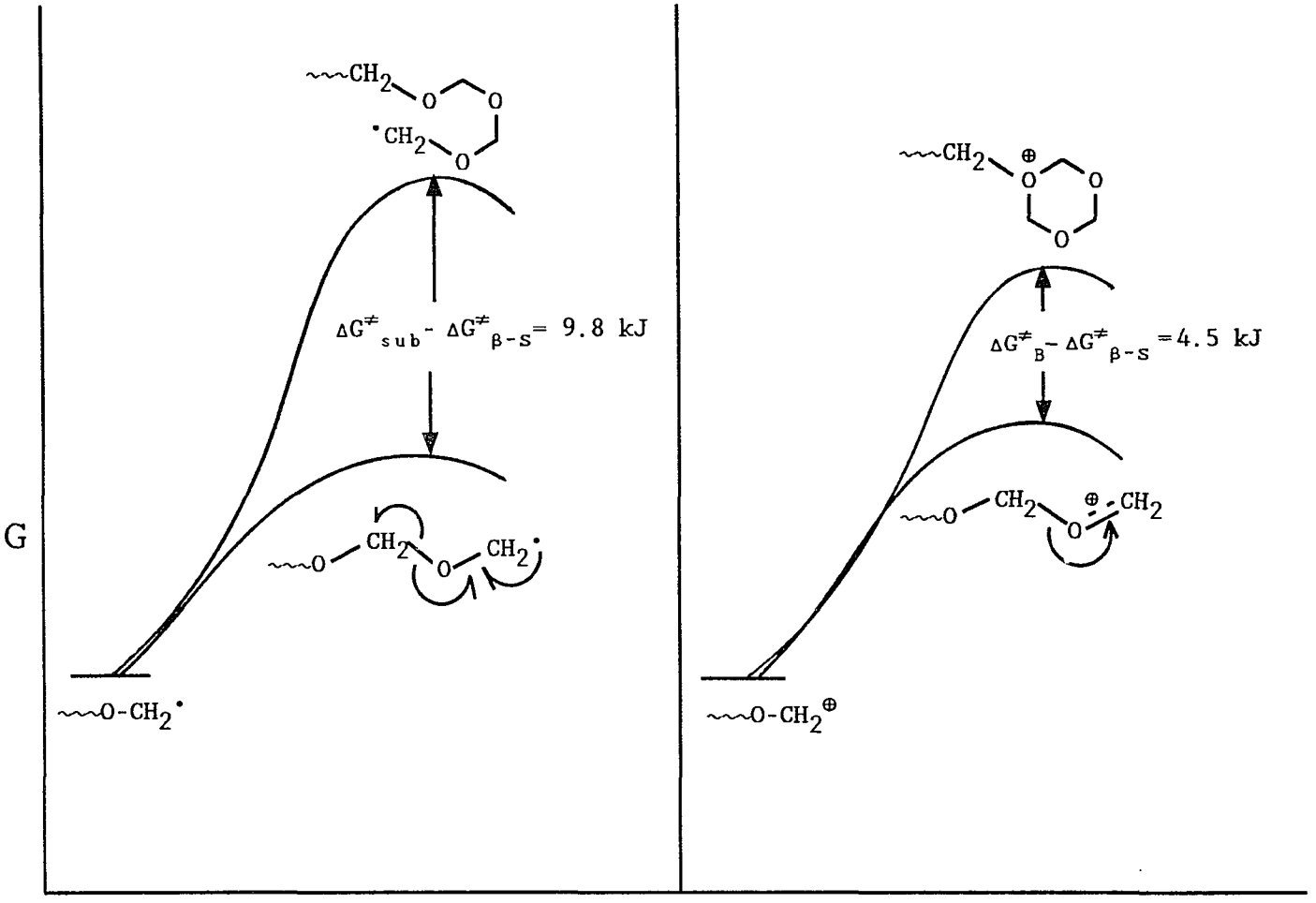
G
$\sim\sim CH_2$
O
O
$\cdot CH_2$
O
$\Delta G^{\neq}_{sub} - \Delta G^{\neq}_{\beta\text{-}s} = 9.8$ kJ
$\sim\sim O$
CH_2
O
$CH_2\cdot$
$\sim\sim O\text{-}CH_2\cdot$
$\sim\sim CH_2$
$\oplus$
O
O
O
$\Delta G^{\neq}_{B} - \Delta G^{\neq}_{\beta\text{-}s} = 4.5$ kJ
$\sim\sim O$
CH_2
O
$\oplus$
CH_2
$\sim\sim O\text{-}CH_2^{\oplus}$
Reaction coordinate

Scheme 2–17

Table 2-9 Comparison of rate data for degradation of TOX-DOL copolymer: Acidic vs. Radical

$R_{Formaldehyde}$	$R_{Cyclic\ Acetals}$	R_{Sum}
Formation rate per chain(sec^{-1})		
Acidic Degradation initiated by CF_3COOH		
3.90×10^{-3}	1.08×10^{-3}	4.08×10^{-3}
Radical Degradation initiated by AIBN		
3.30×10^{-2}	1.47×10^{-3}	3.44×10^{-2}

active chain end, the radical chain end degrade more than eight times faster than the cationic one.

2.4. Conclusions

The present study on the degradation processes of trioxane-dioxolane copolymer provides some valuable information on the fundamental chemistry of chain degradation. Previous works were limited to qualitative aspect of polyacetal degradation. The present investigation gives detailed quantitative data, allowing systematic comparison between acid and radical degradations. From the ^{1}H NMR study for the degradations of TOX-DOL at 120 °C in DMSO-d_6 solution caused by addition of trifluoroacetic acid, AIBN, and Luperox, the kinetic time curves for formaldehyde, formate end group, and cyclic acetals, TOX, DOL, TEX and TOP were obtained. Based on the observations on kinetic behaviors for triad sequences of the degraded copolymer chains and the products formed during degradation, the processes in acidic and radical degradations are compared. Formaldehyde, a main degradation product, is released through unzipping of hemiacetal chain ends and β-scission reaction of the cationic or radical chain ends.

Formate end groups are formed from hydride transfer

reactions during the acidic degradation process and are formed mainly from the β-scission reaction of polymer backbone radicals in the radical degradation process. For a system in the presence of oxygen, formate end groups are also formed from the decomposition of oxidized radicals.

Cyclic acetals are produced by backbiting of the cationic chain ends and intramolecular substitution of radical chain ends. Slightly slower rates of formations for TOX and TEX in the radical process than acidic process are explained by faster β-scission reaction of radical chain end with M unit, leading to low concentration level of consecutive methylene oxide units. The most susceptible triad sequence in radical degradation is the MMM sequence. While for acidic degradation, the triads containing at least one E unit are more favored for protonation. Thus, two process differ fundamentally even though they share most of the degradation products. In the later stage of the degradation processes, shifts of equilibria from TEX to TOX and from TOP to DOL were observed because cyclic acetals, TEX and TOP, reached the maximum of the equilibrium concentrations. In addition to these degradation products, hemiacetal chain ends, secondary oxonium ions and free acids are observed in the acidic degradation process.

A comparison of initial formation rate for formaldehyde in both of processes indicate that β-scission reaction

proceed more efficiently from radical chain ends than cationic chain ends by a factor of 10. The net degradation rate of chain end, in terms of the rate for elimination of monomer units M or E, for radical process is eight times faster than for the cationic one.

2.5. References

1. Patel, V.; Yang, N.-L., Dolce, T., *Am. Chem. Soc. Div. Poly. Mater. Sci. Eng.* **1984**, 51, 149.
2. Felix, R.; Stohler, K. B., *Die Angew. Mak. Chem.*, **1990**, 176/177, 323, 3074.
3. Gerdette, J. L.; Sabel, H. D.; Lemaire, J., *Die Angew. Mak. Chem.*, **1991**, 188, 113.
4. Pesce, R., *Stabilization and Degradation of Acetal Copolymers*, Doctoral Thesis, The City Univesity of New York, **1988**.
5. Penczek, S.; Kubisa, P.; Matjaszwski, K., Cationic Ring Opening Polymerization, part II, Synthetic Applications in *Adv. Polym. Sci.*, **1985**, 68, 114.
6. Cordes, E. H., "Mechanism and Catalysis for the Hydrolysis of Acetals, Ketals and Ortho esters," in Progress in *Physical Organic Chemistry*, **1967**, vol 4, 1. Cordes, E. H., *Chemical Reviews*, **1974**, vol 74, No 5,

581.

7. Pruckmayr, G.; Wu, T. K., *Macromolecules*, **1973**, vol 6, No 1. 33.

8. Yamashita, Y.; Asakura, T.; Okada, M. and Iti, K., *Die Makromol. Chem.*, **1969**, 129, 1.

9. Ishigaki, I.; Ito, A; Iwai, T., *Journal of Polymer Science*, **1972**, Part A-1, vol 10, 1883.

10. Flescher, D.; Schulz, R. C., *Makromol. Chem.*, **1975**, 176, 677.

11. Mengoli, G.; Furlanetto, F., *Die Makromol. Chem.*, **1975** 176, 143.

12. Gutsche, C. D., *"The Chemistry of Carbonyl Compounds"*, Prentice-Hall, Inc. **1967**, p 4.

13. Xiao, F.-F.; Yang, N.-L., Unpublished research result.

14. Hermann, H. D.; Fischer, E.; Weissermel, K., *Makromol. Chem.*, **1966**, 90. 1.

15. Penczek, S.; Kubisa, P.; Matjaszwski, K., Cationic Ring Opening Polymerization, part II, Synthetic Applications in *Adv. Polym. Sci.*, **1985**, 68, 30.

16. Brandup, J.; Immergut, E. H., Eds, with Elias, H.-G., *"Polymer Handbook"*, A Wieley-Interscience, New York, **1975**. p II-3

17. Kuhn, L. P. ; Wellman, C., *Journal of Organic Chemistry*, **1957**, vol 22. 774.

18. Menapace, L. W.; and Kuivila, H. G., *J. Amer. Soc.*,

1964, 86, 3047.

19. Drury, R. F.; Kaplan, L. Kochi, *J. Amer. Chem. Soc.*, **1972**, 94, 3982 in *"Free Radicals"* by Kochi, J. K., vol I, A Wiely-Interscience, New York, **1973**, p 135.
20. Kochi, J. K., *"Free Radicals"*, **1973**, vol I, A Wiely-Interscience, New York, **1973**, p 380.
21. Factor, A.; Russell, C. A.; Traylor, T. G., *J. Amer. Chem. Soc.*, **1965**, 87, 3692.
22. Decker, C., *Journal of Polymer Science, Polymer Chemistry Edition*, **1977**, vol 15, 802.
23. Morelli, F. et. al., *Ann. Chim.* Rome, **1969**, 59, 733.
24. Stanonis, D. J.; King, W. D.; Vail, S. L., *Journal of Appilied Polymer Science*, **1972**, vol 16, 1447.
25. Lazer, M., *"Free Radicals in Chemistry and Biology"*, CRC press, Inc., Boca raton, Florida, **1989**, p 63.
26. March, J., *"Advanced Organic Chemistry"* 3rd. ed. **1985**, A Wiely-Interscience, New York, p 942.
27. Schulz, R. C.; Hellermann, W.; Nienburg, J.; Cyclic Compounds Containing Two or More Oxygen Atoms, in: *Ring-Opening Polymerization*, Chapter 6, vol. 1, Ed. by Ivin, K. J. and T. Saegusa, Elsevier Applied Science Publishers LTD, England, **1984**, p 383
28. Yokoyama, Y.; Okada, M.; Sumimoto, H., *Makromol. Chem.*, **1978**, 179, 1393.

3. SYNTHESIS AND MODIFICATION OF ACETAL COPOLYMER

3.1. Introduction

Through functionalization, one may prepare new acetal copolymers with new properties different from the basic polyacetal system. Various functional groups impart polymer with a range of useful properties.

Copolymers, prepared from copolymerization of trioxane with 5-ethyl-5-hydroxymethyl-1,3-dioxane (EHMDO), possessed low molecular weight, good thermostability and high crystallinity (1).

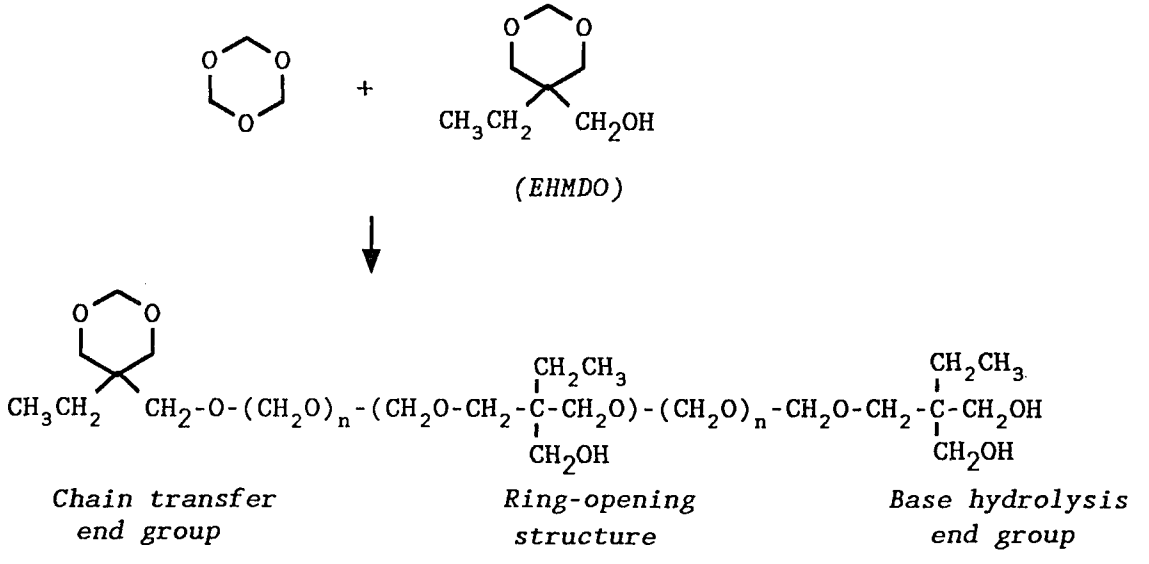

Various types of copolymers or terpolymers, which contain large amounts of comonomer such as dioxolane, dioxepane and bifunctional monomer like 1,4-butanediol diglycidylether, butadiene diepoxide, were prepared by Collins et. al. (2, 3,

4). Some of them are reported as noncrystalline elastomers (2) and had adhesive properties (3) and low glass transition temperatures (4).

Stabilization of polyacetals can only be accomplished based on a full understanding of the degradation mechanism. The process of degradation of acetal polymers can be initiated by acid or radical attack. Auto-oxidative degradation process becomes effective in the presence of oxygen at temperatures above 160^{0}C. The oxidative degradation may be suppressed by antioxidants such as sterically hindered phenols or aromatic amines (5, 6, 7). Acidolysis may be prevented by adding stabilizing agents such as acid acceptors or other agents reacting with free formaldehyde, a degradation product.

In order to stabilize the acetal copolymer, the comonomer units should contain 1) stopper units, 2) H^{+} acceptors, 3) formaldehyde acceptors or 4) radical acceptors. Introduction of these stabilizers to acetal polymer can be achieved through chemical modification of the polymer structure via functionalization. The investigation of the degradation of polyacetal have been documented (8, 9). Functionalization through side chain bromo group has been documented (Sun and Yang in preparation).

The present work pursuits to synthesize thermally stable trioxane copolymers with bound stabilizers through functionalization. Amine and hindered phenol groups can be bound to trioxane copolymer through chemical modifications such as elimination and substitution reaction.

This study presents trioxane copolymer systems carrying backbone vicinal dibromo functional groups and its chemical modifications for the introduction of new functional groups. Functional groups such as amino group and carbon-carbon triple bond are introduced to trioxane copolymer. The structures of new trioxane copolymer system were confirmed by ^1H NMR spectroscopy. Carbon-carbon triple bond was further confirmed by UV-Visible spectroscopy. The trioxane copolymer functionalized with -C≡C- showed stability against harmful degrading agent, Br_2. In the thermogravimetric analysis (TGA), the trioxane copolymers functionalized with -C≡C- and hindered phenol-amine showed better thermal stability to the oxidative degradation than the trioxane copolymer functionalized with -C=C-.

Dibromo functionalized trioxane copolymer was prepared from the copolymerization of 5,6-Dibromo-1,3-dioxepane (DBDXPE) *I* and trioxane (TOX) *II*, in presence of the cationic catalyst, $BF_3O(C_2H_5)_2$ (Scheme 3-1).

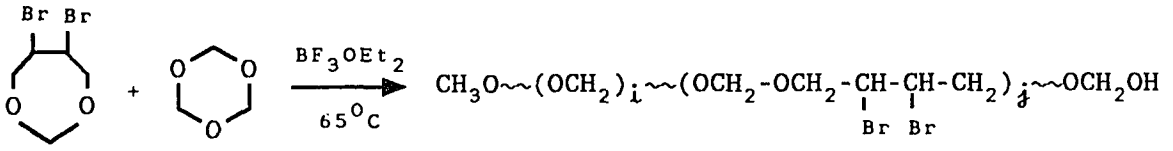

I *III* *Copolymer III*

Scheme 3–1

The crude trioxane copolymer having dibromo groups and the base hydrolyzed copolymer having mono bromo groups were further modified through elimination and nucleophilic substitution reactions. Complete dehydrobromination led to formation of carbon-carbon triple bond along the polymer chain. Amino group was grafted on the trioxane copolymers through substitution of bromo group. Hindered phenol-amine was synthesized and grafted in the side chain of trioxane copolymer by replacing bromo groups. The chemical modifications of trioxane copolymer are outlined in Scheme 3-2.

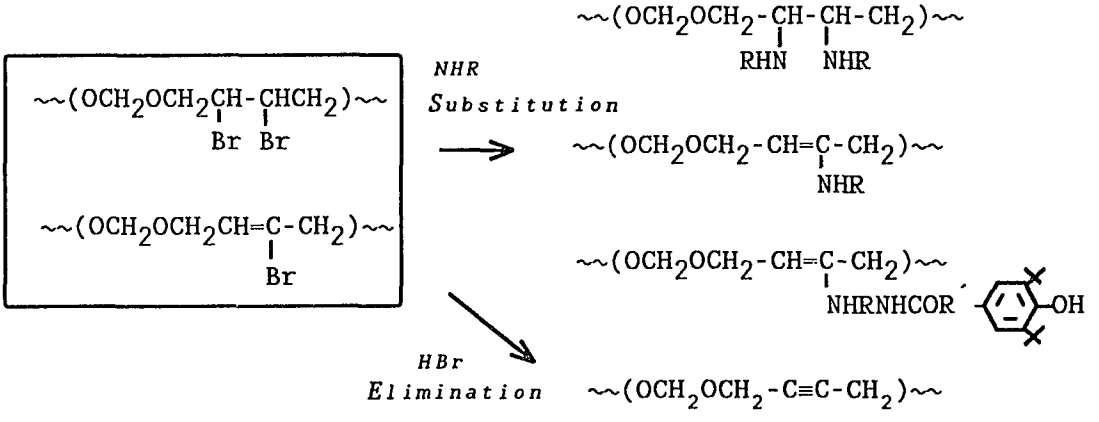

Scheme 3–2

3.2. Synthesis of Trioxane Copolymer with Bromo Groups, Copolymer *III*

3.2.1. Experimental

All starting materials were from Aldrich of the highest purity available unless otherwise stated.

(a) Synthesis of Comonomer *I* (5,6-Dibromo-1,3-Dioxepane)

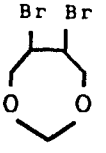

I

5,6-Dibromo-1,3-Dioxepane, *I*, was prepared as follows (10). 1,3-Dioxep-5-ene (10 g) in 10 mL of methanol or carbon tetrachloride (CCl_4) were placed in a 100 mL Erlenmeyerflask, and solution of 5 ~ 6 mL of Br_2 in 10 mL of CCl_4 was added dropwise over a period of 30 minutes at ice temperature. Toward the end of the addition, crystal began to form. The resulting solution was chilled in refrigerator for an hour to complete crystallization and the crystal was collected by filtration and washed with hexane (2 × 5 mL). The yield was about 40 %. ^1H NMR spectra of monomer *I* were obtained at room temperature using DMSO-d_6 as solvent.

(b) Copolymerization of Trioxane with Comonomer *I*

Copolymerization of trioxane with comonomer *I* to give copolymer *III* was carried out in solution using a procedure based on an established method (11). The required amount (1 to 3 g) of distilled trioxane and comonomer were placed in a 100 mL round bottom flask containing 20 mL of cyclohexane. The solution was heated under stirring. When the temperature reached 65 °C, 20 μL of BF_3Et_2O was injected through a serum stopper every 2 minutes until copolymerization occurred to give a white precipitate. The total amount of initiator was about 60 ~ 100 μL. Then the copolymerization was allowed to proceed at 65 °C for 20 hours. At the conclusion of the polymerization, the polymer was removed and pulverized in a Waring blender. The crude copolymer was then stirred in 10 mL of methanol containing 1 % triethanolamine, TEA, for half an hour and then collected by filtration and washed with acetone (3 × 5 mL). The crude copolymer was then filtered and dried under vacuum at 56 °C for 3 hours. Comonomer incorporation and yields are presented in Table 3-1.

(c) Base Hydrolysis of Copolymer *III*

Table 3-1 Copolymerization of trioxane with *I*

Sample [a] #	Mol-% of *I* (feed/incorporation)	Yield (%)
59	1.7/0.2	92
54	2.3/1.1	89
58	3.1/2.4	89
39	5.4/3.5	84
14	7.0/5.9	72
56	12.4/6.1	53

[a] Crude copolymer *III* before base hydrolysis

In order to remove unstable chain end groups, the crude trioxane copolymer *III* was base hydrolyzed using a established procedure (11). A typical example is as follows.

Crude trioxane copolymer *III* (8.9 g) was placed in 250 mL of round bottom flask. N,N-Dimethylformamide (DMF), 45 mL, and benzyl alcohol (45 mL), and 0.9 mL of triethanolamine (TEA, 1 % of total volume) was added. Reaction was kept at 170 ~ 180 °C under stirring for ca. 1.5 hours until no more evolution of formaldehyde was observed. Then, the solution was stirred at room temperature to yield crystalline polymer. The resulting solid was washed with acetone (3 x 5 mL) and dried under the vacuum at 56 °C for 3 hours. For this example, the yield of reaction was 45 % of crude trioxane copolymer *III* with 6.1 mol-% incorporation of comonomer *I*.

(d) ^{1}H NMR analysis

All of 1D and 2D NMR spectra were obtained on an IBM 200-SY NMR spectrometer using NMR 1 software. For the ^{1}H NMR spectrum of crude trioxane copolymer *III*, 1 ~ 2 μL of tripropyl amine was added to the DMSO-d_6 solution of copolymer to suppress the degradation of crude copolymer while NMR transients were acquired. Integration of absorption peak area and peak deconvolution by curve fitting were

carried out using "NMR 1" software.

3.2.2. Results and Discussion

(a) Structure of Comonomer *I*

The ^1H NMR spectrum of *I* with it's chemical shifts assignment is shown in Fig. 3-1 (A). Comonomer *I* is confirmed to be the trans isomer based on the analysis of it's ^1H NMR spectra. Methylene protons, H_1's, between two oxygens are magnetically equivalent in the trans isomer and give a singlet absorption. Methylene protons, H_2 and $H_{2'}$, next to bromine are inequivalent and form an AB systems and basically show two sets of four line absorption in the range of 3.7 to 4.2 ppm. The trans isomer is expected to undergo rapid ring inversion due to ring flexibility. During the ring inversion, protons, $H_{2'}$, cis to a bulky Br group, may be involved in ring conformation changes associated with a number of intermediates and show complicated multiplets absorption. The peak intensity for all four protons H_1, H_2, $H_{2'}$, and H_3 are equal.

For the propose of establishing chemical shift assignment and examining the couplings of protons, a 2D COSY spectrum (Fig. 3-1 (B)) was obtained. In the spectrum, three

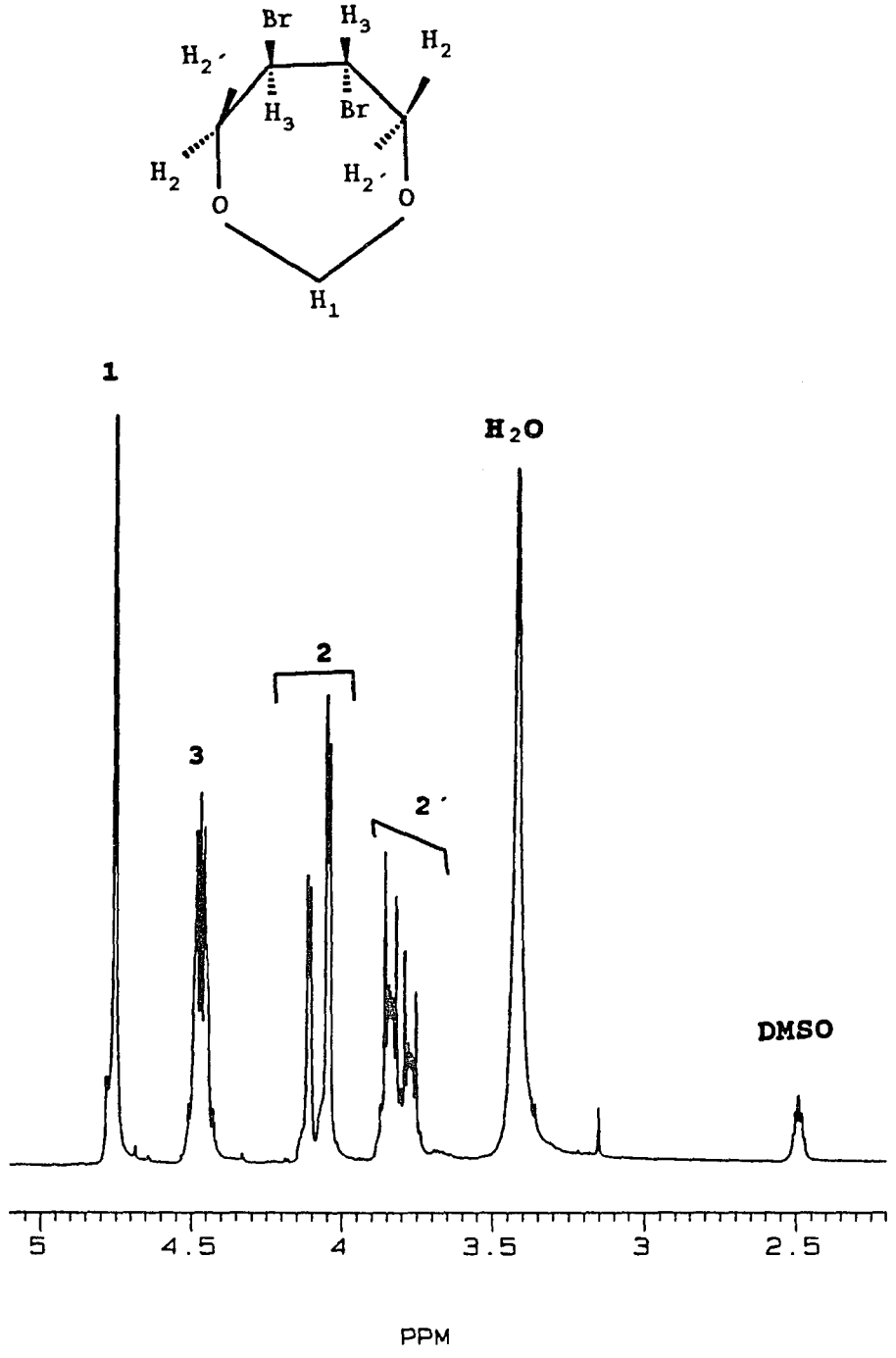

Fig. 3-1 (A) ^{1}H NMR Spectrum of 5,6-dibromo-1,3-dioxepane, *I*, (200 MHz, in DMSO at 25 °C)

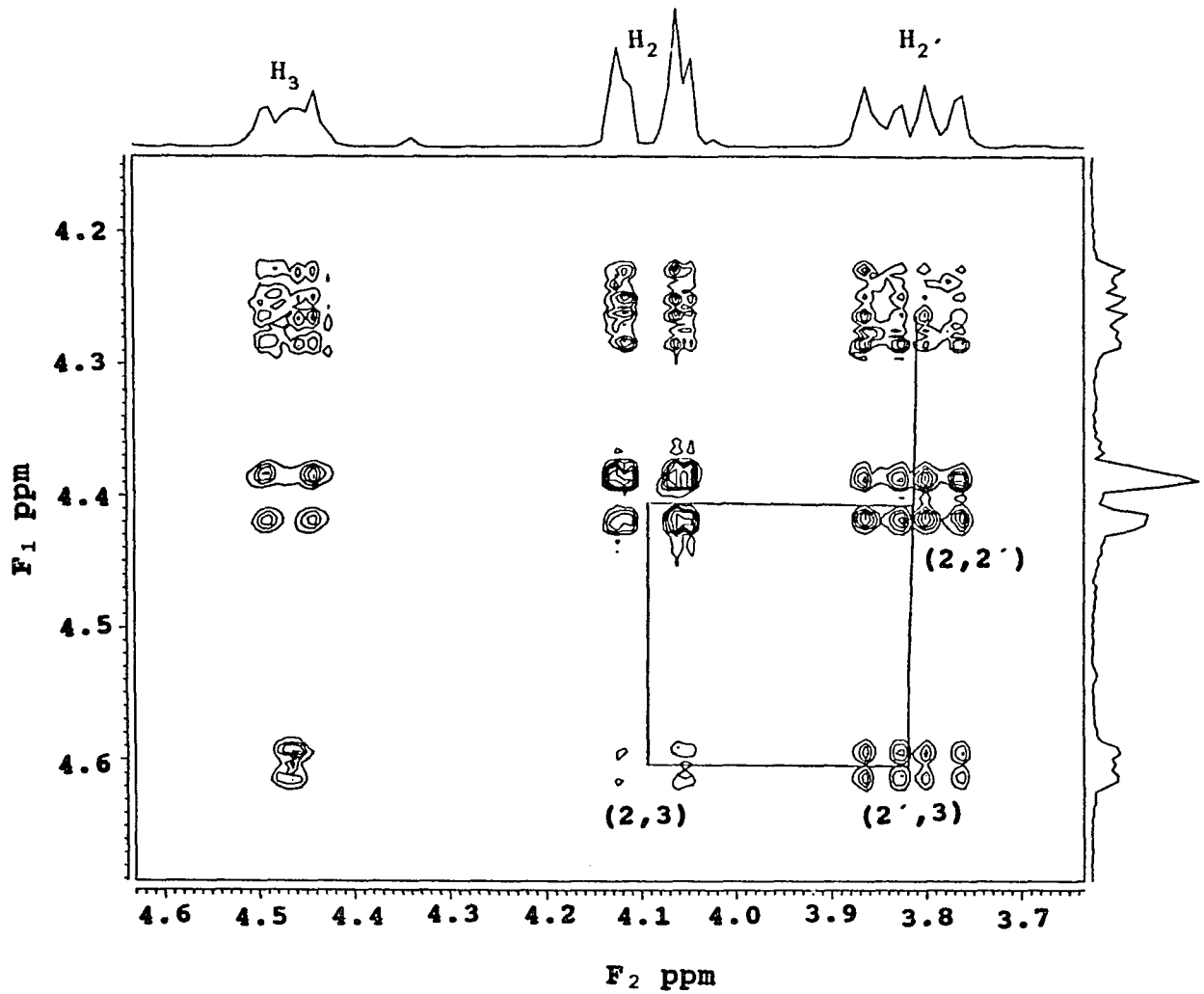

Fig. 3-1 (B) 2D COSY Spectrum of 5,6-dibromo-1,3-dioxepane, *I* (200 MHz, in DMSO at 25 °C)

sets of cross peaks indicate that the protons, H_2, $H_{2'}$, and H_3 are coupled to each other.

(b) Structure of Crude Trioxane Copolymer *III*

The structure of trioxane copolymer *III* is elucidated based on ^1H NMR data. Chemical shifts of trioxane copolymer *III* are assigned using the absorption peaks of a model compound, 2,3-dibromo-1,4-butane-diol, $HOCH_2$-CHBr-CHBr-CH_2OH. The ^1H NMR spectra of the crude trioxane copolymer *III* and a model compound are presented in Fig. 3-2 (A) and (B).

Singlets at 4.83 (H_1), and 4.72 ppm (H_2) represent the protons of methylene oxide units from trioxane and the comonomer *I*, respectively. Methylene protons, H_3's are slightly different and splitted by methine protons, H_4. Hence H_3 protons appears at 3.9 ppm as a quartet:

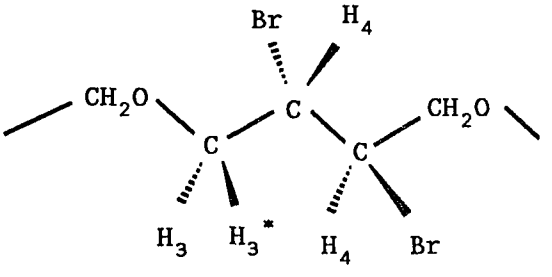

Methine proton, H_4, couples with methylene protons, H_3, and has a close to triplet absorption. A singlet at 3.31 ppm is

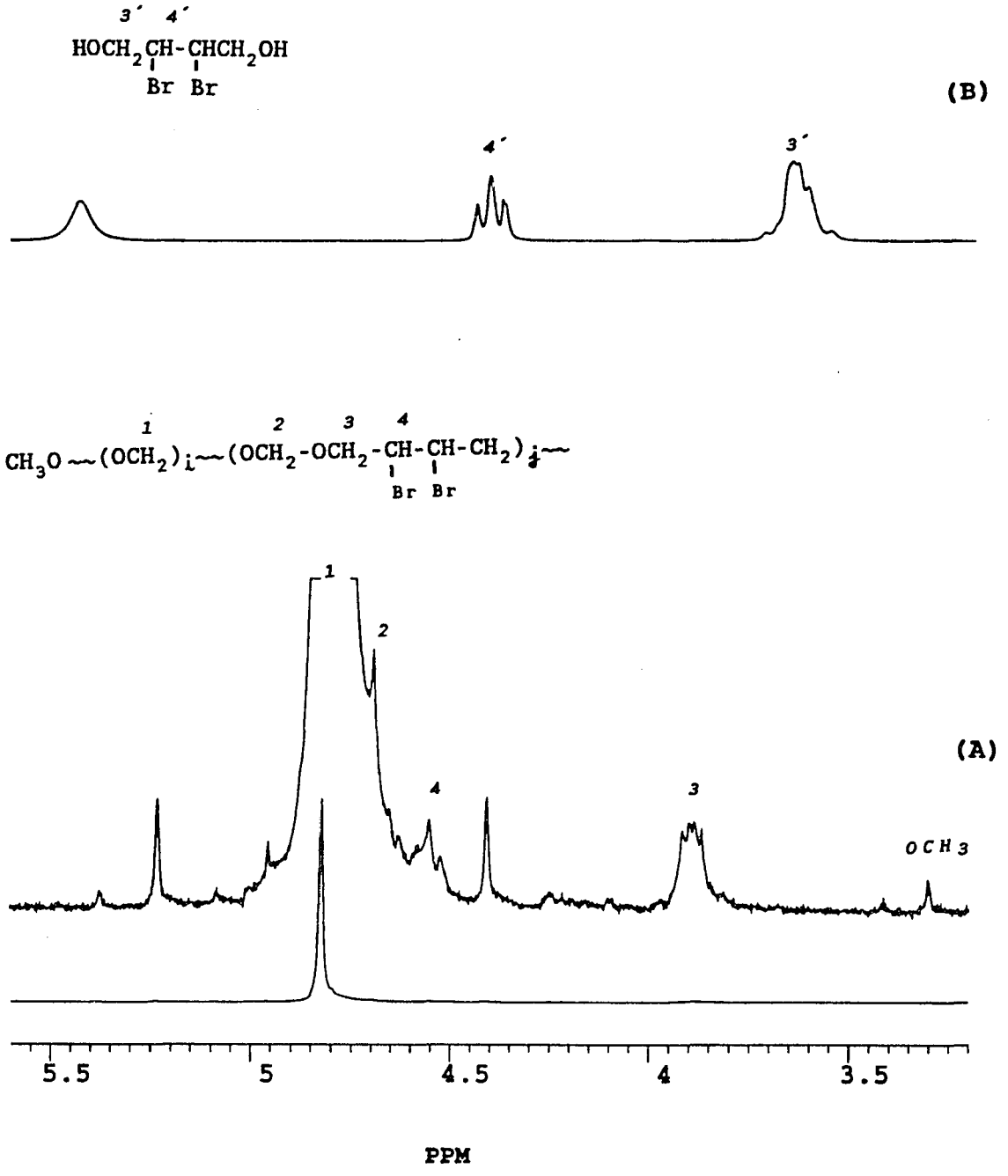

Fig. 3-2 ^{1}H NMR Spectra of (A) crude copolymer *III* and (B) model compound, 2,3-dibromo-1,4-butane-diol (200 MHz, in DMSO at 126 °C)

due to protons on end group methoxy unit, which originated from hydride transfer during the copolymerization (11). As expected, all the proton peaks of the copolymer are observed in low-field compared to those of model compound due to deshielding effect of long oxymethylene units.

The area of absorption peaks in the ^1H NMR spectra were used to calculate incorporation of comonomer *I* as follows:

$$\text{Incorp. mole-\% of } I = \frac{\text{Area of peak } H_3}{\text{Area of peak } (\frac{1}{6} H_1 + \frac{1}{4} H_3)} \times 100\%$$

All expressions of mole percent are based on trioxane as a comonomer unit. The relationship, peak area of (1/4) H_3 = peak area of (1/2) H_4, serves as a verification for internal consistency. Table 3-1 shows mol-% ratio of comonomer *I* in feed to incorporation and the yield of copolymerization. Yield decrease as feed of *I* is increased. The range of copolymer yield was 50-90 %. when comonomer feed is increased from 7.0 to 12.4 mole-%, there is essentially no increase in incorporation and a large decrease in yield is observed.

(c) Structure of Base Hydrolyzed Trioxane Copolymer *IV*

"Scheme 3-3" illustrates the structures of copolymer *IV* after base hydrolysis. During the base hydrolysis reaction,

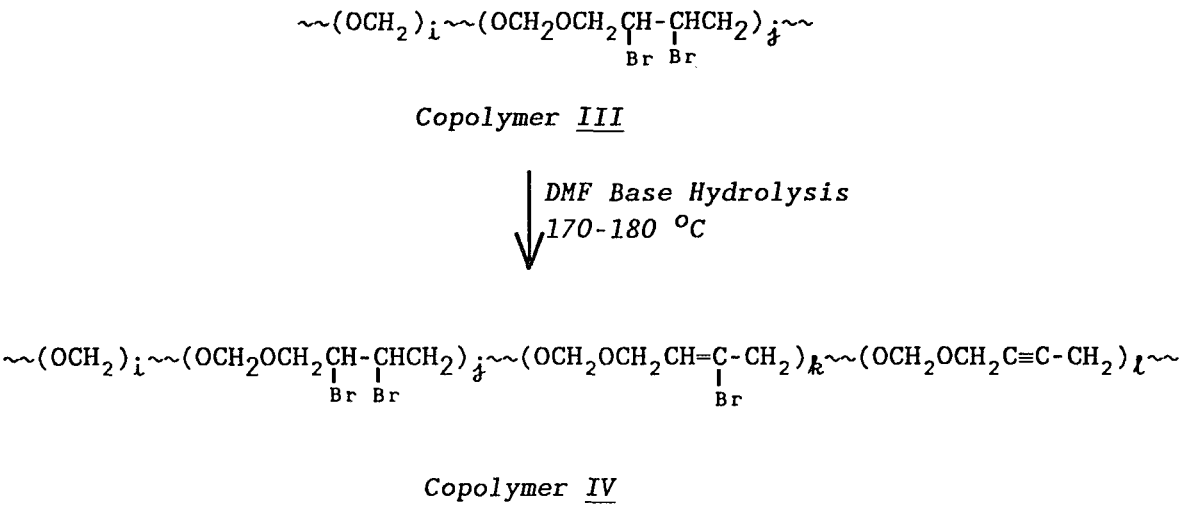

Scheme 3–3

the bromo group can be removed from the polymer chain through dehydrobromination processes in two steps. The reported bond energy of C-Br in a small molecule is a low value of 68 kcal per mol at 25 °C (12). As a result of dehydrobromination under base hydrolysis conditions, "copolymer *IV*" includes three different structure co-units, i.e. triple bond, vinyl bromo and trans-dibromo.

Dehydrobromination is indicated by the appearance of a number of new peaks in the ^{1}H NMR spectrum of the resulting copolymer *IV* (Fig. 3-3 (A) and (B)). The new peaks are

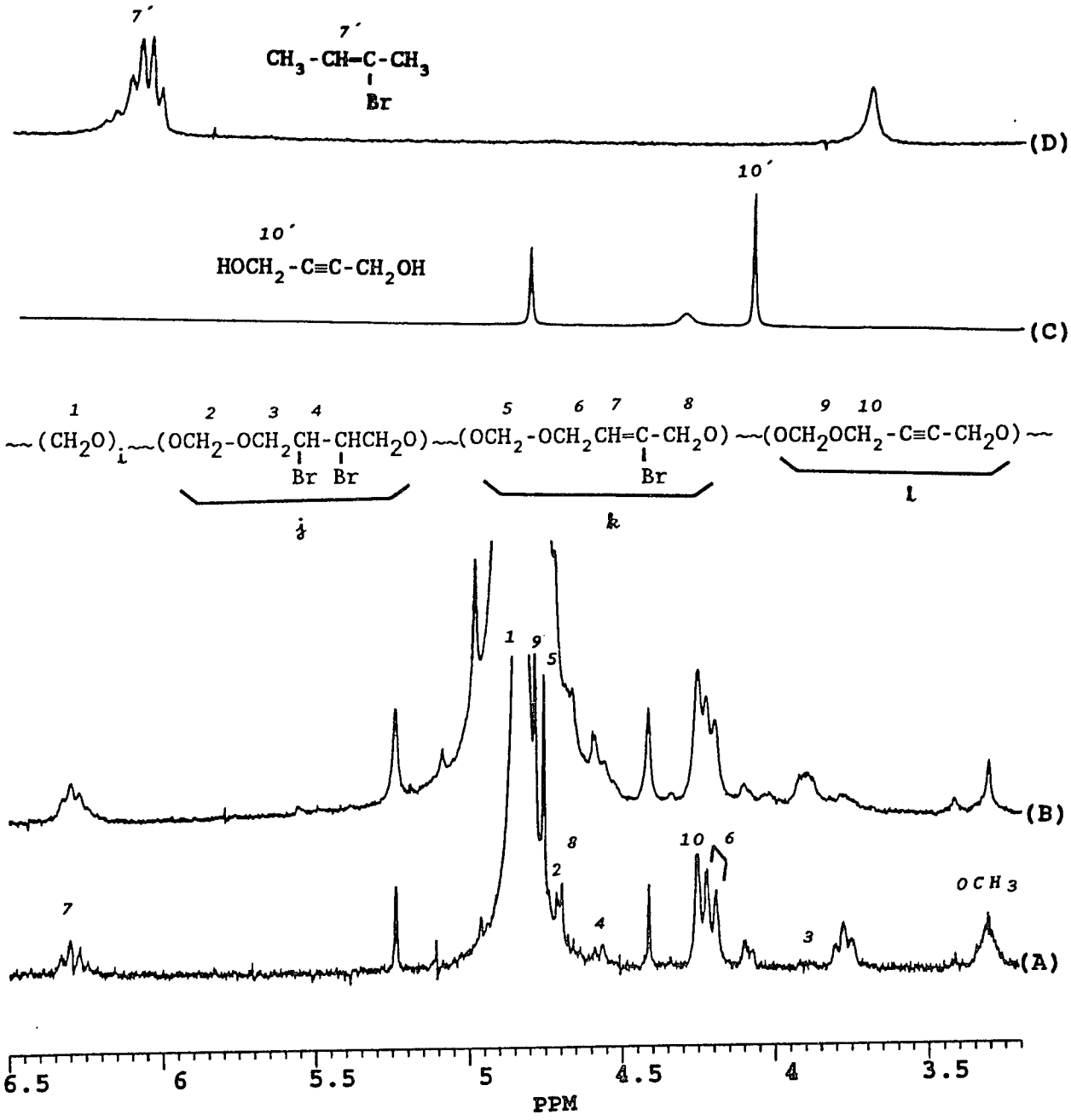

Fig. 3-3 ^{1}H NMR Spectra of base hydrolyzed TOX-copolymer *IV* (A) containing 40 % of original bromo groups and (B) containing 50 % of original bromo groups.
Model compounds (C) 2-butyne-1,4-diol and (D) 2-bromo-2-butene (200 MHz, in DMSO at 126 °C)

assigned to the protons in the co-units: peaks H_5 (s), H_6 (d), H_7 (m), H_8 (s) for ~~$(OCH_2\text{-}OCH_2\text{-}CH{=}CBr\text{-}CH_2)_k$~~ and peaks H_9 (s) and H_{10} (s) for ~~$(OCH_2\text{-}OCH_2\text{-}C{\equiv}C\text{-}CH_2)_l$~~, originating from one step and two step dehydrobromination, respectively. The chemical shifts are assigned based on absorption multiplicity and comparison with the ^1H NMR spectra of two model compounds (Fig. 3-3 (C) and (D)), 2-butyne-1,4-diol, $HOCH_2C{\equiv}CCH_2OH$ and 2-bromo-2-butene, $CH_3\text{-}CH{=}CBr\text{-}CH_3$.

As shown in Fig. 3-3 (A), a singlet at 4.76 ppm and a doublet at 4.21 ppm are assigned to protons, H_5 and H_6, respectively. These protons belong to the co-unit, ~~$(OCH_2\text{-}OCH_2\text{-}CH{=}CBr\text{-}CH_2)_k$~~, which is the product from mono-dehydrobromination of the crude copolymer. A triplet at 6.3 ppm, H_7, is due to the proton on the double bond carbon.

The other new absorptions represent the protons in the "co-unit l", originating from complete dehydrobromination. A singlet at 4.70 ppm, H_9, is from the methylene oxide protons. The methylene oxide protons, H_{10}, next to carbon-carbon triple bond have a singlet absorption at 4.25 ppm, overlapping with doublet peaks due to H_6.

Decrease in the intensities of the peaks H_3 and H_4, and

increase in the intensity of the peak at 3.78 ppm are observed as more bromo groups are eliminated as indicated by bromine elemental analysis (Fig. 3-3 (A), 60 % of bromine eliminated and (B), 50 % of bromine eliminated).

The peak at 3.78 ppm can not be assigned conclusively, but is assumed to be a peak due to reactive side group formed during base hydrolysis reaction. When the copolymer *IV* undergoes further modification reaction, e.g. amination, the peak at 3.78 ppm is no longer visible at the early stage of the reaction.

Although the two co-units, ~~(OCH_2-OCH=CH-CHBr-CH)~~ and ~~(OCH_2-OCH=CH-CH=CH)~~ can be derived from dehydrobromination through elimination of hydrogen at secondary carbon, no corresponding absorption peaks were observed in the ^1H NMR spectrum. Thus, elimination of the hydrogen at tertiary carbon is favored.

Homodecoupling ^1H NMR spectra (Fig. 3-4) further establish the assignment of proton chemical shifts for the base hydrolyzed copolymer *IV*. Decoupling on 3.78 ppm; i.e. H_{10} did not affect any peaks (Fig. 3-4 (A) and (B)). Decoupling on H_7 simplified H_6 from doublet to singlet (Fig. 3-4 (C)). These results indicate that the protons H_6 and H_7 are coupled, while the protons H_{10} show no coupling with these protons. Also, unknown proton peak at 3.78 ppm do not

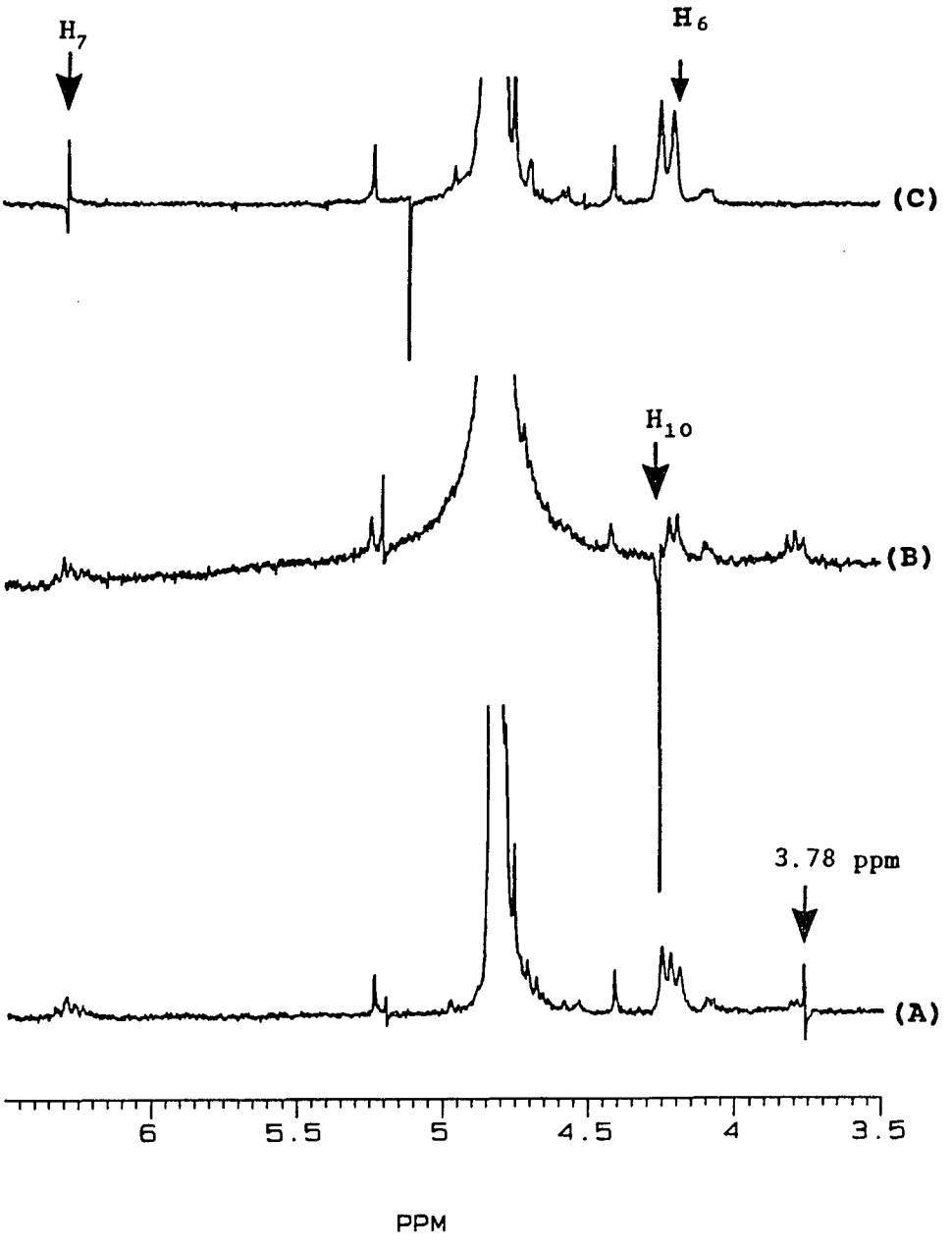

Fig. 3-4 HOMO Neclear decoupling ^{1}H NMR spectra of base hydrolyzed TOX-copolymer *IV*. (A) decoupling on 3.78 ppm (B) decoupling on H_{10} (C) decoupling on H_7 (200 MHz, in DMSO at 126 °C)

have connection to all of the above protons and do not belongs to structures "co-unit *k*" or "co-unit *l*".

The absorption peak areas of the protons of the "co-unit *k*" and the "co-unit *l*" in the ^1H NMR spectrum were used to calculate mol-% of each co-unit as follows:

$$\text{Incorp. mole-\% of "co-unit } k\text{"} = \frac{\text{Area of peak } H_7}{\text{Area of peak } (\frac{1}{6} H_1 + H_7)} \times 100\ \%$$

$$\text{Incorp. mole-\% of "co-unit } l\text{"} = \frac{\text{Area of peak } H_{10}}{\text{Area of peak } (\frac{1}{6} H_1 + \frac{1}{4} H_{10})} \times 100\ \%$$

The peak area of H_{10} is taken after peak deconvolution and the relationship of $H_6 = 2H_7$ serves as verification for internal consistency. (e.g. intensity of H_6 was 13.7, H_7 = 6.95)

Based on NMR data and Br elemental analysis, it was concluded that at least 40 % of Br is removed during base hydrolysis reaction via HBr elimination and that the resultant copolymer *IV* contained the co-unit structures, ~~$(OCH_2\text{-}OCH_2\text{-}CH{=}CBr\text{-}CH_2)_k$~~ and ~~$(OCH_2\text{-}OCH_2\text{-}C{\equiv}C\text{-}CH_2)_l$~~ as major product.

3.3. Chemical Modification Reactions of the Trioxane Copolymers, *III* and *IV*

Both of trioxane copolymers before (copolymer *III*) and after base hydrolysis (copolymer *IV*) are used to create new functional groups.

Amino group is grafted on the trioxane copolymer through substitution of bromo group. Complete dehydrobromination was performed in concentrated sodium hydroxide solution to yield carbon-carbon triple bond along the trioxane copolymer chain backbone.

3.3.1. Experimental

(a) Bromine Elimination Reaction

Dehydrobromination was carried out in NaOH or phenethyl amine solution either of refluxing or heterogeneous. The experimental details are summarized in Table 3-2.

Under heterogeneous conditions, 10 mL of phenethyl amine or sodium hydroxide solution with various concentrations was added to one gram of the base hydrolyzed trioxane copolymer *IV* placed in a 25 mL round bottom flask. The flask was equipped with an water condenser and placed in

Table 3-2 Dehydrobromination of trioxane copolymers

Run #	Sample [b]	Mol-% of co-units		Reagent and reaction (^{o}C/hrs)	Sample [a]	Mol-% of co-units		Yield [e]
		Co-units *j* and *k*,	Co-unit *l*			Co-units *j* and *k*,	Co-unit *l*	
1	48	6.1	/	2N NaOH, 110/24 [c]	53E	*x*	4.8	26
2	56	6.1	/	12N NaOH, reflux/1 [d]	56A	*x*	5.3	23
3	14A	2.6	2.9	2N NaOH, 105-110/2	17A	1.1	4.4	84
4	14A	2.6	2.9	2N NaOH, 100-110/19	30A	2.0	4.1	90
5	48A	3.3	1.1	2N NaOH, 110/3	53B	*x*	3.1	86
6	48A	3.3	1.1	2N NaOH, 110/24	53A	*x*	3.8	75

(Crude copolymer *III* was used in the run # 1 and 2, Base hydrolyzed copolymer *IV* was used used in the run # 3-6)

[b] Before the reaction, [a] After the reaction, [x] No Br content by elemental analysis and ^{1}H NMR

[c] Base hydrolysis was followed heterogeneous dehydrobromination

[d] Reaction was carried ourt in the final stage of base hydroysis

[e] (Final wt./strating wt.) x 100, without correction for loss of Br

an oil bath at 110 °C. The reaction mixture was heated for a period of 1 to 24 hours.

Under refluxing conditions, the desired amount of 12 N NaOH solution was added to the copolymer solution at the final stage of base hydrolysis processes. The solution was then refluxed under stirring.

The product was collected by filtration and washed repeatedly with hot water. In order to remove impurities that might be contained in the filtrated product, it was dissolved in hexafluoroisopropanol and then reprecipitated by addition of methanol. The final product was washed with acetone and vacuum dried at 56 °C.

(b) Amine Substitution Reaction

Trioxane copolymers with amino side chain were synthesized via substitution of bromo group in co-unit by amines.

The procedure for amine substitution reaction in the present work was as follows: the trioxane copolymer sample (1 g) was added to a 25 mL round bottom flask containing a desirable amount of amine with or without solvent. The flask fitted with a water condenser was heated to the required

temperature and for a selected period of time.

The reaction conditions for the various samples are tabulated in Table 3-3. At the completion of amine substitution reaction, base hydrolysis reaction was immediately carried out. Complete elimination of the bromo groups were accomplished by successive NaOH dehydrobromination reaction. At the end of the reaction, the solution was slowly cooled to room temperature. The product was collected by filtration and reprecipitated by addition of hexafluoroisopropanol and then washed with methanol to remove impurities. Finally, the reprecipitated copolymer was washed with acetone repeatedly and vacuum dried at 56 °C.

(c) Preparation of 3,5-di-tert-butyl-4-hydroxyhydrocinnamic acid, V

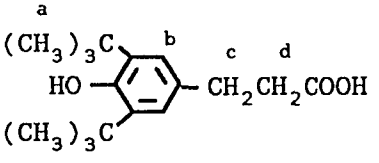

V

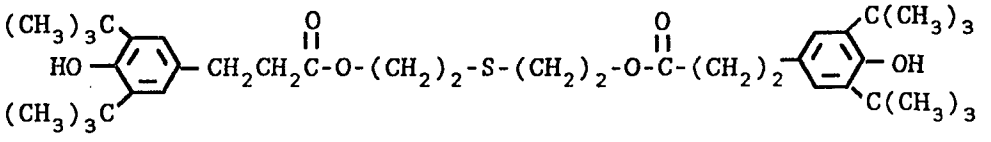

Irganox 1035

Thiodiethylene bis(3,5-di-tert-butyl-4-hydroxy)hydrocinnamate

An aqueous KOH solution (1M, 100 mL) was added to

Table 3-3 Amine substitution reaction of trioxane copolymers

Run #	Sample [b] #	Co-units with bromo groups (Mol-%)	Reagent and reaction (^{o}C/hrs)	Solvent (mL)	Sample [a] #	Co-units with amino groups (Mol-%)	Yield (Wt.%)
1	39 [c]	3.9	2g, Butylamine, 65/56 [e]	/	39A	*x*	56
2	"	"	2g, Butylamine, 65/56 [e]	/	40	0.2	71
3	"	"	1g, Dedecylamine,65/56 [e]	2, DMSO	38B	*x*	49
4	"	"	6 mL, Octylamine, 140/5 [e]	/	51	0.3	68
5	56 [c]	6.1	1g *VI*, 140/8 [e]	3, DMF	60	>1.0	25
6	43 [f]	1.6	10mL, Octylamine, 140/5	/	52	1.2	/
7	48A [d]	3.3	1g *VI*, 140/5	2, DMSO	47A	0.4	/
8	14A [d]	2.6	1g *VI*, 140/5	4, DMSO	61	1.0	29
9	"	"	12 mL, Octylamine, 140/7	6, DMF	62	1.2	20

[b] Before the reaction, [a] After the reaction, [c] Crude copolymer *III*, [d] Base hydrolyzed copolymer *IV*

x Amine was not grafted, [e] DMF base hydrolysis and NaOH dehydrobromination followed the substitution reation

[f] Copolymer prepared from Br addition to trioxane copolymer, -$(CH_2O)_x$-$(CH_2O$-CH_2-CH=CH-$CH_2O)_y$-

Irganox 1035 (5g, 0.007 mol) and the mixture was then heated in a steam bath for 4 hours under stirring to a clear dark brown color solution. The solution was cooled to room temperature and concentrated HCl solution was added dropwise until no more precipitate was formed. Finally, the precipitation was collected by filtration and dried over magnesium sulfate. The yield was about 80 %. The structure of *V* was confirmed by ^1H NMR spectra in DMSO-d_6 at 120 °C. The observed chemical shifts are follows: δ 1.38 (18H, s, H_a), 6.95 (2H, s, H_b), 2.71 (2H, t, H_c), 2.51 (2H, t, H_d)

(d) Synthesis of Phenolic Amine *VI*, N-(ω-aminohexyl)-(3,5-di-tert-butyl-4-hydroxyl)hydrocinnamamide

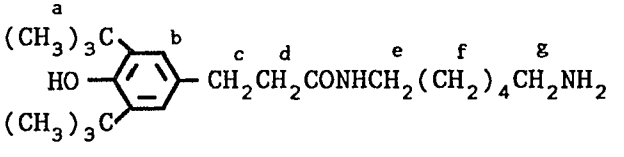

VI

The preparation of this derivative is based on a typical procedure for preparing the amides from corresponding amine salts.

1,6-Hexane diamine (3 g, 0.027 mol) was added to *V* (3.135 g, 0.011 mol) and the mixture was heated slowly to 150 °C and allowed to react at the temperature for six hours

resulting in a green-brown color mixture. The mixture, cooled down to room temperature, became a viscous liquid, which was washed with water repeatedly to remove water soluble components. The products was then dried in vacuum. It was ground to powder form and dried again in vacuum at room temperature. The final product, m. p. 72 ~ 75 °C, was a dark green powder with a yield about 40 %. The structure of *VI* was confirmed by ^1H NMR spectrum in DMSO-d_6 at 120 °C. The chemical shifts are follows: δ 7.83 ppm (NH, t), 6.92 (2H, s, H_b), 6.56 (OH, s), 3.02 (2H, m, H_e), 2.9 (2H, m, H_g), 2.71 (2H, t, H_c), 2.32 (2H, t, H_d), 1.38 (18H, s, H_a), 1.29 (8H, m, H_f)

(e) UV Analysis

UV Absorption measurement were carried out in order to confirm the presence of the carbon-carbon triple bond in the main chain of the trioxane copolymer after chemical modification of the trioxane copolymers. The absorption spectrum of the modified copolymer dissolved in hexafluoroisopropanol (6 g/L) was obtained by Varian DMS 300 UV Visible Spectrometer in a 1 cm absorption cell in the absorption range of 200 nm to 800 nm.

(f) Bromine Resistance Test

In order to ascertain the interaction of stabilizing effect of triple bond co-unit against harmful degradating agent, the effect of Br_2, a strong degrading agent, on the viscosity of polymer solutions was examined.

The trioxane copolymer solutions (0.2 % wt/wt) were made by dissolution of the copolymer with 1.8 mol-% incorporated ethylene oxide or copolymer with 1.4 mol-% of "co-unit *l*", in 10.00 mL of distilled hexafluoroisopropanol (HFIP). The bromine solution (4.0×10^{-3} M) was prepared dissolving bromine (2.0×10^{-4} mL) in 10.0 mL of HFIP. To the trioxane copolymer solution, 20.00 μL of the bromine solution was quickly added while stirring. The solution was then introduced into a Ubbelohde viscometer operating at 25 °C. Reduced viscosities were calculated using a predetermined solvent flow time of 128.0 seconds according to the following formula:

$$\eta_{red} = \frac{\eta_{sp}}{C} = \frac{(t/t_o) - 1}{C} = \frac{(t/128) - 1}{0.319\ (g/dL)}$$

where t is flow time of copolymer solution, t_o is flow time of HFIP, C is concentration of copolymer solution.

(g) IR Analysis of Functionalized Trioxane Copolymer with Hindered Phenol-Amine

The copolymer sample used for the Fourier Transfer Infrared (FT-IR) study were prepared by the potassium bromide pellet method. FT-IR spectrum were recorded on a Bio-Rad Digilab FTS-40 Division FT Infrared Spectrometer.

(h) Thermogravimetric Analysis

Thermogravimetric analysis (TGA) was used to examine the improved thermal stabilities of the modified copolymers with various functional groups. Thermograms of the polymers were obtained on a Dupont 2100 Thermogravimetric Analyzer. Temperature of the TGA was calibrated by determining melting temperature of indum (m.p = 156 °C) and tin (m.p = 232 °C), standard samples. The polymer samples, (ca. 5 ~ 7 mg), were heated at a rate of 10 °C per minute under air or nitrogen flow (60 mL/min).

(i) Viscosity Measurement

The molecular weight of acetal copolymer before and

after hindered amine graft were estimated from the inherent viscosity of the copolymers in hexafluoroisopropanol (HFIP) solution at 25.0 °C with a concentration of 0.200 (g/dL).

3.3.2. Results and Discussion

(a) Functionalized Trioxane Copolymer with Carbon-Carbon Triple Bond

^{1}H NMR spectra of trioxane copolymer with carbon carbon triple bond (5.3 mol-% incorporation, run #2, Table 3-2) were obtained in DMSO-d_6 solution at 137 °C. The ^{1}H NMR spectrum (Fig. 3-5) shows the trioxane copolymer structure with "co-unit *l*" only. Co-units *j* and *k* were not detected (compared with Fig. 3-3). In the UV absorption spectrum (Fig. 3-6) of the copolymer, the characteristic absorption band of carbon-carbon triple bond at 207 nm was observed, confirming the presence of the carbon-carbon triple bond in the copolymer after chemical modification of the copolymers *III*, or *IV*. Thus, sodium hydroxide dehydrobromination under the experimental conditions can give mainly triple bond functionality. The reactions were efficient under the conditions of refluxing for one hour (run #2) or heating at 110 °C for 24 hours (run #7) (Table 3-2) to give conversions

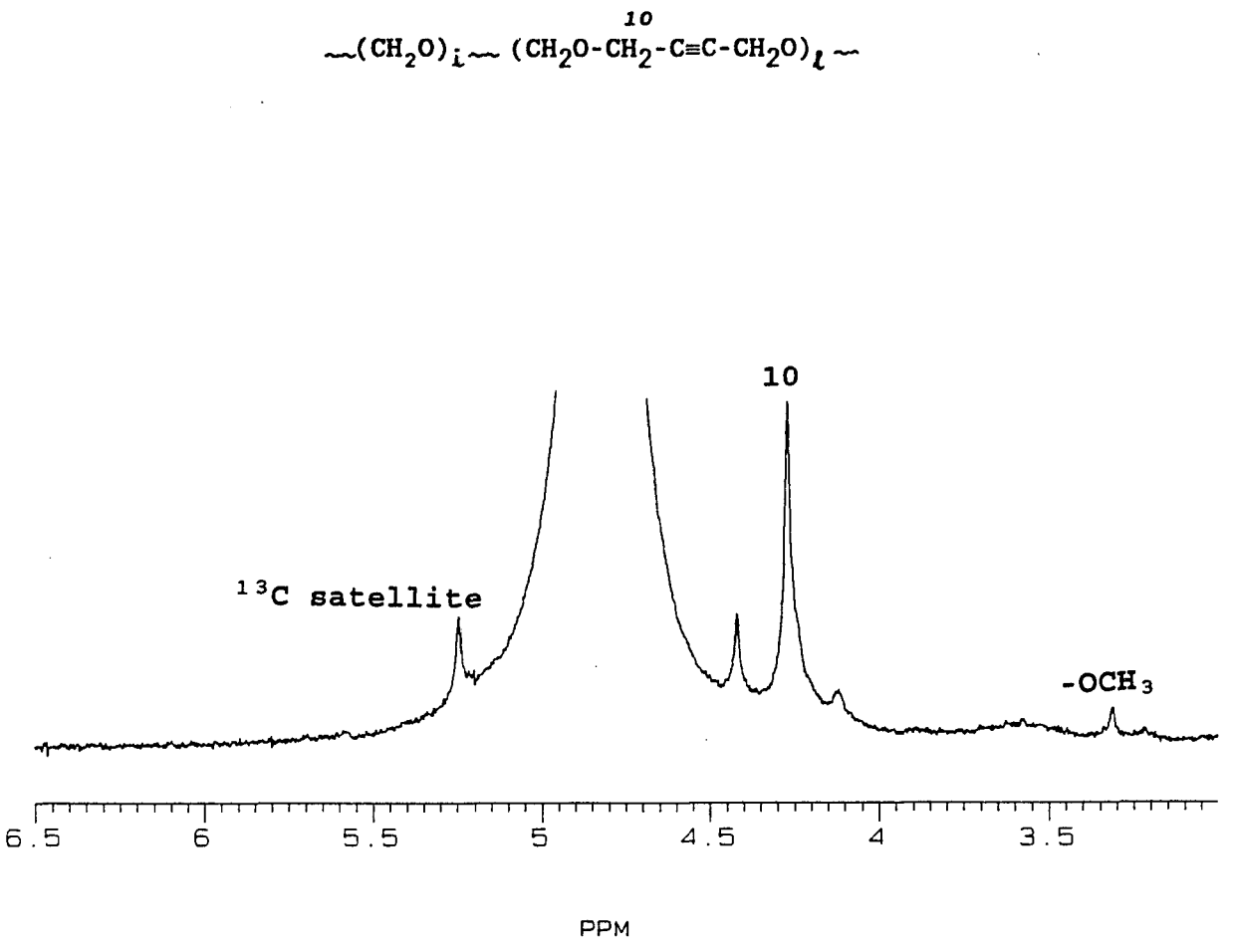

Fig. 3-5 ^{1}H NMR Spectrum of TOX-copolymer with "co-unit *l*" (200 MHz, in DMSO at 137 °C)

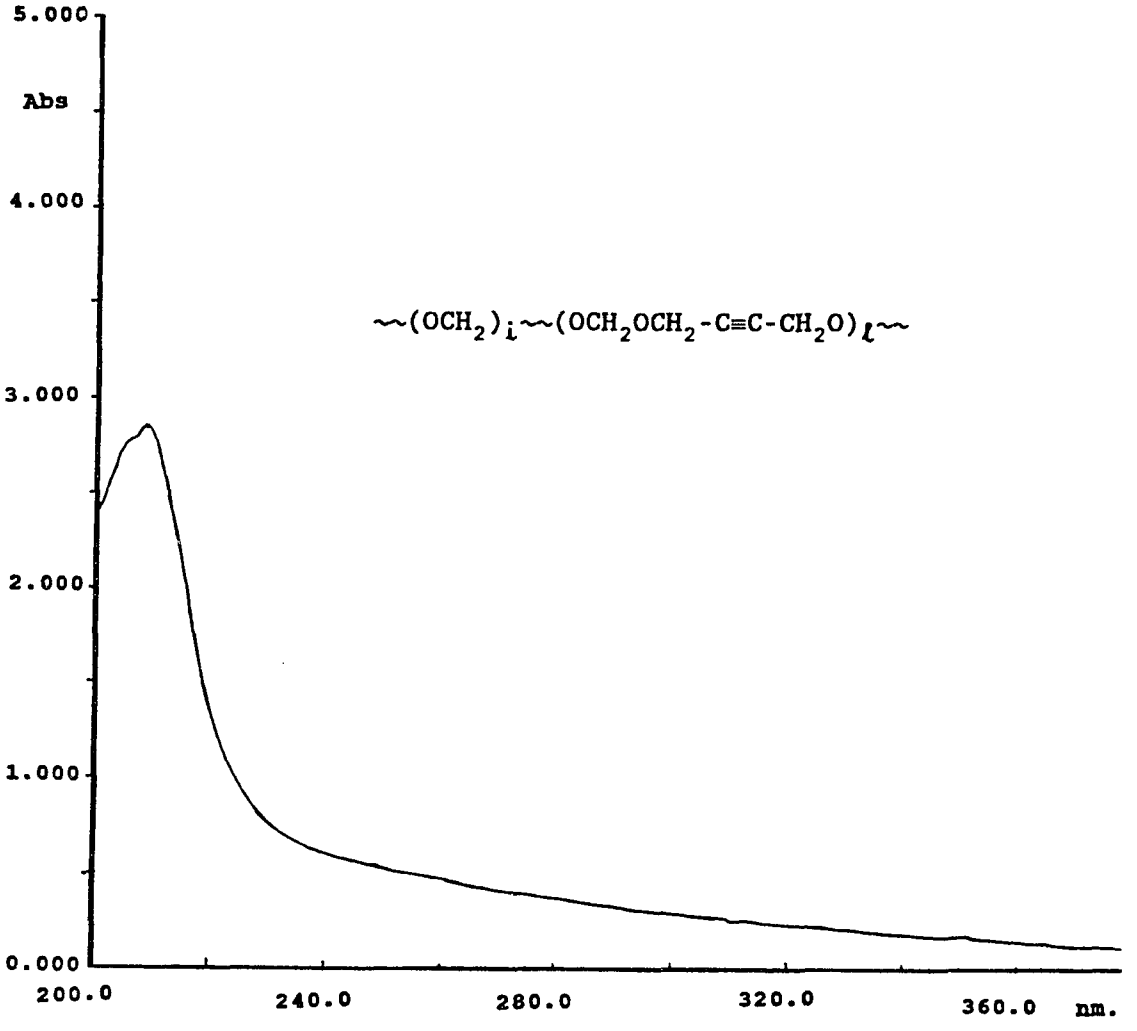

Fig. 3-6 UV Absorption spectrum of copolymer solution (6g/L) in hexafluoro-isopropanol

86% (5.3%/6.1%) and 85% (2.7%/3.3%) of dehydrobromination respectively. The low yield for run #2 is due to the loss of unstable end group. Run #7 gave good conversion and high yield and at the same time all bromine was eliminated.

(b) Stability of Functionalized Trioxane Copolymer with Carbon-Carbon Triple Bond

In the presence of bromine at a concentration of 4.0×10^{-3} M, the reduced viscosity (η_{red}) of TOX-ethylene oxide copolymer with 1.8 mol-% of ethylene oxide decreased from 2.2 (dL/g) to 1.4 (dL/g) within 35 minutes (Fig. 3-7). Under the identical conditions, the reduced viscosity of TOX-copolymer with 1.4 mol-% incorporation of "co-unit *l*" remained unchanged. The molecular weight of the copolymer with "co-unit *l*" is lower than the TOX-ethylene oxide copolymer and hence more stable end groups is associated with the former copolymer. Nevertheless, this experimental result indicates that -C≡C- can function as an efficient stabilizer. The triple bond of the "co-unit *l*" may react with harmful species which can initiate the degradation of acetal copolymer.

It has been reported that in the study of TOX-copolymer stability against bromine degradation, the reduced viscosity of TOX-copolymer with 1.8 mol-% incorporation of

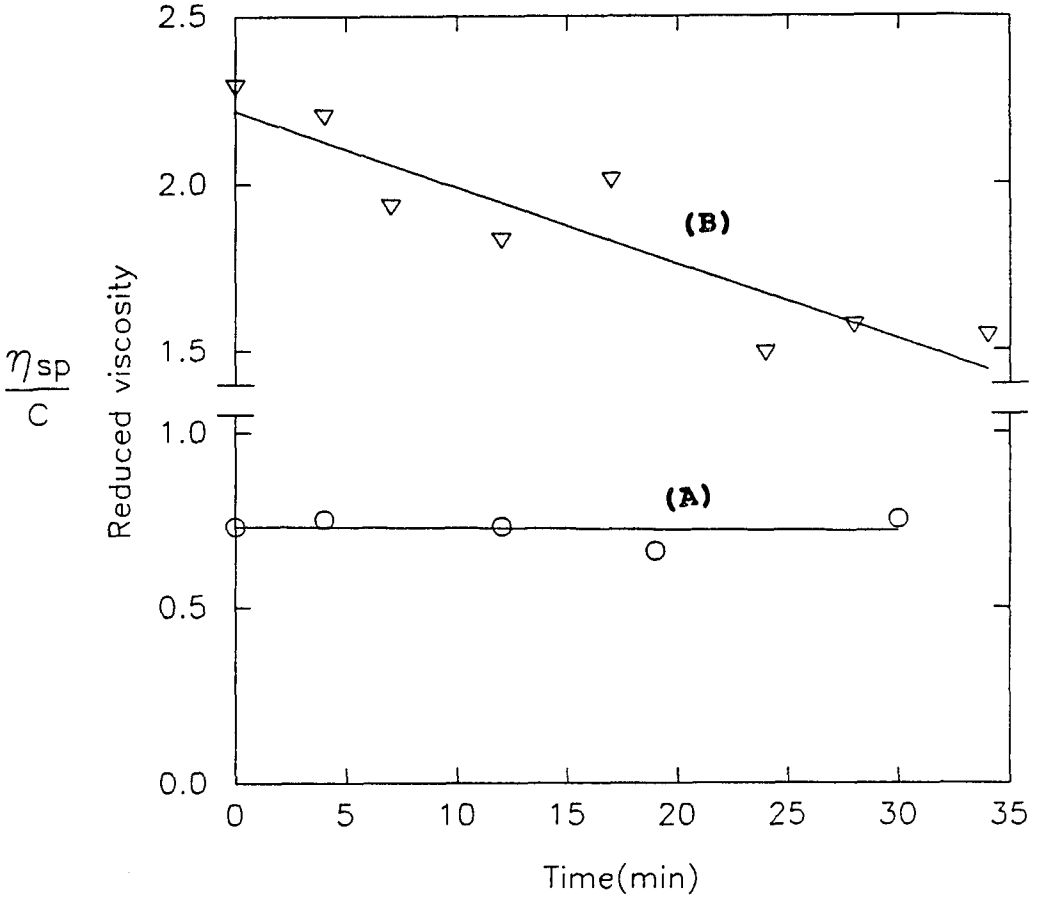

Fig. 3-7 TOX-Copolymer stability against bromine degradation as determined by monitoring reduced viscosity as a function of time at 25 °C in hexafluoroisopropanol
[polymer] = 0.32 g/dL
[Br_2] = 4.0 x 10^{-3} M
(A) with 1.4 mol-% of "co-unit *l*"
(B) with 1.8 mol-% of ethylene oxide

~~$(OCH_2\text{-}OCH_2\text{-}C{=}C\text{-}CH_2)_y$~~ decreased from 1.1 dL/g to 0.2 dL/g in less than 20 minutes at the concentration of 3×10^{-3} M of Br_2 (13). Therefore, it is believed that -C≡C- works more efficiently than -C=C- as a stabilizer by reacting with harmful degrading species. The action is thought as the formation of stable products through the addition reactions as follows:

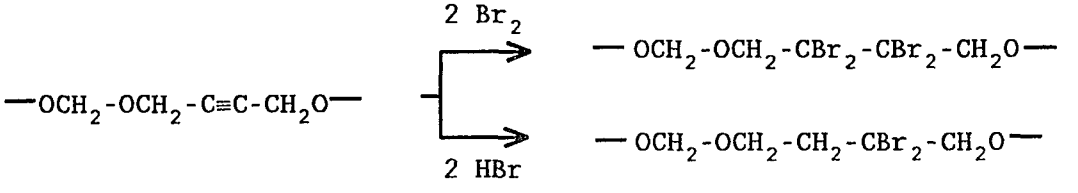

Two moles of bromine may be added to triple bonds to give tetrabromo products. Two moles of hydrogen bromide, generated from the hydrogen abstraction from the copolymer chain by Br•, may be added to triple bond (14, 15).

TGA Thermograms of trioxane copolymer with 8.2 mol-% of oxy-butenylene unit, ~~$(OCH_2\text{-}OCH_2\text{-}C{=}C\text{-}CH_2)_y$~~ and 5.3 mol-% of "co-unit ℓ", ~~$(OCH_2\text{-}OCH_2\text{-}C{\equiv}C\text{-}CH_2)_\ell$~~, were obtained with a heating rate of 10 °C per minute under nitrogen flow (Fig. 3-8) and air flow (Fig. 3-9). Under nitrogen flow, the thermal stability of trioxane copolymer with 8.2 mol-% of oxy-butenylene unit, ~~$(OCH_2\text{-}OCH_2\text{-}C{=}C\text{-}CH_2)_y$~~ is superior to that of trioxane copolymer with 5.3 mol-% of "co-unit ℓ",

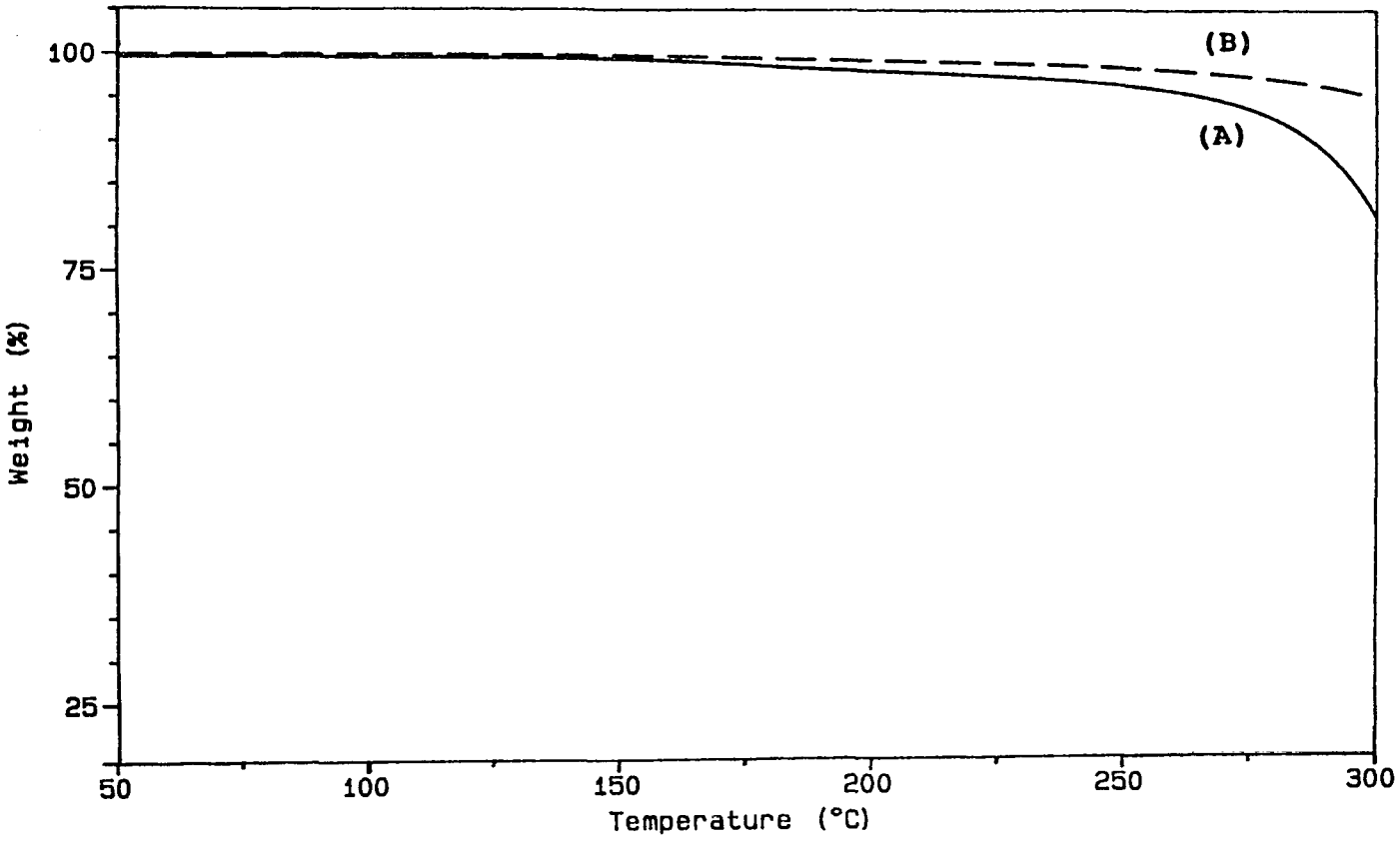

Fig. 3-8 TGA Thermograms of TOX-copolymers (A) with 5.3 mol-% of "co-unit *l*" (B) with 8.2 mol-% of co-unit, $\sim\sim(OCH_2OCH_2\text{-}CH{=}CH\text{-}CH_2)_y\sim\sim$ (heating rate 10 °C/min in N_2 flow)

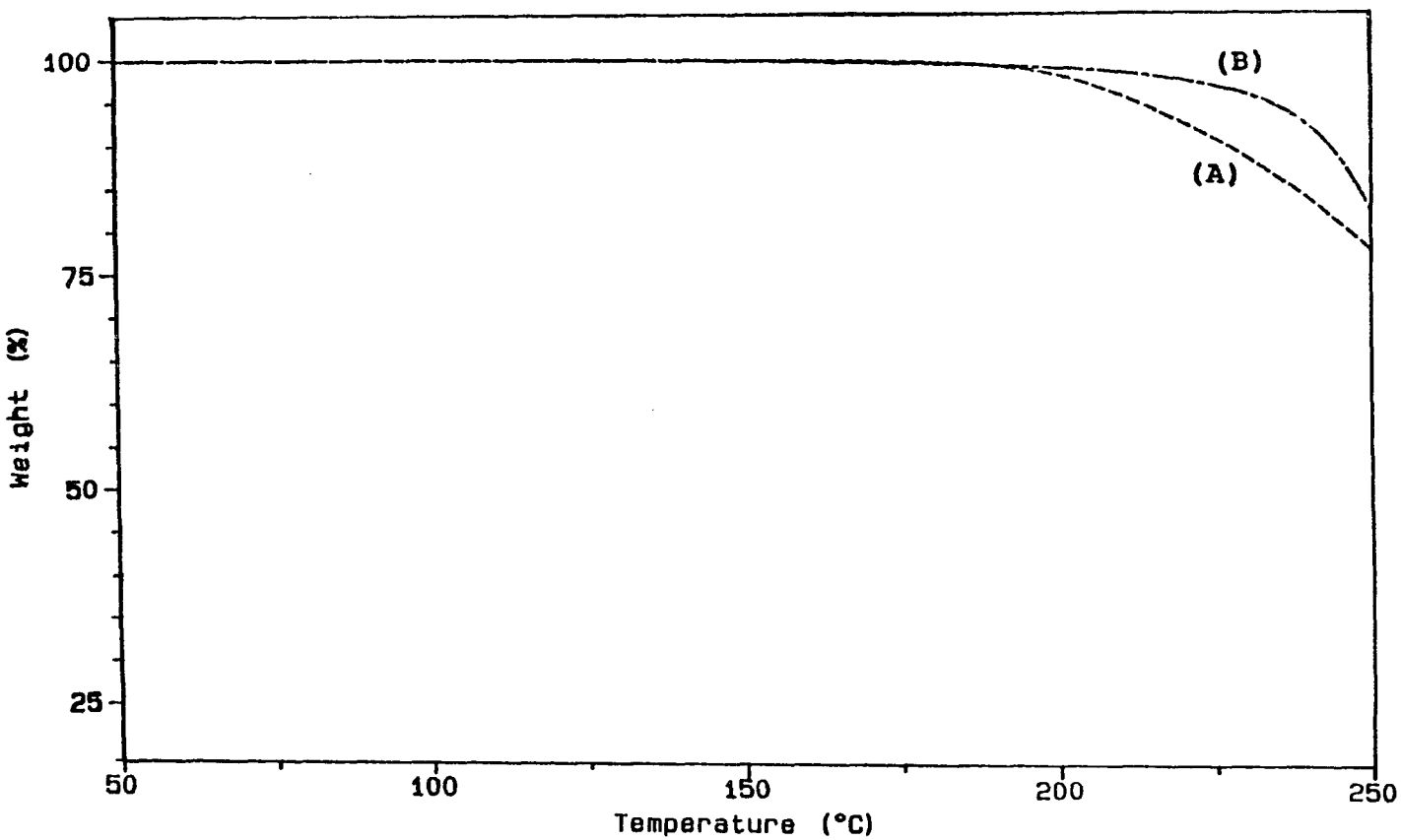

Fig. 3-9 TGA Thermograms of TOX-copolymers (A) with 8.2 mol-% of co-unit, ~~$(OCH_2OCH_2\text{-}CH{=}CH\text{-}CH_2)_y$~~ (B) with 5.3 mol-% of "co-unit l" ~~$(OCH_2OCH_2\text{-}CH{=}CNHR'\text{-}CH_2)_n$~~ (heating rate 10 °C/min in air flow)

~~$(OCH_2\text{-}OCH_2\text{-}C{\equiv}C\text{-}CH_2)_{\ell}$~~. This indicate that copolymer with higher incorporation of -C=C- is more stable than the copolymer with low incorporation of -C≡C-. However, TGA thermograms under air flow (Fig. 3-9), shows better thermal stability of trioxane copolymer with lower incorporation of "co-unit ℓ", ~~$(OCH_2\text{-}OCH_2\text{-}C{\equiv}C\text{-}CH_2)_{\ell}$~~ compared with trioxane copolymer with higher comonomer incorporation of oxy-butenylene unit, ~~$(OCH_2\text{-}OCH_2\text{-}C{=}C\text{-}CH_2)_{y}$~~. This result can be attributed to the ability of -C≡C- acting more efficiently as a trap for oxygen and other reactive intermediate than -C=C- during the oxidative degradation. The oxygen may react with double bond to give a epoxide intermediate, which usually cleaves to aldehydes or ketones (16). However, the intermediate formed from the addition of oxygen with triple bond may not lead bond scission (17).

(c) Functionalized Trioxane Copolymer with Amine and Hindered Phenol-Amine

The copolymer with amino side chain was synthesized via substitution reaction of the bromo groups in the co-unit by an amine. The details of the experimental conditions and the results are summarized in Table 3-3.

The expected co-unit structures are

~~$(OCH_2OCH_2\text{-}CHNHR\text{-}CHNHR\text{-}CH_2)_{m}$~~ and

~~$(OCH_2OCH_2\text{-}CH{=}CNHR\text{-}CH_2)_n$~~ originated from structures of ~~$(OCH_2OCH_2\text{-}CHBr\text{-}CHBr\text{-}CH_2)_j$~~ and ~~$(OCH_2OCH_2\text{-}CH{=}CBr\text{-}CH_2)_k$~~, respectively. However, substitution of the bromo groups by bulky amine must take place mostly in the "co-unit *k*" since the formation of two bulky amino groups next to each other as in "co-unit *m*" is very unlikely.

^1H NMR spectra of amine grafted or hindered phenol bound TOX-copolymer (with 0.4 mol-% incorporation of *VI*) was obtained in DMSO-d_6 at 120 °C. A ^1H NMR spectrum of octyl amine grafted acetal copolymer (with incorporation of 1.2 mol-% octyl amine and 3.3 mol-% "co-unit *l*") is presented in Fig. 3-10. The peak due to proton H_{12} overlaps with water peak and the methine peak, H_{11}, was not observed in the spectrum. It is assumed that the peak, H_{11}, overlaps with main unit peak, H_1. The chemical shift of H_{11} in unsaturated ethylene, trans to amine groups, is calculated based on the substituent constants literature values for chemical shift of substituted ethylenes (18). The calculated chemical shift value is 4.62 ppm. The incorporation of amine was calculated from the peak intensity of methyl protons, H_{14}:

$$\textit{Incorp. mole-\% of "co-unit n"} = \frac{\textit{Area of peak } (\frac{1}{3} H_{14})}{\textit{Area of peak } (\frac{1}{6} H_1 + \frac{1}{3} H_{14})} \times 100\%$$

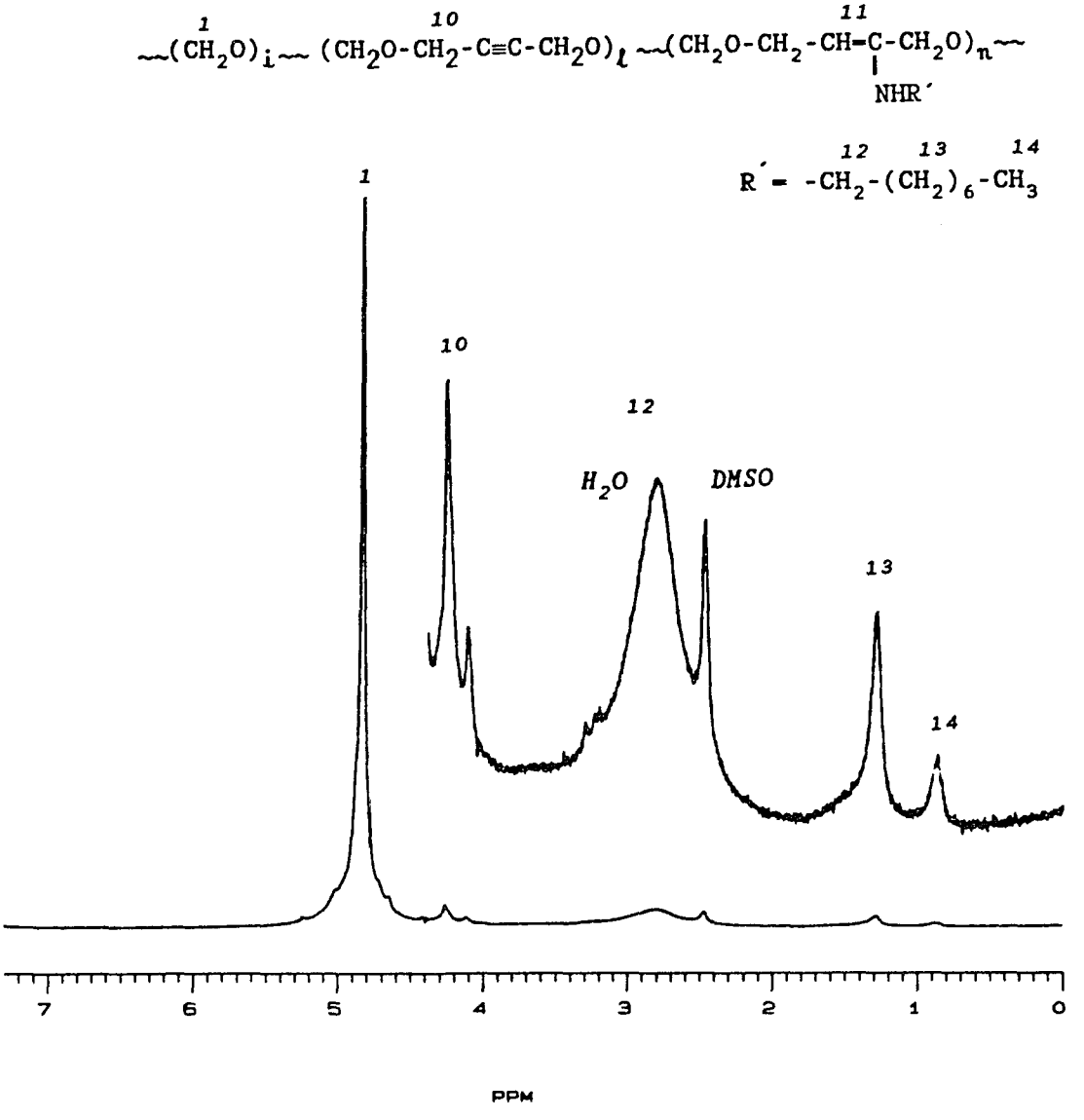

Fig. 3-10 ^{1}H NMR Spectrum of functionalized TOX-copolymer with 3.3 mol-% of "co-unit *l*" and 1.2 mol-% of "co-unit n", ~$(OCH_2OCH_2$-CH=CNHR´-$CH_2)_n$~~ (200 MHz, in DMSO-d_6 at 120 °C)

Based upon calculations on ^1H NMR data, up to 40 % of bromo group in the crude copolymer was replaced by amine. The remaining bromo groups were further eliminated via the process of heterogeneous NaOH dehydrobromination. Thus, the structure of the copolymer derived after substitution and dehydrobromination consists of two co-units, ~~$(OCH_2\text{-}OCH_2\text{-}C{\equiv}C\text{-}CH_2)_{\ell}$~~ and ~~$(OCH_2OCH_2\text{-}CH{=}CNHR\text{-}CH_2)_{n}$~~. Complete removal of the bromo groups was confirmed by bromine elemental analysis.

Hindered phenol along with secondary amino group can be bound to acetal copolymer via substitution of bromo group. For this propose, phenolic amine *VI* was synthesized.

^1H NMR spectrum of TOX-copolymer with 0.4 mol-% hindered phenol *VI*, including 2.9 mol-% of "co-unit ℓ" and 2.2 mol-% "co-unit k" is shown in Fig. 3-11. The chemical shifts for peaks of "co-unit n" were assigned by comparison of the peaks with those of unbound hindered amine *VI* (Fig. 3-12). The methine proton peak, H_{11}, was not observed due to overlapping with the peak H_1. Slight shifts of absorptions to downfield for protons H_{14}, H_{15}, H_{16} and upfield for H_{18}, in bound hindered phenol were observed after grafting to copolymer. The peaks for H_{14} shifted from 2.71 ppm to 2.75 ppm. The peak for H_{15} and H_{16} shifted from 2.32 ppm to 2.37 ppm and from 3.02 ppm to 3.07 ppm, respectively. The key proton, H_{18}, confirming the bonding of *VI* to copolymer

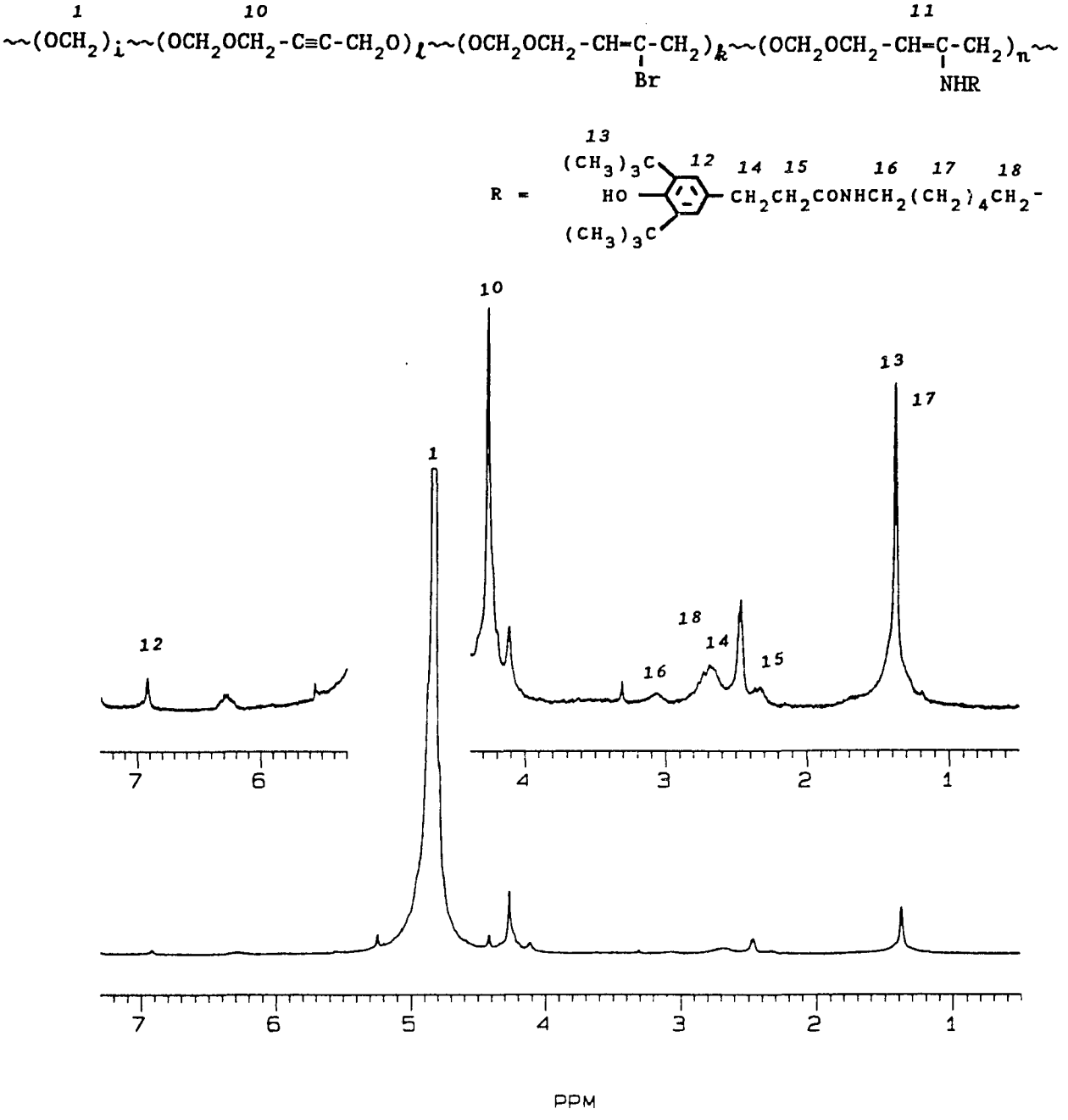

Fig. 3-11 ^{1}H NMR Spectrum of hindered phenol-amine functionalized TOX-copolymer with 0.4 mol-% of "co-unit n", ~~$(OCH_2OCH_2\text{-}CH{=}CNHR\text{-}CH_2)_n$~~", 2.2 mol-% of "co-unit k", and 2.9 mol-% of "co-unit l" (200 MHz, in DMSO-d_6 at 120 °C)

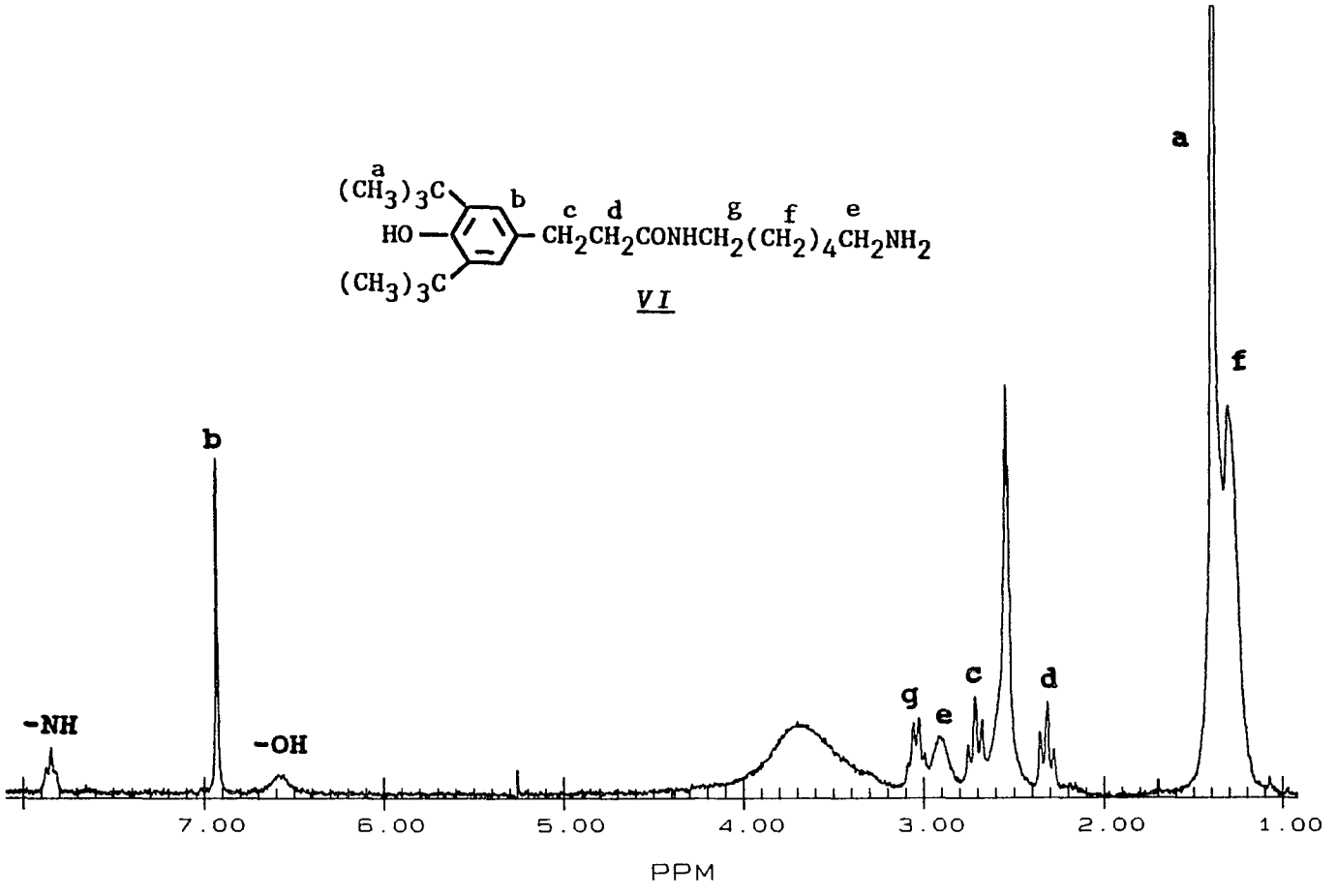

Fig. 3-12 ^{1}H NMR Spectrum of hindered phenol-amine, *VI* (200 MHz, in DMSO-d_6 at 120 °C)

through showing a shift to upfield from 2.9 ppm to 2.8 ppm. This result is consistent with the reported chemical shift values at slightly high field for methylene next to secondary amine than the methylene next to primary amine. The reported chemical shift values of methylene peaks next to amine group of hexylamine, $CH_3(CH_4)C\underline{H}_2NH_2$, and di-n-hexylamine, $CH_3(CH_2)_4C\underline{H}_2NHC\underline{H}_2(CH_2)_4CH_3$, are 2.75 ppm and 2.6 ppm, respectively (19).

The incorporation of hindered phenol unit was calculated from the total intensity of H_{13} and H_{17} as follows:

$$\textit{Incorp. mole-\% of "co-unit n"} = \frac{(H_{13} + H_{17})/26}{(H_1/6) + (H_{13} + H_{17})/26} \times 100\%$$

In the IR spectrum (Fig. 3-13) of functionalized TOX-copolymer with hindered phenol *VI* (sample # 60), peaks at 2300 cm^{-1} due to NH stretching and at 1665 cm^{-1} due to C=O stretching indicate that during the base hydrolysis reaction followed after the modification reaction, amide group of the hindered phenol *VI* was retained.

Higher molecular weight of the copolymer (sample #60, MW $\approx 2 \times 10^4$) with 1 mol-% of *VI* grafted compared to the parent crude copolymer (sample #56, MW $\approx 7 \times 10^3$, with 6.1 mol-% "co-unit *j*") before the reaction indicates that some

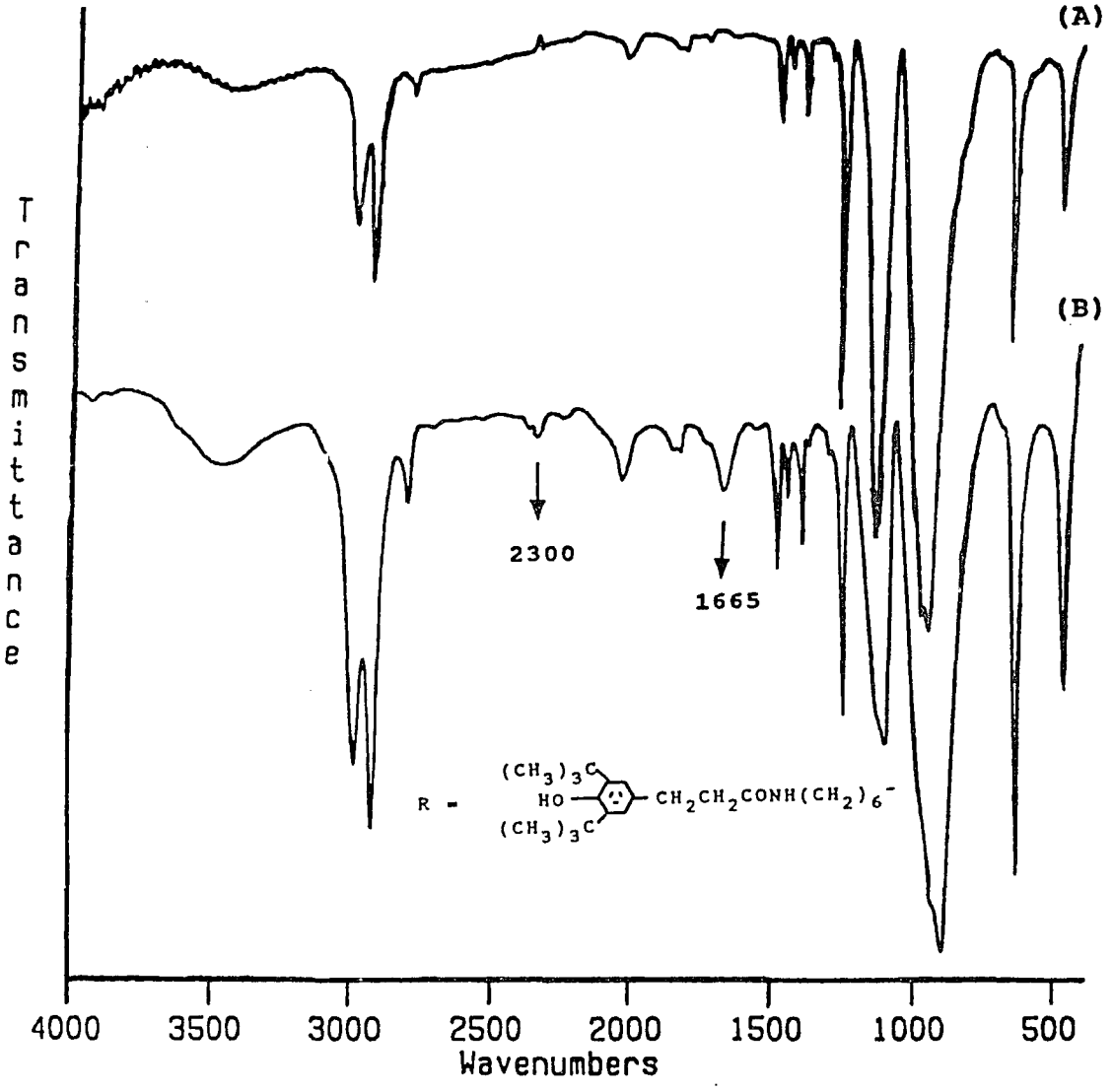

Fig. 3-13 IR Spectra of TOX-copolymers

(A) crude copolymer *III* before modification reaction

(B) functionalized with 1.0 mol-% of "$\sim\sim(OCH_2OCH_2\text{-}CH{=}CNHR\text{-}CH_2)_n\sim\sim$" and 3.3 mol-% of "co-unit *l*"

extent of branching may be formed during the successive processes of base hydrolysis and dehydrobromination reactions which followed the substitution reaction. This may be caused by formaldehyde generated by the crude copolymer during this series of reactions.

(d) Thermal Stability of Functionalized Trioxane Copolymers

TGA Thermogram of amine grafted copolymer showed improved thermal stability over bromo group functionalized copolymer (Fig. 3-14). TGA thermograms of the functionalized trioxane copolymer with octylamine (1.0 mol-% incorporation) and hindered phenol-amine (1.2 mol-% incorporation) were obtained in 10 °C per minute of heating rate under nitrogen and air flow, and are presented in Fig. 3-15 and Fig. 3-16, respectively. The functional groups are as follows:

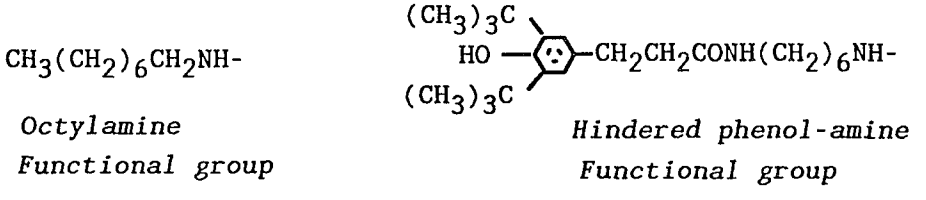

Under both nitrogen flow and air flow, the trioxane copolymer with hindered phenol-amine shows better thermal stability compared with the trioxane copolymer with comparable level of octylamine.

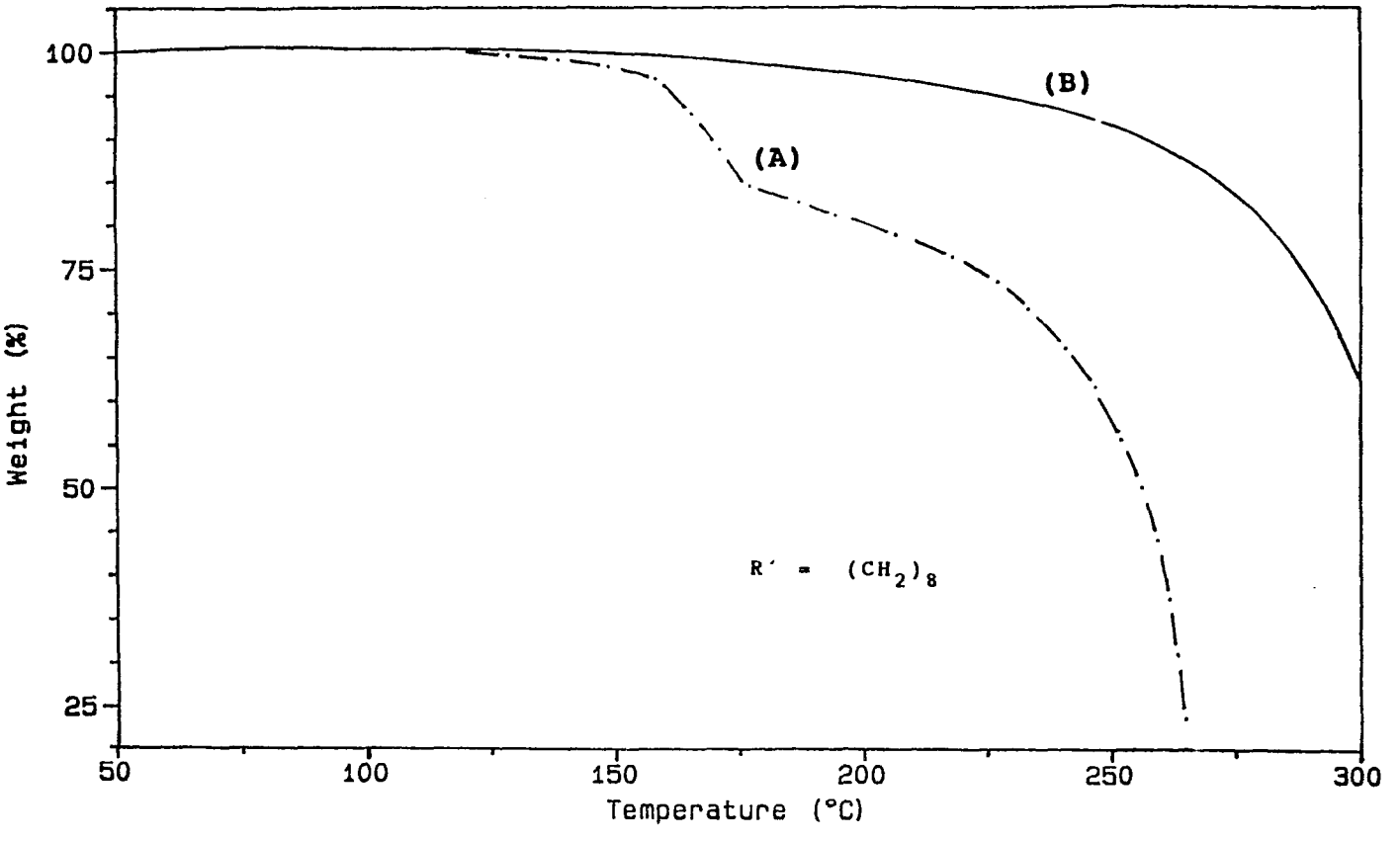

Fig. 3-14 TGA Thermograms of TOX-copolymer (A) with 3.5 mol-% of "co-unit j", $\sim\sim(OCH_2OCH_2\text{-}CHBr\text{-}CHBr\text{-}CH_2)_j\sim\sim$, (B) with 3.3 mol-% of "co-unit l" and 1.2 mol-% of "co-unit n", $\sim\sim(OCH_2OCH_2\text{-}CH{=}CNHR'\text{-}CH_2)_n\sim\sim$, (heating rate 10 °C/min in N_2 flow)

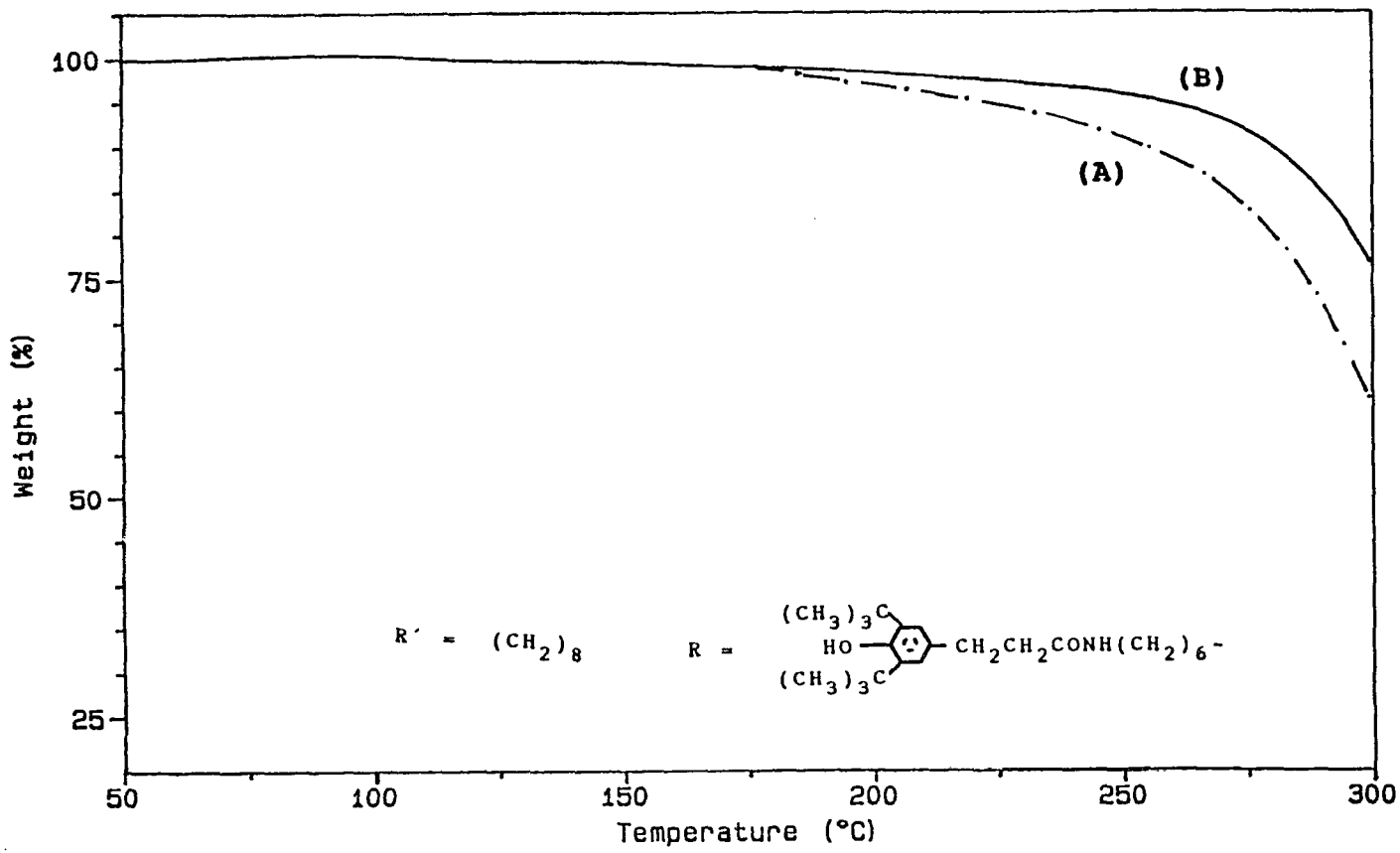

Fig. 3-15 TGA Thermograms of TOX-copolymers (A) with 1.2 mol-% of ~~$(OCH_2OCH_2\text{-}CH{=}CNHR'\text{-}CH_2)_n$~~ and 3.3 mol-% of "co-unit *l*" (B) with 1.0 mol-% of "co-unit *n*", ~~$(OCH_2OCH_2\text{-}CH{=}CNHR\text{-}CH_2)_n$~~ and 3.3 mol-% of "co-unit *l*" (heating rate 10 °C/min in N_2 flow)

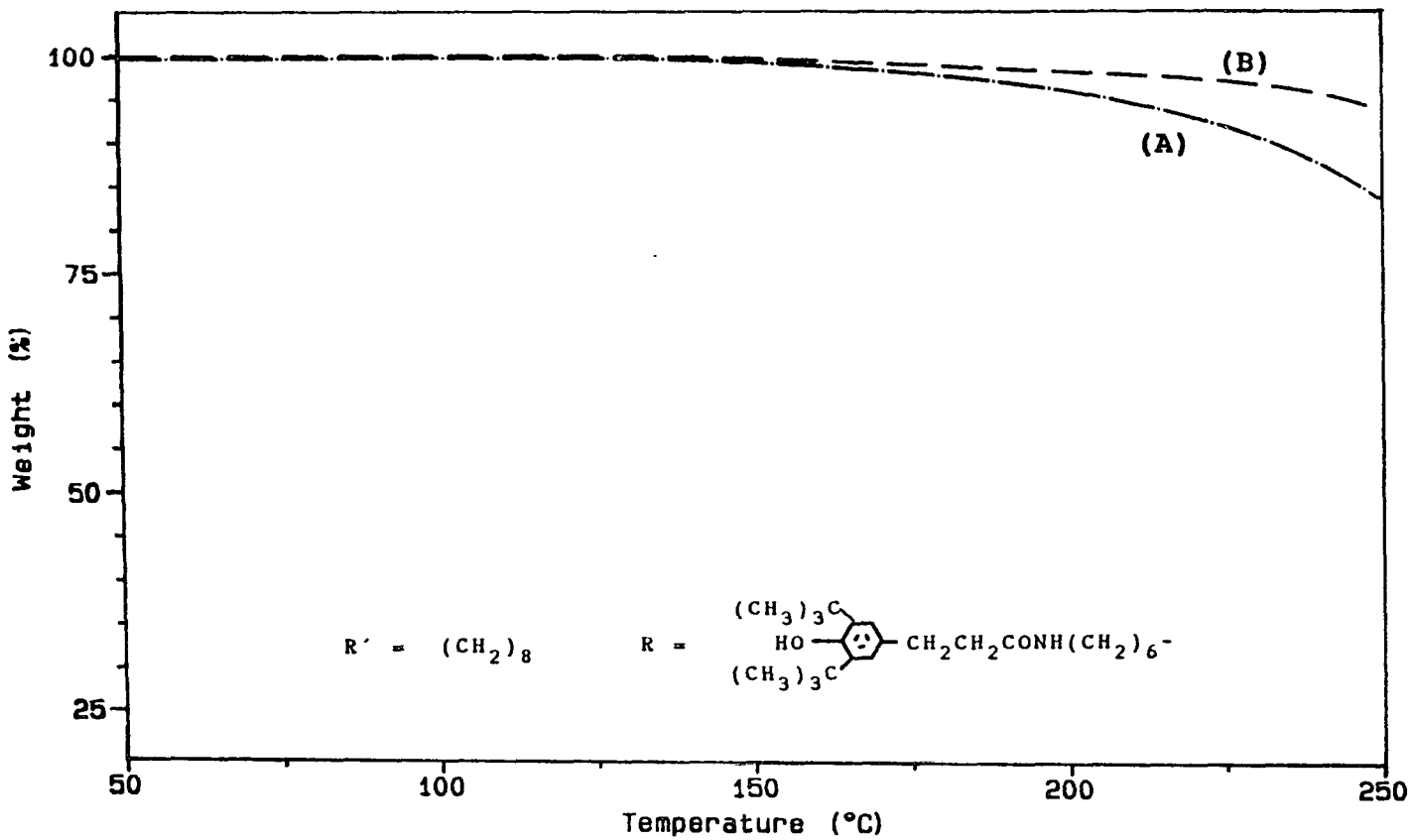

Fig. 3-16 TGA Thermograms of TOX-copolymers (A) with 1.2 mol-% of ~~$(OCH_2OCH_2$-CH=CNHR´-$CH_2)_n$~~ and 3.3 mol-% of "co-unit *l*" (B) with 1.0 mol-% of "co-unit *n*", ~~$(OCH_2OCH_2$-CH=CNHR-$CH_2)_n$~~ and 3.3 mol-% of "co-unit *l*" (heating rate 10 °C/min in air flow)

This can be attributed to the efficient actions of hindered phenol-amine as a radical scavenger as well as an acceptor of acid and formaldehyde during thermal degradation. Amide group can remove formaldehyde from degraded polyacetal copolymer systems, i.e.:

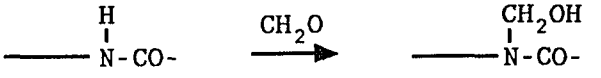

Hindered phenol group acts as antioxidant. The mechanism is illustrated in Scheme 3-4 (20).

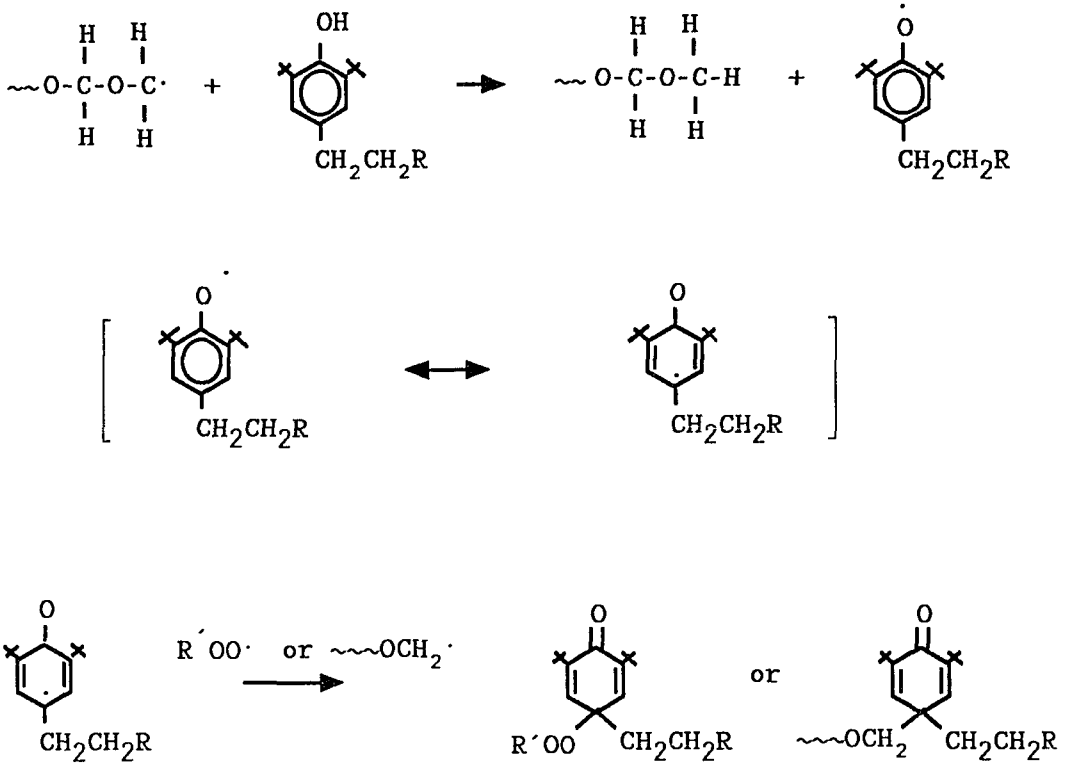

Phenoxyl radical *Resonance stabilized adducts*

Scheme 3–4

It donates hydrogen to polymeric alkyl radicals or peroxyradicals (ROO•), inhibiting further β-scission or initiation of degradation. The phenoxyl radical combines with peroxy radical or degrading polymer radical chain and forms resonance stabilized adduct through π electron delocalization.

Figure 3-17 shows TGA thermograms of functionalized trioxane copolymers with various groups. Under air flow, the thermograms were obtained for the following functionalized

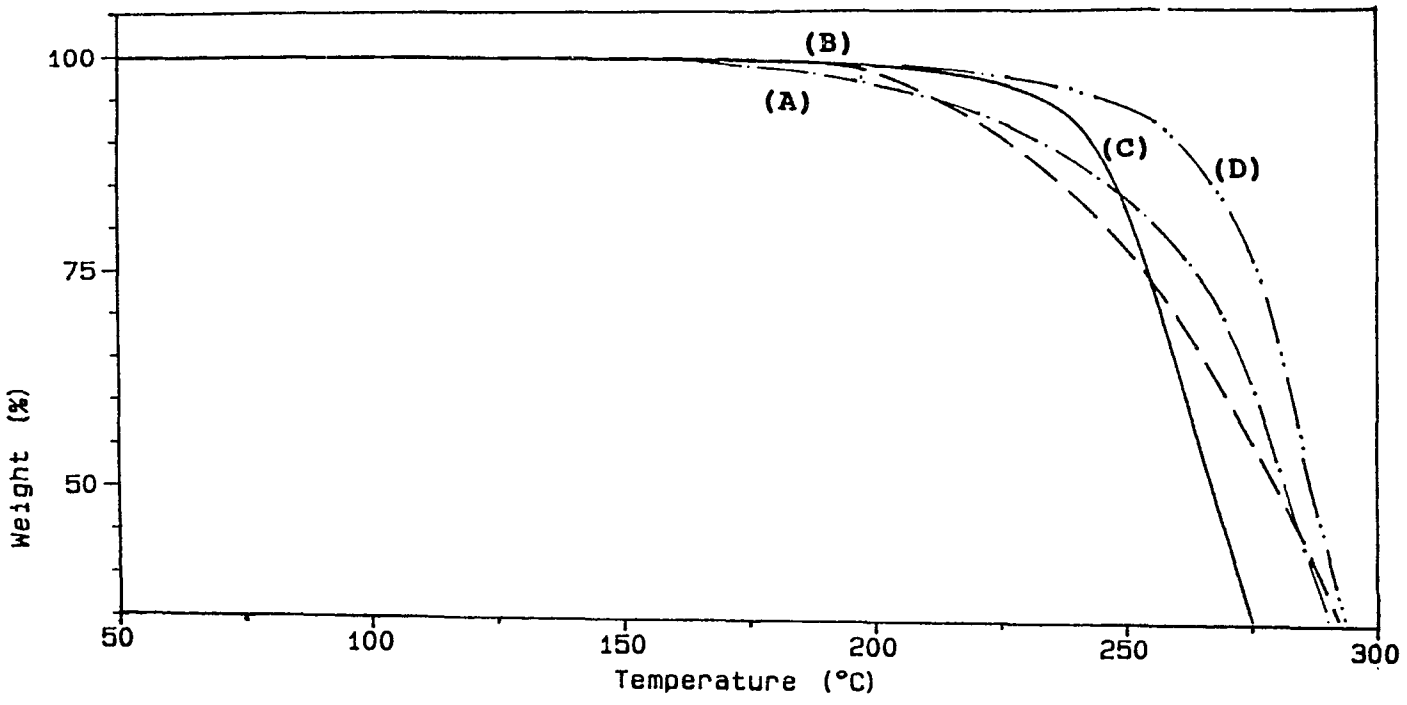

Fig. 3-17 TGA Thermograms of TOX-copolymers (A) with 1.2 mol-% of ~~$(OCH_2OCH_2\text{-}CH{=}CNHR'\text{-}CH_2)_n$~~ and 3.3 mol-% of "co-unit ℓ" (— · —) (B) with 8.2 mol-% of "co-unit γ ", ~~$(OCH_2OCH_2\text{-}CH{=}CH\text{-}CH_2)_\gamma$~~ (— —)
(C) with 5.3 mol-% of "co-unit ℓ" (——)
(D) with 1.0 mol-% of "co-unit n", (— ··—)
~~$(OCH_2OCH_2\text{-}CH{=}CNHR\text{-}CH_2)_n$~~ and 3.3 mol-% of "co-unit ℓ"
(heating rate 10 °C/min in air flow)

trioxane copolymer: (A) 1.0 mol-% of octyl amine and 3.3 mol-% of "co-unit *l*", (B) with 8.2 mol-% of oxybutenylene co-unit, (C) with 5.3 mol-% of "co-unit *l*" and (D) hindered phenol-amine 1.2 mol-% and 3.3 mol-% of "co-unit *l*". The stability of trioxane copolymers increases in the increasing order of (A)< (B)< (C)< (D). Comparing curve C with D, one can arrive at the conclusion that bound hindered phenol-amine at 1.0 mol-% is far more efficient than 2 mol-% of -C≡C-. From D versus B, one mol-% of bound antioxidant is again far superior to a high level (i.e. 8.2 mol-%) of -C=C-.

3.3.4. Conclusions

Polyacetal copolymers with dibromo functional group was synthesized for functionalization. Amino and triple bond functional groups can be successfully incorporated into the crude copolymer via substitution and elimination reactions of bromo groups. Thermal stability of copolymers demonstrated that the co-unit, ~~(OCH_2-OCH_2-C≡C-CH_2)~~, is not only a efficient stopper unit against unzipping process, but also functions as good stabilizer against oxidative thermal degradation. It was shown that bound hindered phenolic amine served as an excellent antioxidant to improve

thermostability of the polyacetal copolymer. It's hindered penol group suppress radical degradation through free radicals deactivation, while amine and amide groups retard acidic degradation through acting as a H^+ and as a CH_2O acceptor, respectively.

3.5. References

1. Zheng, Y., *Acetal Copolymers: Synthesis and Modification* Doctoral Thesis, The City Univesity of New York, **1992**.
2. Collins, G. L.; Pleban, W. M.; Hayes, M. J., *WO* 9,104,282 (1991), assigned to Hoechst Celanese.
3. Wissbrun, K. F., *U. S. Pat.* 4,937,312 (1990), assigned to Hoechst Celanese.
4. Collins, G. L.; Ying, *WO* 9,109,082 (1991), assigned to Hoechst Celanese.
5. Stohler, F. R.; Berger, K., *Die Angew. Makromol. Chem.*, **1990**, 176/177, 323, p 3074.
6. Baker, S. J.; Price, M. B., *Polyacetals*, American Elsevier Publishers Co, New York, **1961**, p 23.
7. Scott, G., *Polymer Stabilization and Degradation*, Klemchuk, P. P., Ed.; ACS Symposium series no. 280, American Chemical Society: Washington, DC, **1985**, p 173.
8. Imai, E.; Ito, S., *Gyomu Nenpo-Tochigi-Ken Ken'nan Kogyo Shidosho*, **1987**, p 31.

9. Yang, N.-L.; Patel, V.; Dolce, *Am. Chem. Soc. Div. Polym. Mater. Sci. Eng.*, **1984**, 17, p 149.

10. Brannock, K. C.; Lappin, G. R., *J. Org. Chem.*, **1956**, 21, 1366.

11. Pesce-Rodriguez R.; Wang, S.; Auerbach, Andrew; Paul, James; Yang, N-L., *Makromol. Chem.*, **1990**, 191, 99.

12. Saul, P., *The Chemistry of the Carbon-Halogen Bond*, part 2, John Wiely and Sons, New York, **1973**, p 687.

13. Pesce, R., *Stabilization and Degradation of Acetal Copolymers*, Doctoral Thesis, The City Univesity of New York, **1988**.

14. March, J., *"Advanced Organic Chemistry"* 3rd ed. **1985** A Wiely-Interscience, New York, p 680.

15. March, J., *"Advanced Organic Chemistry"* 3rd ed. **1985** A Wiely-Interscience, New York, p 726.

16. Adam and Baader, *Angew. Chem. Int. Ed. Engl.*, **1984**, 23, p 437.

17. Dao, L. T. A.; Blau, K., Pritzkow, W.; Schmidt-Renner, W.; Voerckel, V.; Willecke, L., *J. Prakt. Chem.*, **1984**, 115, 531; *Chem. Abs.*, **1984**, 100, 5586.

18. Pascual, C.; Meier, J.; Simon, W., *Helv. Chim. Acta*, **1966**, 49, p 164 in *"Spectrometric Identification of Organic Compounds"* by Silverstein, Robert M.; Bassler, G. Clayton; Morrill, Terence C., **1980**, John Wiely &

Sons, New York, p 228.

19. "The Aldrich Library of NMR Spectra", Edition II, vol 1. by Aldrich Chemical Company, Inc. **1983**, p 239, 256.

20. "Encyclopedia of Polymer Science and Engineering", vol 2, by Mark, H. F.; Bikales, N. M.; Overberger, C. G.; Menges, G., vol. 2, A Wiely-Interscience Publication, John Wiely & Sons, New York, **1983**, p 76.